



DEVELOPMENT OF WEB-BASED SPATIAL DECISION SUPPORT SYSTEM
FOR LANDSLIDE SUSCEPTIBILITY ASSESSMENT IN XISHUANGBANNA,
CHINA



A Thesis Submitted to the Graduate School of Naresuan University
in Partial Fulfillment of the Requirements
for the Master of Science in Disaster Management - (Plan A Type A2) International
Program
2021
Copyright by Naresuan University

DEVELOPMENT OF WEB-BASED SPATIAL DECISION SUPPORT SYSTEM
FOR LANDSLIDE SUSCEPTIBILITY ASSESSMENT IN XISHUANGBANNA,
CHINA



A Thesis Submitted to the Graduate School of Naresuan University
in Partial Fulfillment of the Requirements
for the Master of Science in Disaster Management - (Plan A Type A2) International
Program
2021
Copyright by Naresuan University

Thesis entitled "Development of Web-based Spatial Decision Support System for
Landslide Susceptibility Assessment in Xishuangbanna, China"

By GEN LONG

has been approved by the Graduate School as partial fulfillment of the requirements
for the Master of Science in Disaster Management - (Plan A Type A2) International
Program of Naresuan University

Oral Defense Committee

..... Chair
(Associate Professor Uruya Weesakul, Ph.D.)

..... Advisor
(Associate Professor Sarintip Tantanee, Ph.D.)

..... Co Advisor
(Assistant Professor Korakod Nusit, Ph.D.)

..... Internal Examiner
(Polpreecha Chidburee, Ph.D.)

Approved

.....
(Associate Professor Krongkarn Chootip, Ph.D.)

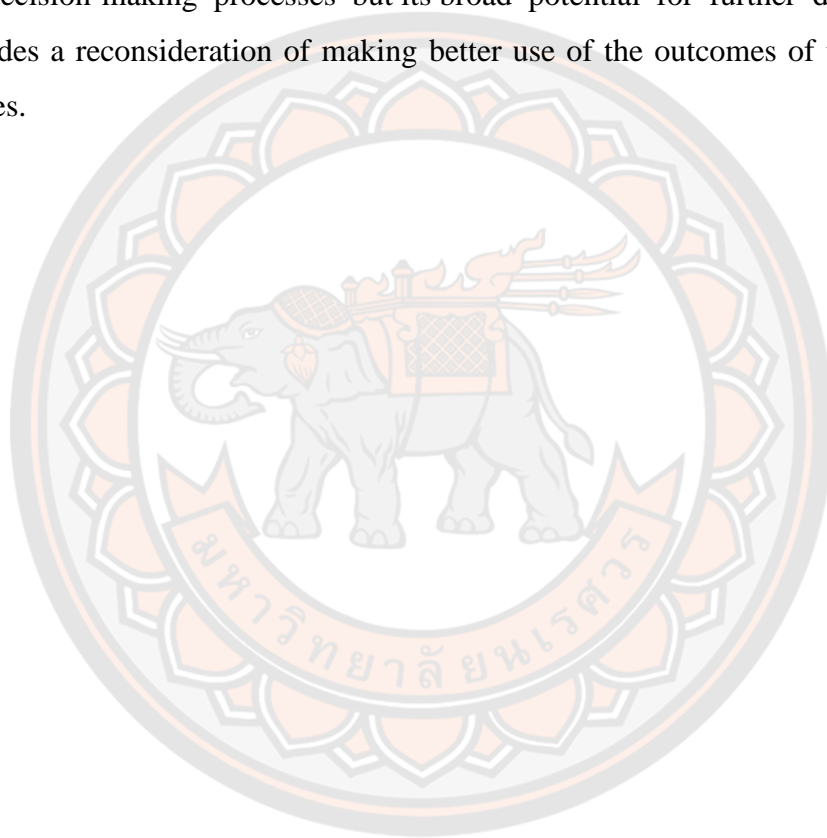
Dean of the Graduate School

Title	DEVELOPMENT OF WEB-BASED SPATIAL DECISION SUPPORT SYSTEM FOR LANDSLIDE SUSCEPTIBILITY ASSESSMENT IN XISHUANGBANNA, CHINA
Author	GEN LONG
Advisor	Associate Professor Sarintip Tantanee, Ph.D.
Co-Advisor	Assistant Professor Korakod Nusit, Ph.D.
Academic Paper	M.S. Thesis in Disaster Management - (Plan A Type A2) International Program, Naresuan University, 2021
Keywords	Landslide, Landslide Susceptibility Assessment, Frequency Ratio, Relative Frequency, Predictor Rate, Remote Sensing, Geographic Information System, Xishuangbanna, Spatial Decision Support System, Web-based Spatial Decision Support System

ABSTRACT

Climate change, human activities such as rapid and unplanned urban expansion, increase the risk of natural hazards. Landslide is one of the most severe that cause imponderable loss of human life and property and showing a trend of increasing occurrence worldwide. Both national and provincial scales of landslide-prone area zonation studies have been found but no regional such study yet for Xishuangbanna Prefecture, Yunnan Province, China. The Frequency Ratio (FR) is selected as the mapping model due to its popularity, simplicity, and understandability. Fourteen most frequently used landslide conditioning factors (LCFs) have been extracted from a comprehensive literature review (52 studies) firstly, then 27 scenarios have been designed to produce the 27 landslide susceptibility maps, and the Area Under the Curve (AUC) of each map has been calculated and compared. Finally, seven of the fourteen factors are identified as the more effectively decisive LCF for the study area, the final landslide susceptibility mapping (LSM) was done based on these 7 LCFs. The AUC values of the final landslide susceptibility map with inputting landslide inventory dataset and verification dataset are 85.8% and

84.0%, respectively, which means the model acquired a very good result for both success and prediction rate. Innumerable landslide susceptibility assessment (LSA) studies have been done by researchers in recent decades, but most of the outcomes of these works have been archived and rare of them have been well used for supporting decision-makers in real situations. The last objective of the study is to adopt the outcomes of the study to develop a Web-based Spatial Decision Support System (Web-based SDSS), which not only can be used as an effective aiding tool to support the decision-making processes but its broad potential for further development also provides a reconsideration of making better use of the outcomes of these GIS-based studies.



ACKNOWLEDGEMENTS

I could not ever have been able to finish my thesis without the guidance of all my committee members, help from all lecturers and friends, and support from the scholarship and my family.

First, I would like to show my sincere gratitude to the Faculty of Engineering, Naresuan University for providing the scholarship for the tuition fee, which is a priceless opportunity to chase my higher education in Master of Science in Disaster Management at Naresuan University, Thailand.

Foremost, I would like to express my sincere gratitude to my advisor Assoc. Prof. Dr. Sarintip Tantaneer and co-advisor Assist. Prof. Dr. Korakod Nusit for the continuous support of my master's study and research, for their patience, motivation, enthusiasm, and immense knowledge. Their guidance helped me in all the time of research and writing of this thesis. I could not have imagined having a better advisor and mentor for my study.

Besides my advisor and co-advisor, I would like to thank the rest of my thesis committee, Assoc. Prof. Dr. Uruya Weesakul, Dr. Bhichit Rattakul, and Dr. Polpreecha Chidburee for their encouragement, insightful comments, and suggestions.

I do not forget to thank all the lecturers both inside and outside the Faculty of Engineering, especially those who gave me precious lectures on the subject. Without them, I would not have done my thesis precisely. I will never forget their motivation and guidance.

I am very grateful to all the faculty staff who always help me with providing information, documents, and guidance.

Finally, yet importantly, I would like to thank all of my family and my friends for providing me both emotional and financial support, encouragement, throughout the years especially during this particular time of COVID-19. My achievement would not be possible without them.

Thank you so much.

TABLE OF CONTENTS

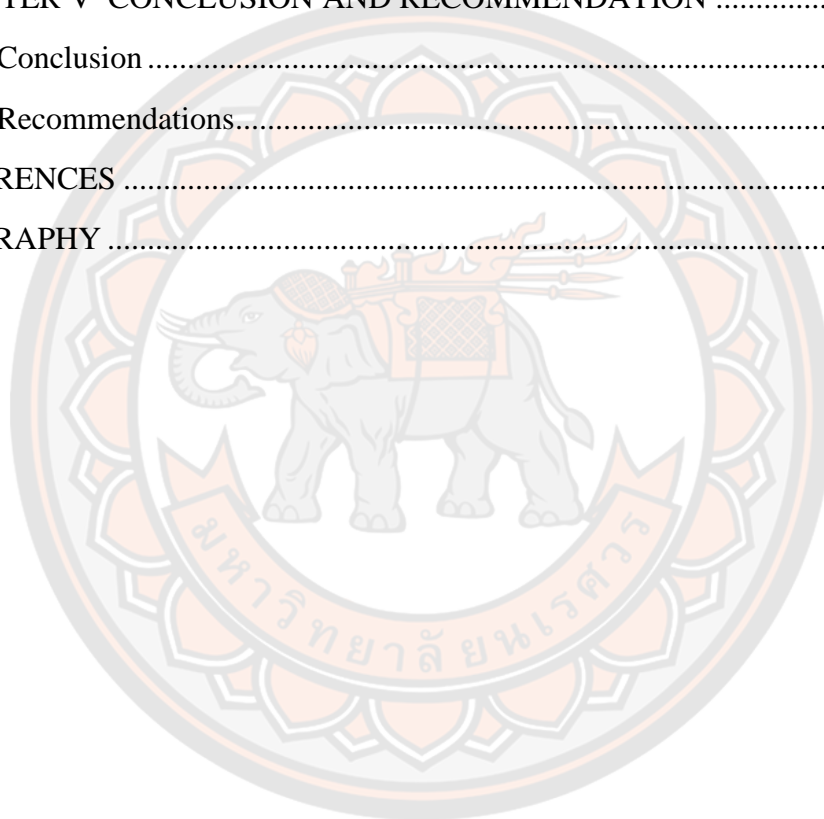
	Page
ABSTRACT.....	C
ACKNOWLEDGEMENTS.....	E
TABLE OF CONTENTS.....	F
LIST OF TABLES.....	K
LIST OF FIGURES.....	L
ABBREVIATION.....	P
CHAPTER I INTRODUCTION.....	1
1.1 Background.....	1
1.2 Statement of the Problems.....	3
1.3 Purposes of the Study.....	4
1.4 Expected Outcome.....	4
1.5 Significance of Study.....	5
1.5.1 Innovation of the Study.....	5
1.5.2 Practical Application Value of the Study.....	6
1.6 Scope of Study.....	7
1.7 Key Words.....	8
CHAPTER II LITERATURE REVIEW.....	9
2.1 Landslide.....	9
2.1.1 Landslides Formation Mechanism.....	9
2.1.2 Negative Impacts of Landslides.....	10
2.2 Landslides in China.....	10
2.3 Landslides in Yunnan.....	11
2.4 Landslides in Xishuangbanna.....	11
2.5 Landslide Susceptibility Concept.....	12
2.5.1 Landslide Susceptibility and Landslide Hazard.....	12

2.5.2 Importance of Landslide Susceptibility Assessment (LSA).....	13
2.6 Landslide Susceptibility Mapping (LSM)	13
2.7 Landslide Susceptibility Mapping (LSM) Approach	14
2.7.1 Qualitative Approach	14
2.7.2 Semiquantitative Approach	15
2.7.3 Quantitative Approach	15
2.8 Landslide Causative Factors	16
2.8.1 Slope Angle	27
2.8.2 Distance to Rivers	27
2.8.3 Slope Aspect.....	27
2.8.4 Lithology	28
2.8.5 Land Use and Land Cover (LULC).....	28
2.8.6 Distance to Faults	28
2.8.7 Distance to Roads	28
2.8.8 Curvature	29
2.8.9 Elevation.....	29
2.8.10 Precipitation.....	29
2.8.11 Normalized Difference Vegetation Index (NDVI).....	30
2.8.12 Soil Texture	30
2.8.13 Topographic Wetness Index (TWI).....	30
2.8.14 Stream Power Index (SPI).....	31
2.8.15 Rubber Plantation Density (RPD)	31
2.9 Geographic Information System (GIS) and Remote Sensing (RS) in Landslide Susceptibility Assessment (LSA)	31
2.10 Frequency Ratio (FR) Model.....	32
2.11 Relative Frequency (RF) and Predictor Rate (PR)	34
2.12 Landslide Susceptibility Index (LSI).....	35
2.13 Receiver Operating Characteristic (ROC) Curve and Area Under the Curve (AUC).....	35
2.14 Decision Support System.....	37

2.15 Spatial Decision Support System.....	37
2.16 Web-based Spatial Decision Support System.....	38
CHAPTER III METHODOLOGY	41
3.1 Introduction.....	41
3.1.1 Overall Research Methodology	41
3.2 Study Area	41
3.2 Data Preparation	44
3.2.1 Landslide Inventory.....	46
3.2.2 Landslide Conditioning Factor Sources	47
3.3 Method.....	48
3.3.1 Landslide Conditioning Factor Identification	48
3.3.2 Landslide Susceptibility Mapping.....	50
3.3.2.1 Factor Classification.....	51
3.3.2.2 Landslide Susceptibility Mapping with Identified Factors	52
3.3.2.3 Frequency Ratio (FR) Calculation	52
3.3.2.4 Relative Frequency (RF) Calculation.....	52
3.3.2.5 Predictor rate (PR) Calculation	53
3.3.2.6 Landslide Susceptibility Map (LSM) Generation	53
3.3.3.7 Mapping Results Verification	53
3.3.3 Design of Web-based Spatial Decision Support System.....	53
CHAPTER IV RESULTS AND DISCUSSION.....	56
4.1 Results.....	56
4.1.1 Factor Classification Results	56
4.1.1.1 Slope Angle	56
4.1.1.2 Distance to River	56
4.1.1.3 Slope Aspect.....	56
4.1.1.4 Lithology	57
4.1.1.5 Land Use and Land Cover (LULC).....	57
4.1.1.6 Distance to Fault.....	57

4.1.1.7 Distance to Road	57
4.1.1.8 Curvature	58
4.1.1.9 Elevation.....	58
4.1.1.10 Precipitation.....	58
4.1.1.11 Normalized Difference Vegetation Index (NDVI).....	59
4.1.1.12 Soil Texture	59
4.1.1.13 Topographic Wetness Index (TWI).....	60
4.1.1.14 Stream Power Index (SPI).....	60
4.1.1.15 Rubber Plantation Density (RPD)	60
4.1.2 Frequency Ratio (FR), Relative Frequency (RF), and Predictor Rate (PR) Value Calculation Results	67
4.1.2.1 Frequency Ratio Value Results	67
4.1.2.2 Relative Frequency Value Results	67
4.1.2.3 Predictor Rate Value Results.....	68
4.1.3 Landslide Susceptibility Mapping (LSM) and AUC Results.....	80
4.1.3.1 Landslide Susceptibility Mapping (LSM) Results for Cases of Inputting All 14 Factors and Removing Factor in Turn	80
4.1.3.2 Area Under the Curve (AUC) values for Cases of Inputting All 14 Factors and Removing Factor in Turn.....	84
4.1.3.3 Landslide Susceptibility Mapping (LSM) Results for Cases of Inputting 3 Minimum Factors and Adding Factor in Turn.....	88
4.1.3.4 Area Under the Curve (AUC) Values for Cases of Inputting 3 Minimum Factors and Adding Factor in Turn.....	92
4.1.3.5 Area Under the Curve (AUC) Value Variation for Both Removing and Adding Single Factor Cases.....	95
4.1.4 Results of Final Factors Selection and Predictor Rate (PR) Value, and Final Landslide Susceptibility Mapping Results.....	97
4.1.4.1 Final Factors Selection Results	97
4.1.4.2 Predictor Rate (PR) Value for Final Factors	97
4.1.4.3 Landslide Susceptibility Mapping (LSM) Results with Final Landslide Conditioning Factors (LCFs)	98

4.1.4.4 Landslide Susceptibility Mapping (LSM) Result Verification .	104
4.1.5 Web-based Spatial Decision Support System Results	104
4.2 Discussion.....	124
4.2.1 Landslide Conditioning Factors Identification.....	124
4.2.2 Landslide Susceptibility Mapping with the 7 Final Landslide Conditioning Factors	128
4.2.3 Development of the Web-based Spatial Decision Support System	129
CHAPTER V CONCLUSION AND RECOMMENDATION	130
5.1 Conclusion	130
5.2 Recommendations.....	131
REFERENCES	133
BIOGRAPHY	148



LIST OF TABLES

	Page
Table 1 The Producing Time of the Data Used in the Study	7
Table 2 Literature Review Statistic on Utilization of Landslide Conditioning Factors	18
Table 3 Time Range Statistics of Data Adopted from Literature Review	45
Table 4 The Landslide Inventory and the Randomly Divided Training, Verification Datasets	46
Table 5 Landslide Inventory Distribution in Each Classification and the Area Percentage of Each Classification of LCFs	61
Table 6 Frequency Ratio and Relative Frequency Value for Each Classification of Each Factor, and Predictor Rate Value for Each Factor	69
Table 7 Predictor Rate Value (PRV) Results of All 14 Input Factors and Removing One Factor in Turn.....	77
Table 8 Predictor Rate Value (PRV) Results of Minimum 3 Input Factors and Adding One Factor in Turn.....	77
Table 9 The Area Percentage of Each Landslide Susceptibility Level of Inputting all 14-Factor Case and Removing Factor Cases, and the Area Percentage Variation of High and Very High Level.....	83
Table 10 Area Under the Curve (AUC) Values for Cases of Inputting All 14 LCFs and Removing One LCF in Turn	84
Table 11 The Area Percentage of Each Landslide Susceptibility Level of Inputting 3 Minimum Factors (Slope Angle, Lithology, and LULC) Case and Adding Factor Cases, and Their Area Percentage Variation of High and Very High Level	91
Table 12 Area Under the Curve (AUC) Values for Cases of Inputting All 14 Factors and Removing Factors in Turn	92
Table 13 Predict Rate (PR) Values for Final 7 LCFs	97
Table 14 Landslide Susceptibility Distribution in Township-Level of Final Landslide Susceptibility Mapping (LSM) Result	99
Table 15 Landslide Susceptibility Distribution in Township-Level of Final Landslide Susceptibility Mapping (LSM) Result	101

LISTOF FIGURES

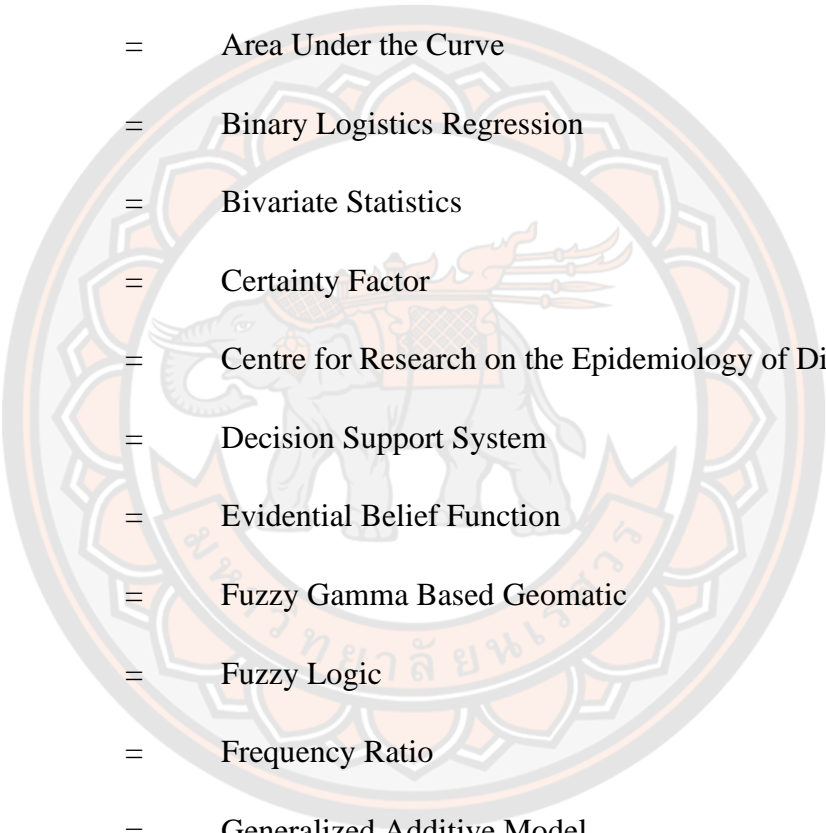
	Page
Figure 1 The Illustration of Reclassify Function of ArcGIS	34
Figure 2 An Example of ROC Curves with Good (AUC = 0.9) and Satisfactory (AUC = 0.65) Results of Specificity and Sensitivity	36
Figure 3 The Progression of Spatial Decision Support Systems Development.....	39
Figure 4 The Overall Research Methodology.....	41
Figure 5 Study Area.....	42
Figure 6 The Southeast Asia Rubber Plantation Zone (a), and the Xishuangbanna Rubber Plantation Zone (b).....	43
Figure 7 Landslide Conditioning Factors (LCFs) Identification Workflow.....	50
Figure 8 General Landslide Susceptibility Mapping (LSM) Process of the Study.....	51
Figure 9 Final Landslide Susceptibility Mapping Workflow	52
Figure 10 Design of Web-based SDSS for LSA in Xishuangbanna, China.....	55
Figure 11 USDA Soil Texture Triangle.....	59
Figure 12 Landslide Inventory Mapping Result (a), and the Rubber Plantation Zone Map (b) (Zhu et al., 2014) in Xishuangbanna.....	61
Figure 13 Maps of Landslide Inventory Distribution in the Classification of Slope Angle (a), Distance to River (b), Slope Aspect (c), Lithology (d), Land Use and Land Cover (LULC) (e), and Distance to Fault (f)	65
Figure 14 Maps of Landslide Inventory Distribution in the Classification of Distance to Road (a), Curvature (b), Elevation (c), Precipitation (d), Normalized Differential Vegetation Index (NDVI) (e), and Soil Texture (f).	66
Figure 15 Maps of Landslide Inventory Distribution in the Classification of Topographic Position Index (TWI) (a) and Stream Power Index (b)	67
Figure 16 Landslide Number and Percentage in Each Classification, Area Percentage and RF Value of Each Classification of Slope Angle (a), Distance to River (b), Slope Aspect, Lithology (c), LULC, and Distance to Fault (d).....	72
Figure 17 Landslide Number and Percentage in Each Classification, Area Percentage, and RF Value of Each Classification of Distance to Road (a), Curvature (b), NDVI (c), Elevation (d), Precipitation (e), and Soil Texture (f).....	73

Figure 18. Landslide Number and Percentage in Each Classification, Area Percentage, and RF Value of Each Classification of TWI (a) and SPI (b)	74
Figure 19 Maps of Relative Frequency (RF) Value for Each Classification of Slope Angle (a), Distance to River (b), Slope Aspect (c), and Lithology (d).....	74
Figure 20 Single Layer Maps of Relative Frequency (RF) Value for Each Classification of LULC (a), Distance to Fault (b), Distance to Road, Curvature (c), Elevation (e), and Precipitation (f).....	75
Figure 21 Single Layer Maps of Relative Frequency (RF) Value for Each Classification (a) of NDVI (b), Soil Texture (c), TWI, and SPI (d)	76
Figure 22 Predictor Rate value (PRV) Results of Inputting All 14 Factors and Removing One Factor in Turn	79
Figure 23 Predictor Rate value (PRV) Results of Inputting 3 Minimum Factors and Removing One Factor in Turn	79
Figure 24 Landslide Susceptibility Mapping (LSM) Results for the Case of Inputting All 14 Factors (a), Removing Slope Angle (b), Removing Distance to River (c), and Removing Slope Aspect (d) from the 14 Factors.....	80
Figure 25 Landslide Susceptibility Mapping (LSM) Results for the Case of Removing Lithology (a), Removing LULC (b) Removing Distance to Fault (c), Removing Distance to Road (d), Removing Curvature (e), and Removing Elevation (f) from the 14 Factors	81
Figure 26 Landslide Susceptibility Mapping (LSM) Results for the Case of Removing Precipitation (a), Removing NDVI (b), Removing Soil Texture (c), Removing TWI (d), and Removing SPI (e) from the 14 Factors.....	82
Figure 27 AUC Results for Cases of Inputting All 14 LCFs (a), Removing Slope Angle (b), Removing Distance to River (c), Removing Slope Aspect (d), Removing Lithology (e), and Removing LULC (f) from the 14 LCFs.....	85
Figure 28 AUC Results for the Case of Removing Distance to Fault (a), Removing Distance to Road (b), Removing Curvature (c), Removing Elevation (d), Removing Precipitation (e), and Removing NDVI (f) from the 14 LCFs.....	86
Figure 29 AUC Results for the Case of Removing Soil Texture (a), Removing TWI (b), and Removing SPI (c) from the 14 LCFs.....	87
Figure 30 Area Under the Curve (AUC) Value Comparison Between the Case of Inputting All 14 LCFs and Cases of Removing Other 14 Factors in Turn	87
Figure 31 Landslide Susceptibility Mapping (LSM) Results for the Case of Inputting 3 Minimum Factors (a), Adding Distance to River Into the 3-Factor Group (b),	

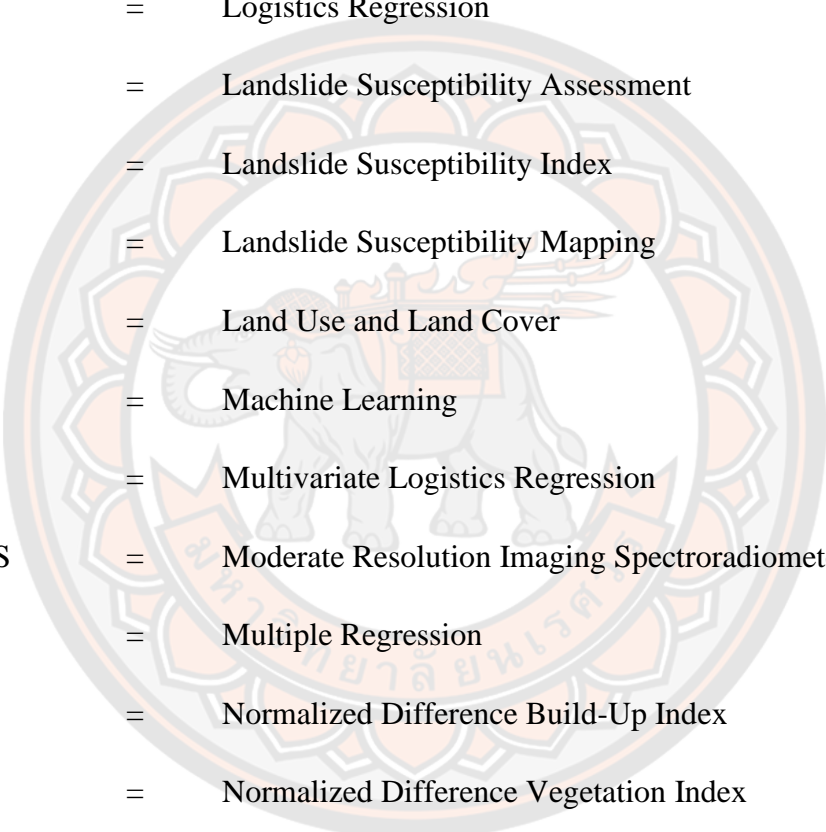
Adding Slope Aspect (c), Adding Distance to Fault (d), Adding Distance to Road (e), and Adding Curvature (f) to the 3-Factor Group	89
Figure 32 Landslide Susceptibility Mapping (LSM) Results for the Case of Adding Elevation (a), Adding Precipitation (b), Adding NDVI (c), Adding Soil Texture (d), Adding SPI (e), and Adding TWI (f) to the 3-Factor Group	90
Figure 33 AUC Results for the Case of Inputting 3 Minimum LCFs (a), Adding Distance to River (b), Adding Slope Aspect (c), Adding Distance to Fault (d), Adding Distance to Road (e), and Adding Curvature (f) to the 3 Minimum LCFs.....	93
Figure 34 AUC Results for the Case of Adding Elevation (a), Adding Precipitation (b), Adding NDVI (c), Adding Soil Texture (d), Adding TWI (e), and Adding SPI (f) to the 3 Minimum LCFs.....	94
Figure 35 AUC Value Comparison Between the Case of Inputting 3 Minimum LCFs and Case of Adding Other 11 Factors in Turn.....	95
Figure 36 AUC Value Variation of Both Removing and Adding Distance to River, Aspect, Fault, Distance to Road, Curvature, Elevation, Precipitation, NDVI, Soil Texture, TWI, and SPI.....	96
Figure 37 PR Value for Final 7 Landslide Conditioning Factors (LCFs).....	98
Figure 38 Final Landslide Susceptibility Mapping (LSM) Result (a), the Susceptibility Proportion for Each Level (b), and the Susceptibility Proportion for the County-Level Administrative Division.....	99
Figure 39 Final Landslide Susceptibility Mapping (LSM) Result for the Township-Level Administrative Division.....	100
Figure 40 Landslide Susceptibility Proportion for Township-Level Administrative Divisions	101
Figure 41 AUC Results of the Final Landslide Susceptibility Mapping Result with Inputting Both Landslide Inventory Training and Verification Data	104
Figure 42 Location Identification Page of “General Module”	106
Figure 43 Example of Location Identification Function.....	107
Figure 44 Program Introduction Page of “General” Module.....	110
Figure 45 Data Type and Source Page of “General” Module.....	111
Figure 46 Methodology Page of “General” Module.....	112
Figure 47 About Us Page of “General” Module.....	113
Figure 48 Slope Angle Sample Page of “Single Layer” Module.....	114

Figure 49 Factor Weight & AUC Value Page of “Remove Factor” Module	115
Figure 50 Landslide Susceptibility Mapping Result Sample Page of Inputting All the 14 Factors of “Remove Factor” Module	116
Figure 51 Factor Weight & AUC Value Page of “Add Factor” Module.....	117
Figure 52 Landslide Susceptibility Mapping Result Sample Page of Inputting 4 Factors That Adding Distance to River to the 3 Minimum Factors of “Remove Factor” Module	118
Figure 53 Page of AUC Value Compare of Both Cases of Removing and Adding Factor Except for the Obligatory 3 Minimum Factors (Slope Angle, Lithology, and LULC) of “Final Results” Module	119
Figure 54 Page of Factor Weight Value for the Final 7 Factors of “Final Results” Module	120
Figure 55 Page of Landslide Susceptibility Mapping Result of Inputting Final 7 Factors for County-Level of “Final Results” Module.....	121
Figure 56 Page of Landslide Susceptibility Mapping Result of Inputting Final 7 Factors for Township-Level of “Final Results” Module	122
Figure 57 Page of Statistic Chart of Landslide Susceptibility Mapping Result for Township-Level of Inputting Final 7 Factors of “Final Results” Module.....	123

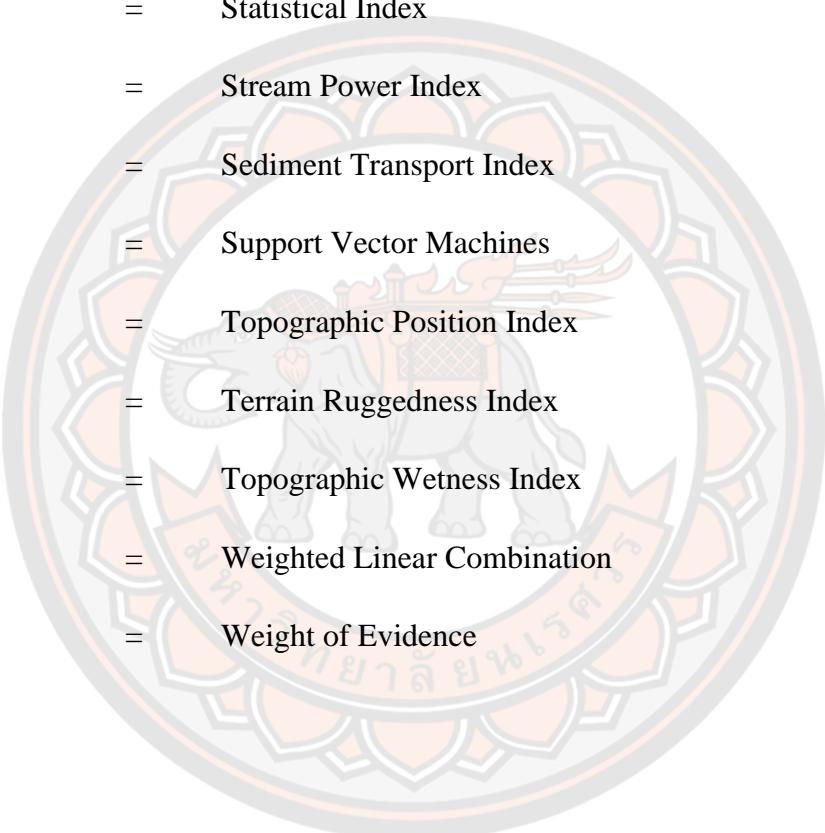
ABBREVIATION



AHP	=	Analytic Hierarchy Process
ANN	=	Artificial Neural Network
ASTERGDEM	=	Advanced Spaceborne Thermal Emission and Reflection Radiometer Global Digital Elevation Model
AUC	=	Area Under the Curve
BLR	=	Binary Logistics Regression
BS	=	Bivariate Statistics
CF	=	Certainty Factor
CRED	=	Centre for Research on the Epidemiology of Disasters
DSS	=	Decision Support System
EBF	=	Evidential Belief Function
FGBG	=	Fuzzy Gamma Based Geomatic
FL	=	Fuzzy Logic
FR	=	Frequency Ratio
GAM	=	Generalized Additive Model
GDP	=	Gross Domestic Product
GFM	=	Geomorphological Field Mapping
GIS	=	Geographic Information System
HSMCE	=	Hybrid Spatial Multi-Criteria Evaluation
IoE	=	Index of Entropy



Lao PDR	=	Lao People's Democratic Republic
LCF	=	Landslide Conditioning Factor
LHA	=	Landslide Hazard Assessment
LIM	=	Landslide Inventory Map
LNRF	=	Landslide Nominal Risk Factor
LR	=	Logistics Regression
LSA	=	Landslide Susceptibility Assessment
LSI	=	Landslide Susceptibility Index
LSM	=	Landslide Susceptibility Mapping
LULC	=	Land Use and Land Cover
ML	=	Machine Learning
MLR	=	Multivariate Logistics Regression
MODIS	=	Moderate Resolution Imaging Spectroradiometer
MR	=	Multiple Regression
NDBI	=	Normalized Difference Build-Up Index
NDVI	=	Normalized Difference Vegetation Index
FR	=	Frequency Ratio
NGCC	=	National Geomatics Center of China
PR	=	Predictor Rate
PRC	=	The People's Republic of China
RESDC	=	Resource and Environment Science and Data Center of China
RF	=	Relative Frequency



ROC	=	Receiver Operating Characteristic
RPD	=	Rubber Plantation Density
RS	=	Remote Sensing
SDSS	=	Spatial Decision Support System
SE	=	Shannon Entropy
SI	=	Statistical Index
SPI	=	Stream Power Index
STI	=	Sediment Transport Index
SVM	=	Support Vector Machines
TPI	=	Topographic Position Index
TRI	=	Terrain Ruggedness Index
TWI	=	Topographic Wetness Index
WLC	=	Weighted Linear Combination
WoE	=	Weight of Evidence

CHAPTER I

INTRODUCTION

1.1 Background

Natural hazards cause noticeable casualties and destruction in the present world (Kumar & Anbalagan, 2016). Over the past few decades, due to climate change, rapid and unplanned urban expansion especially in less developed regions, as well as other human activities, increase the risk of natural hazards. As one of the most destructive natural disasters that cause imponderable loss of human life and property, landslide is no exception showing a trend of increasing occurrence worldwide. In numbers, every year, tens of thousands of people died from landslides and caused billions of dollars loss. Furthermore, landslides pose serious impacts to people's normal life by destroying infrastructures such as highways, waterways, and pipelines (Lee & Pradhan, 2006; Mind'je et al., 2019; Vakhshoori & Zare, 2016).

As a consequence, instead of being regarded as only the incidental results of other phenomena such as earthquakes, floods in the early stages, independent landslide study interests are having been enhanced among international researchers (Abedini & Tulabi, 2018). There are two reasons for this: First, there is a growing understanding of the socioeconomic impact of landslides; second, there is a growing strain on the environment because of urbanization and development. It is reported that development on sloping urban areas, induces slope instability and in turn causes landslides (Aleotti & Chowdhury, 1999). On the other hand, requirements of economic growth and population pressure have also put a strain on slope stability in mountainous locations with the infrastructure expansion and residential zones shifting on natural slopes. Furthermore, other human activities including slope cut, deforestation, land cover change, mining, etc., would cause slope failures, in particularly during triggering phenomena such as extreme high return period and prolonged rainstorms. (Le et al., 2021).

Disaster risk management has been a prominent topic across the world, with the focus shifting from post-disaster to pre-disaster stages (Mind'je et al., 2019). Critical management relies on thorough information regarding hazard characteristics, capacity, susceptibility, and vulnerability in pre-disaster phases such as risk assessment, hazard identification, preparedness, and preventative efforts (UNISDR, 2016). To help decision-makers conduct a better urban plan, it is of great significance to identify and predict where is more prone to landslides, accordingly they can take preventive measures and minimize the damage of landslides (Rasyid et al., 2016). Furthermore, the landslide-prone zoning products can facilitate the decision-making processes such as helping the decision-makers in taking essential steps in soil and natural resource management and protection, as well as achieving a better plan for city and village growth (Abedini & Tulabi, 2018; Arabameri et al., 2020). Nowadays many modeling methods have been adopted by researchers in identifying landslide-prone areas worldwide. In disaster management, knowing the process of landslide occurrence is critical, it may not be possible to regulate nature and prevent natural phenomena such as landslides from occurring, but it is possible to mitigate their impacts and damages. As a result, it is vital to appropriately identify places that disasters are probable to occur by evaluating various conditioning factors based on scientific knowledge in order to mitigate the latter (Mind'je et al., 2019). Assessments and management of future hazard can get benefit from a developed landslide susceptibility map (LSM). It is also critical for land use, infrastructure, and new construction engineering, to lower the expenses of living in areas prone to landslides (Zhang et al., 2016).

Decision Support System (DSS) has been an important aiding tool for the decision-making process while a major limitation of DSSs is their inability to take spatial and temporal data into account, despite many useful data being spatially referenced (Sugumaran & Sugumaran, 2007). Geographic Information Systems (GIS), which has traditionally been employed in fields such as utilities, environmental and urban planning, real estate, governance, and natural resource management, has the potential to shorten this restriction of DSSs. The GIS-based Spatial Decision Support System (SDSS) was built to effectively support decision-making for solving semi-structured spatial related problems. SDSS is a framework for connecting database

management systems to graphical presentation, tabular reporting capabilities, analytical models, and expertise of decision-makers (Ghavami, 2019). SDSS has been used in many fields, such as agriculture, business, energy, fire protection, land planning, site selection, transportation, water resource management, disaster management (DM), etc.

During the last decades, the rapid rise of the computer, Internet, and especially World Wide Web (WWW) technologies has had a great influence on architecture, landscape architecture, and urban planning education and practice. The ability to overcome constrained resources in terms of time, data, and communication, is one of the most significant advantages of employing web services in spatial decision-making. The typical Web-based SDSS is an integration application of Web-based GIS and DSS, where GIS information is implemented in WWW/Internet environment, and Open Source GIS software is used (Jeong & García-Moruno, 2016). Because GIS provides a wide range of visual and computational support capabilities that may be utilized by both planners and lay participants on the web for selection, prioritizing, and integration of decision alternatives, Web-based SDSS has been recommended as an effective tool for participatory planning. Web-based SDSSs not only give participants the flexibility to work from different locations and at different times to suit their needs, but they also give everyone an option to participate (Jelokhani-Niaraki & Malczewski, 2015). Individual decision-makers' decision times were shortened and their accuracy was raised by using GIS as a component of SDSS (Herold et al., 2005).

1.2 Statement of the Problems

Lin, & Wang (2018) analyzed spatial and temporal characteristics of disastrous landslides from 1950 to 2016 on a national scale in China. Yanhui Zhu et al. (2018) assessed the landslide and debris flow hazard risk in Yunnan Province of China. However, scientific literature revealed that no landslide-related research has ever been done on a regional scale in Xishuangbanna Prefecture, Yunnan Province, despite it is a slope instability-prone area, therefore, it is at stake and significant to assess the landslide susceptibility in Xishuangbanna on a regional scale. Moreover, it

is essential to select the appropriate techniques and methods to improve the accuracy and quality of prediction of future landslides.

The influential landslide conditioning factors (LCFs) in one place can be completely different from those in another. However, there is no standard method to determine the LCFs.

Innumerable landslide susceptibility assessment studies have been done by researchers. However, most of the GIS-based outcomes of these works have been archived and rarely have been well used for supporting decision-making processes in real situations.

1.3 Purposes of the Study

The major aims of the study are zoning the landslide-prone areas with the application of Geographic Information System (GIS), by adopting the frequency ratio (FR) method, in Xishuangbanna, Yunnan Province, China. Of which, there are four specific objectives as follows:

- To extract and analyze the possible landslide causative factors from previous studies then identify the effectively decisive factors that influence the occurrence of landslides within Xishuangbanna.
- To assess and map the landslide susceptibility spatial distribution using FR model in the study area.
- To develop a Web-based SDSS using the outcomes of the study to effectively support decision-making processes.

1.4 Expected Outcome

The expected outcomes of this study are:

- Get the reasonable and effective landslide conditioning factors (LCFs) for Xishuangbanna.
- Get the instructive landslide susceptibility map(s) that is poorly known in the previous studies for the study area.
- Get a Web-based SDSS platform adopting the derived landslide susceptibility map(s) and other outcomes of the study.

The final zonation map(s) of landslide susceptibility for Xishuangbanna will be classified into five-level landslide susceptibility classifications including a) very low, b) low, c) medium, d) high, and e) very high.

The proposed Web-based SDSS will allow decision-makers/users to identify the susceptibility level of a clicked location, as well as view and download the related outcomes of the study simply by using a web browser on any device, anytime and anywhere.

1.5 Significance of Study

Losses resulting from landslides can only be reduced in two ways: either by modifying the hazard itself or by reducing human vulnerability to it. Nevertheless, both approaches require the natural hazard to be zoned first (C. F. Chung & Y. Leclerc, 2003). The significance of this study mainly includes:

- Breaking through the zero-landslide prone zoning product situation for the study area, to provide an alternative aiding tool for decision-makers.
- Extracting the overall possibly reasonable landslide conditioning factors (LCFs) through a comprehensive literature review.
- Finding out the effective LCFs for the study area, by innovatively comparing the area under the curve (AUC) values of different scenarios that when the specific factors are adopted or not.
- Considering uniquely adopting the rubber plantation density (RPD) as an important LCF based on the local vegetation cover status of the study area.
- By developing the Web-based SDSS which is adopting the outcomes of the study, will increase the values of the LSM process, and facilitate the decision-making processes, which can also provide a new consideration for other researchers.

1.5.1 Innovation of the Study

The study reviewed 52 previous studies regarding the methodology, conditioning factor types, and numbers used in each study. The innovation points of the study can be described as follows:

- a) Conduct the first landslide-prone area assessment study and provide the first landslide susceptibility mapping production on a regional scale;

b) Many researchers claim that there is not a standard procedure to select the decisive landslide causative factors, it may differ among areas. The present study is the first to extract the factors used by researchers from a mass of previous studies, then get the 14 most frequently used factors by setting the utilization frequency threshold of 21% (11 times out of 52 studies), which shows the higher frequency than the rest (at most 3 times, most are only 1 time). Which provides a supporting ground for the selection of the effective landslide conditioning factors;

c) Normally, the AUC value is used for the validation of both the success rate (verify by using landslide inventory training dataset) and the prediction rate (verify by using landslide inventory verification dataset) as the last step of implementation of the study. In this study, we are the first to adopt this AUC method into the identification process of landslide conditioning factors, by comparing the model prediction quality of both when a specific factor is adopted and absent;

d) Come up with the idea of integrating the landslide susceptibility assessment outcomes with the Internet environment and SDSS, to support decision-making processes as well as provide an idea for researchers to make better use of the results of LSA.

1.5.2 Practical Application Value of the Study

a) As the first regional LSM production for the study area, it can be useful as an aiding tool for the decision-makers;

b) The statistics from the 52 previous studies in regard to the landslide conditioning factors used and utilization frequency can be used as a reference for other scholars in their future research;

c) The innovative use of the AUC method into the identification process of the landslide conditioning factors for a specific area also can provide a reference for other researchers;

d) It can provide a way to expand and make further use of the conventional LSA results.

1.6 Scope of Study

The scope of the study is presented as follows:

- **Area:** The study area is Xishuangbanna Prefecture, Yunnan Province, the People's Republic of China (PRC), lies at (21°0'-22°40'N, 99°55'-101°50'E), borders Myanmar to the southwest and Lao People's Democratic Republic (Lao PDR) to the south (Cao et al., 2017). The administrative region includes one county-level city (Jinghong) in the center and two counties (Menghai, Mengla) in the west and east respectively.

- **Method:** Determine the overall possible landslide causative factors from the literature review, then analyze them using substitution method with the aids of the AUC, finally filter out the unreasonable or unhelpful ones for improving the model quality. The landslide inventory is used to reveal the relationships between the spatial distribution of each landslide conditioning factor and historical landslides. The frequency ratio (FR) and the predictor rate (PR) model which is developed based on FR are selected to mapping the landslide susceptibility using landslide susceptibility index (LSI), with the aid of GIS tools, then assess the prediction quality of using the FR method in landslide susceptibility assessment (LSA) for Xishuangbanna. Eventually, making use of the final LCF group and the mapping results that derived from different LCF weight values, a Web-based SDSS for landslide platform will be developed.

- **Time range of data:**

Table 1 The Producing Time of the Data Used in the Study

No.	Data name	Producing time
1	Landslide inventory	1956 - 2019
2	Digital elevation model (DEM)	2000 - 2013
3	River network	2018
4	Road network	2020
5	Fault	2020
6	Precipitation	1901-2017
7	Landsat 8 OLI/TIRS Level-2 Data Products	2020

No.	Data name	Producing time
8	Land use and land cover (LULC)	2020
9	Lithology	2004
10	Soil	1990

1.7 Key Words

Landslide, Landslide Susceptibility Assessment, Frequency Ratio, Relative Frequency, Predictor Rate, Remote Sensing, Geographic Information System, SDSS, Web-based SDSS, Xishuangbanna.



CHAPTER II

LITERATURE REVIEW

2.1 Landslide

Landslide has been one of the most catastrophic natural hazards, posing a constant threat to human communities across the world. They are the 7th most common major hazard in terms of the devastation of property and human life, infrastructure, and landscapes (Abedini & Tulabi, 2018; Dao et al., 2020; Intarawichian & Dasananda, 2011; Shano et al., 2021). Even in many countries, landslides cause more economic damage and deaths than other natural disasters such as earthquakes, windstorms and floods, (Solaimani et al., 2012).

Landslide has the definition that it is the downhill movement of a large amount of material on a slope, according to engineering geology (Abedini & Tulabi, 2018). Landslides are the flow of rubble, rock, or soil mass down a slope, which is more prone to occur in mountainous places and endangers people's lives and property. Landslides happen on a lesser scale than other natural catastrophes, but they have a wider spread and are, in many situations, more destructive. Landslides are responsible for 17% of all the natural disaster deaths worldwide, according to the data obtained from the Centre for Research on the Epidemiology of Disasters (CRED), and some researchers believe this trend will continue due to rapid urbanization, deforestation, and extreme regional precipitation brought on by climate change. In addition, an earthquake, typhoon, or flood may also be the trigger of landslides. What's more, the damage extent resulting from landslides is also expected to rise in the coming decades (Nohani et al., 2019).

2.1.1 Landslides Formation Mechanism

Earth's life cycle process involves rocks being born, growing old, dying, and then re-emerging in the molten core of the planet. Landslide is a normal component of the process (El Jazouli et al., 2019). Landslides are defined as earthen materials sliding along a slope owing to gravity, and it is primarily a geological event

that happens when the material's force surpasses the soil's shear force resistance (Arabameri et al., 2020).

Various causal factors influence the occurrence of landslides. The stability of slopes is influenced by topography, rainfall, tectonics, lithology, vegetation, and also human activities, which all influence the susceptibility of a landscape to landslides (Dao et al., 2020; El Jazouli et al., 2019). Furthermore, landslides are occurring more frequently for three key reasons. First, natural resources overusing and vegetation damage have exacerbated surface soil instability. Second, land urbanization, particularly in mountainous areas, increases the number of people exposed to landslides. Third, there has been a rise in extreme precipitation in China, as well as an increase in the areas receiving abnormally intense precipitation (Lin & Wang, 2018). Additionally, areas with fine grit, moraines, or highly fractured and altered rocks such as clays, marls, gypsum, are particularly sensitive to landslides. (El Jazouli et al., 2019).

2.1.2 Negative Impacts of Landslides

Landslides devastate residential areas, highways, infrastructure, agricultural fields, gardens, grasslands, etc. (Abedini & Tulabi, 2018). According to CRED data, landslides are responsible for at least 17% of all deaths caused by natural disasters worldwide (Shahabi et al., 2014). Landslides kill over 1,000 people per year throughout the world, causing \$4 billion in property damage (Pradhan, 2010). Meanwhile, Landslides have environmental as well as socioeconomic costs affecting human populations. Landslides can destroy the forest, disturb wildlife habitat, remove productive soils, and disrupt road traffic. Landslides can also cause a tsunami, seiches, floods in some cases (Laila Fayeze et al., 2018).

2.2 Landslides in China

China has been one of the countries that has suffered many fatalities as a consequence of landslides. According to the China Institute of Geo-Environment Monitoring, more than 10,000 landslides occurred in China in 2014, 400 individuals were killed or missing and 218 were injured (<http://www.cigem.gov.cn>). According to the China Statistical Yearbook, 373,630 landslides occurred in China between 2000 and 2015, resulting in 10,996 deaths. The Sichuan Basin and its

surrounding mountains, The Yun Gui (Yunnan and Guizhou) Plateau, the Yangtze River middle reaches, the southeast hilly area, and the Loess Plateau are the most frequent site for deadly landslides in China. The northeast Changbai Mountain area, the western section of the Kunlun Mountains, and the northwest Tianshan region all experienced devastating landslides (Lin & Wang, 2018).

Five southeastern provinces including Guangdong, Hunan, Fujian, Zhejiang and Jiangxi, five southwestern provinces including Sichuan, Yunnan, Guangxi, Chongqing, and Guizhou, Hubei, Gansu, Shaanxi, and Shanxi, are among the 14 hotspot provinces of occurrence of fatal landslides, accounting for 86 percent of the total deadly landslides and resulting deaths and injuries. In particular, deadly landslides happened most frequently in Sichuan and Yunnan provinces, with 277 and 253 incidents, respectively, and caused a largest number of deaths with 82 and 67 deaths every year (Lin & Wang, 2018).

2.3 Landslides in Yunnan

One of the provinces that have been hit by landslides and debris flows is Yunnan, in the year 2013 alone, it has witnessed 425 geological hazards in Yunnan Province, which reported 69 casualties and caused about 0.52 billion yuan of direct economic losses. Among the geological hazards, there were 247 landslides and 68 debris flows (Yanhui Zhu et al., 2018).

2.4 Landslides in Xishuangbanna

Although no regional landslide susceptibility/hazard assessment research was found from the literature, in the last few decades, the massive population growth (grew by 13% from 2005 to 2020) (Statistics, 2020), rapid urbanization as well as dramatic land-use change (Cao et al., 2017) have expanded the landslide-prone regions of Xishuangbanna, putting people, property, and infrastructure at risk of landslides. As the farmers described: landslides during the rainy season take place much more frequently than in the past, water sources are polluted, and the water level is lower than past as well. They got water from the river near the village before but now they must construct a water pipe system to drainage water from high mountains (Groetz et al., 2010). Research also shows that the highest risk region of precipitation

in Yunnan, which is considered as an important LCF for landslides occurrence, is southwestern Yunnan, among which Xishuangbanna is one of the highest (Yanhui Zhu et al., 2018).

2.5 Landslide Susceptibility Concept

Various definitions were found in the literature review. As described in (Marsala et al., 2019), the concept of landslide susceptibility is a qualitative or quantitative assessment of the area (or volume), geographic distribution, and classification of landslides that occurred or might occur in a given location (Shahabi et al., 2014). Landslide susceptibility is the likelihood of future slope failure given a set of geo-environmental conditions, or it refers to the extent to which places can be influenced by future slope movement. It's a prediction of "where" landslides are most likely to occur (Shahabi et al., 2014; Shano et al., 2021). Wu et al. (2016) also state that landslide susceptibility is defined as the geographical probability of landslides occurring.

Researchers generally make four fundamental assumptions as follows for assessment and zonation of landslide hazards:

- a) Landslides will always happen under the same geological, geomorphological, hydrogeological, and climatic circumstances as before;
- b) There are identifiable physical factors that regulate the major conditions that induce land sliding;
- c) The hazard of a landslide can be assessed;
- d) All types of land sliding can be identified and classified (Aleotti & Chowdhury, 1999).

2.5.1 Landslide Susceptibility and Landslide Hazard

Different terminologies were found to be regularly used in past landslide research, such as landslide susceptibility, landslide hazard, landslide inventory, and landslide risk, each of these terms has its own, data types, applications, mapping scales, stages of studies, and purposes. Among these terms, landslide hazard and susceptibility study are the most perplexing. They have different definition, however, most researchers use them interchangeably rather than using them individually (Shano et al., 2021). The risk of potentially harmful phenomena

occurring during a particular timeframe and within a certain area is characterized as the landslide hazard (Kumar & Anbalagan, 2016), while several scholars claim susceptibility holds only for 'where' landslides may occur (Shano et al., 2021; Van Westen et al., 2003). The uncertainties and complexities of quantitatively determining the vulnerability of the elements at risk make it hard to achieve an accurate risk assessment. Therefore, rather than hazard, susceptibility is more frequently used for assessing the occurrence possibility of landslides in a particular area based on the local environmental conditions (Aleotti & Chowdhury, 1999). Thus, the concept of landslide susceptibility was selected to zoning the landslide-prone areas in the study.

2.5.2 Importance of Landslide Susceptibility Assessment (LSA)

The evaluation and identification of landslide-prone regions became a critical step in the spatial planning process since it allowed for the early implementation of preventative and corrective measures (Marsala et al., 2019). LSA is the first stage in assessing the hazard and risk of landslides, assessment of landslide hazards has become an essential research task not only for engineers but also for urban planners and government decision-makers, the final products are critical in environmental impact and land-use planning assessment, as well as in building early warning system. (Abbaszadeh Shahri et al., 2019; Intarawichian & Dasananda, 2011; Persichillo et al., 2016). For this, studies related to the determining of LCFs and the prediction of future landslide events through LSA approaches have become an important hotspot in the last decade (Mind'je et al., 2019), LSA is effective in preventing or reducing potential damages (Fang et al., 2020).

2.6 Landslide Susceptibility Mapping (LSM)

LSM is the zoning by assessing the occurrence probability of landslides in a certain area (Meena et al., 2019). LSM has been adopted in recent decades as the subject of research worldwide (Arabameri et al., 2020), it is commonly acknowledged that disaster prevention and mitigation measures cannot be effectively executed without the vital information provided by adequate landslide-related maps (Arabameri et al., 2020; Hervás & Bobrowsky, 2009; Marsala et al., 2019; Wu et al., 2016). LSMs may be used as strong instruments to predict the places where landslides are likely to occur, and so assist to make the best possible use of the land while preventing

landslides, particularly in mountainous places (Nohani et al., 2019; Zhang et al., 2016). The preparation of an LSM is an important stage in total landslide hazard management, and the fundamental motive behind is land conservation and management (Arabameri et al., 2020; Shahabi et al., 2014). However, the frequency or the time of occurrence of future landslides are not assessed in the LSM process (Persichillo et al., 2016).

2.7 Landslide Susceptibility Mapping (LSM) Approach

In general, the approaches for LSM can be categorized into quantitative or qualitative methods (Aleotti & Chowdhury, 1999; Hervás & Bobrowsky, 2009; Marsala et al., 2019; Milevski et al., 2019; Nohani et al., 2019; Shano et al., 2021; Wu et al., 2016). However, some scholars also propose that some of the qualitative techniques such as AHP, which also consider the ranking or weighting of factors, should be categorized as the third group, namely semi-quantitative methods (L. Fayez et al., 2018; Kumar & Anbalagan, 2016; Mind'je et al., 2019; Nohani et al., 2019; Zhang et al., 2016). Nevertheless, each approach has both advantages and disadvantages, an agreement that which method is the best does not exist (Wu et al., 2016; Zhang et al., 2016)

Despite the categories of the LSM approaches, all need the following procedures in implementation:

- 1) Mapping historical landslides in a given region;
 - 2) Identifying a group of geomorphological/geological factors that are thought to be associated with slope instability either directly or indirectly;
 - 3) Analyzing the relationship between these factors and slope instability;
- and
- 4) Dividing the study area into zones with different landslide susceptibility (Zhang et al., 2016).

2.7.1 Qualitative Approach

Qualitative methods (heuristic, landslide inventory, geomorphological approaches), are acknowledged as partially subjective, which is limited by unconsidered features or insufficient knowledge on which expert choices (the selection, weighting, and the combination function of the variables) are based, and

relatively low prediction accuracy (Hervás & Bobrowsky, 2009; Huang et al., 2018; Milevski et al., 2019; Mind'je et al., 2019; Wu et al., 2016; Zhang et al., 2016). In qualitative approaches, actual landslides are compared to geomorphology or geology features, and the input data is generally collected from field observations, potentially supplemented by aerial photo interpretation (Aleotti & Chowdhury, 1999). Though strongly dependent on the experience of surveyors, the advantage of the qualitative approach is its only practicability for all scale ranges of landslides (Shano et al., 2021).

2.7.2 Semiquantitative Approach

The advantage of semiquantitative approaches is they can partly reduce the subjectivity inherent to qualitative methods. For instance, by applying a semiquantitative model based on multi-criteria evaluation, whereby the assigned weighting can be re-evaluated to achieve a good consistency ratio (Hervás & Bobrowsky, 2009). Examples of semiquantitative models are fuzzy logic (FL) (Devkota et al., 2012), weighted linear combination (WLC) (Hung et al., 2015), AHP (El Jazouli et al., 2019; Intarawichian & Dasananda, 2010; Kumar & Anbalagan, 2016; Le et al., 2021; Milevski et al., 2019; Phrakonkham et al., 2020; Wicaksono et al., 2020; Yanhui Zhu et al., 2018; Zhang et al., 2016), etc. Semi-quantitative techniques, on the other hand, have the drawback of using subjective judgments and failing to quantify the weight of each LCF (Zhang et al., 2016).

2.7.3 Quantitative Approach

Quantitative approaches have the advantage of being less subjective than qualitative approaches but have high demands for quantity and quality of data (Zhang et al., 2016). Comparatively, quantitative methods are typically preferable and more commonly used for LSA because they produce more accurate results than qualitative methods (Abbaszadeh Shahri et al., 2019). Quantitative models can be divided into deterministic models and data-driven models (Marjanović et al., 2011). Due to the difficulty in obtaining comprehensive and sufficient soil mechanical and hydrological characteristics, the deterministic model is not suitable for large areas. Whereas the data-driven models are more effective and widely used in large areas. Data-driven models assume that the area under similar environmental conditions to previous events are more prone to landslides, and LCFs and landslides are uniformly

distributed in an area (Huang et al., 2018; Persichillo et al., 2016; Shano et al., 2021). In recent decades, many researchers have conducted LSA using statistical models combined with other data-driven approaches such as the frequency ratio (FR) model (L. Fayeze et al., 2018; Intarawichian & Dasananda, 2011; Khan et al., 2019; Mind'je et al., 2019; Zhang et al., 2020), support vector machines (SVM) (Marjanović et al., 2011), artificial neural network model (ANN) (Abbaszadeh Shahri et al., 2019; Dao et al., 2020; Valencia Ortiz & Martínez-Graña, 2018), statistical index (SI) (Milevski et al., 2019), logistics regression (LR) (Yalcin et al., 2011), etc. Out of all these data-driven methods, the FR method is widely used for LSA due to its good performance (Laila Fayeze et al., 2018). However, a quantitative model is superior only if validity and accuracy conditions are met (C.-J. F. Chung & Y. Leclerc, 2003).

2.8 Landslide Causative Factors

To develop a model for LSA, identifying the proper LCFs is crucial. LCFs have the characteristics of easy obtainability, representativeness, and practicality. However, factors that influence landslides in a specific region can be totally different from those in another. With the assumption that landslides are more likely to occur again under the same environmental conditions as the past events, the collecting of landslide inventory data and understanding of landslide formation mechanism are required to identify the relevant LCFs that may have relationship with landslide occurrence as well as the local surrounding environment such as topography, geomorphology, geotechnical properties, weather conditions, land cover and anthropogenic, etc. Furthermore, in some circumstances, factors such as heavy rainfall, seismic shaking, blasting, drilling, water level changes, storm waves, and so on can all play a crucial role in the landslide occurrence. As a result, assessing the influence of these LCFs on the geographical distribution of landslides is critical to comprehend their operational mechanism and subsequently develop a LSM (Anbalagan et al., 2015; Marsala et al., 2019; Mind'je et al., 2019; Nohani et al., 2019; Yanhui Zhu et al., 2018).

According to literature (52 previous studies that retrieved by using the keywords “landslide susceptibility”) (**Table 2**), over the past few decades, dozen types of LCFs have been studied and adopted by researchers in their previous LSA

studies, at least 5 (Hidayat et al., 2019; Sangeeta & Maheshwari, 2018; Srivastava et al., 2010; Yanhui Zhu et al., 2018) and at most 16 LCFs (Arabameri et al., 2020) are adopted according to each of the individual studies. Among the LCFs, some are widely accepted and frequently used in the literature, whereas others are used only by a few researchers. There are 14 of which the utilization frequency ranges from 21% to 100% (at least 11 and at most 52 times out of the 52 studies), which are Slope Angle (F1), Distance to River (F2), Slope Aspect (F3), Lithology (F4), Land Use and Land Cover (LULC) (F5), Distance to Fault (F6), Distance to Road (F7), Curvature (F8), Elevation (F9), Precipitation (F10), Normalized Difference Vegetation Index (NDVI) (F11), Soil Texture (F12), Topographic Wetness Index (TWI) (F13) and Stream Power Index (SPI) (F14). Other factors such as Slope Length (Pourghasemi et al., 2013; Pourghasemi et al., 2012), Profile Curvature (Huang et al., 2018; Javier & Kumar, 2019), Relative Relief (Anbalagan et al., 2015; Huang et al., 2018), Distance to Reservoir (Kumar & Anbalagan, 2016), Seismicity (Sangeeta & Maheshwari, 2018; Yalcin et al., 2011; Yanhui Zhu et al., 2018), Topographic Position Index (TPI) (Arabameri et al., 2020; Srivastava et al., 2010), Convergence Index (Arabameri et al., 2020), material depth (L. Fayez et al., 2018), Geomorphology (L. Fayez et al., 2018), Normalized Difference Build-Up Index (NDBI) (Huang et al., 2018), Sediment Transport Index (STI) (Devkota et al., 2012), Catchment Area (Persichillo et al., 2016), Catchment Slope (Persichillo et al., 2016), Terrain Ruggedness Index (TRI) (Persichillo et al., 2016), Building Density (Wicaksono et al., 2020), however, their utilization frequency are less than 7% (at most 3 times out of the 52 studies) and most of them are uniquely used only by one researcher, thus have been filtered to be shown in the table. There are no standard steps to determine the LCFs, for the current study, only the 14 most frequently adopted LCFs are considered based on their universality and data availability, in addition, a unique and innovative factor namely Rubber Plantation Density (RPD) is adopted based on the local vegetation feature, the rationality and applicability of all the 15 LCFs for the study area are to be discussed in the following section.

Table 2 Literature Review Statistic on Utilization of Landslide Conditioning Factors

Author (year)	Title	Methods	Factor														
			Number	1	2	3	4	5	6	7	8	9	10	11	12	13	14
Intarawichian and Dasananda (2011)	Frequency ratio model-based landslide susceptibility mapping in lower Mae Chaem watershed, Northern Thailand	FR	10	✓	✓	✓	✓	✓	✓	✓	✓	✓	✓	✓	✓	✓	✓
Yanhui Zhu et al. (2018)	Landslide and Debris Flow Hazard Risk Analysis and Assessment in Yunnan Province	AHP	5	✓			✓	✓									✓
Zhang et al. (2016)	Integration of the Statistical Index Method and the Analytic Hierarchy Process technique for the assessment of landslide susceptibility in Huizhou, China	SI, AHP	9	✓	✓	✓	✓	✓	✓	✓	✓	✓	✓	✓	✓	✓	✓
Milevski et al. (2019)	Statistical and expert-based landslide susceptibility modeling on a national scale applied to North Macedonia	SI, AHP	8	✓	✓	✓	✓	✓	✓	✓	✓	✓	✓	✓	✓		✓
Pourghasemi et al. (2013)	Landslide susceptibility mapping by binary logistic regression, analytical hierarchy process, and statistical index models and assessment of their performances	BLR, AHP, SI	12	✓	✓	✓	✓	✓	✓	✓	✓	✓	✓	✓	✓	✓	✓
Pourghasemi et al. (2012)	Application of fuzzy logic and analytical hierarchy process (AHP) to landslide susceptibility mapping at Haraz watershed, Iran	FL, AHP	11	✓	✓	✓	✓	✓	✓	✓	✓	✓	✓	✓	✓	✓	✓

Author (year)	Title	Methods	Factor															
			Number	1	2	3	4	5	6	7	8	9	10	11	12	13	14	
Arabameri et al. (2020)	Landslide Susceptibility Evaluation and Management Using Different Machine Learning Methods in The Gallicash River Watershed, Iran	ML	16	✓	✓		✓	✓	✓	✓	✓	✓	✓	✓	✓	✓	✓	✓
	Kumar and Anbalagan (2016)	Landslide susceptibility mapping using analytical hierarchy process (AHP) in Tehri reservoir rim region, Uttarakhand	AHP	12	✓	✓	✓	✓	✓	✓	✓	✓	✓	✓	✓	✓	✓	✓
Yalcin et al. (2011)	A GIS-based comparative study of frequency ratio, analytical hierarchy process, bivariate statistics and logistics regression methods for landslide susceptibility mapping in Trabzon, NE Turkey	FR, BS, LR	7	✓	✓	✓	✓	✓	✓	✓	✓	✓	✓	✓	✓	✓	✓	✓
Khan et al. (2019)	Landslide susceptibility assessment using Frequency Ratio, a case study of northern Pakistan	FR	7	✓	✓	✓	✓	✓	✓	✓	✓	✓	✓	✓	✓	✓	✓	✓
	Javier and Kumar (2019)	Frequency Ratio Landslide Susceptibility Estimation in a Tropical Mountain Region	FR	12	✓	✓	✓	✓	✓	✓	✓	✓	✓	✓	✓	✓	✓	✓
L. Fayez et al. (2018)	Application of frequency ratio model for the development of landslide susceptibility mapping at part of Uttarakhand State, India	FR	11	✓	✓	✓	✓	✓	✓	✓	✓	✓	✓	✓	✓	✓	✓	✓

Author (year)	Title	Methods	Factor														
			Number	1	2	3	4	5	6	7	8	9	10	11	12	13	14
Shano et al. (2021)	Landslide susceptibility mapping using frequency ratio model: the case of Gamo highland, South Ethiopia	FR	8	✓	✓	✓	✓	✓	✓	✓	✓	✓	✓	✓	✓	✓	✓
Hidayat et al. (2019)	Analysis of Landslide Susceptibility Zone using Frequency Ratio and Logistic Regression Method in Hambalang, Citeureup District, Bogor Regency, West Java Province	FR	5	✓	✓	✓	✓	✓	✓	✓	✓	✓	✓	✓	✓	✓	✓
Anbalagan et al. (2015)	Landslide hazard zonation mapping using frequency ratio and fuzzy logic approach, a case study of Lachung Valley, Sikkim	FR, FL	8	✓	✓	✓	✓	✓	✓	✓	✓	✓	✓	✓	✓	✓	✓
Vakhshoori and Zare (2016)	Landslide susceptibility mapping by comparing weight of evidence, fuzzy logic, and frequency ratio methods	WOE, FL, FR	10	✓	✓	✓	✓	✓	✓	✓	✓	✓	✓	✓	✓	✓	✓
Huang et al. (2018)	Landslide susceptibility assessment in the Nantian area of China: a comparison of frequency ratio model and support vector machine	FR, SVM	10	✓	✓	✓	✓	✓	✓	✓	✓	✓	✓	✓	✓	✓	✓
Pradhan (2010)	Landslide Susceptibility mapping of a catchment area using frequency ratio, fuzzy logic and multivariate logistic regression approaches	FL, FR, MLR	10	✓	✓	✓	✓	✓	✓	✓	✓	✓	✓	✓	✓	✓	✓

Author (year)	Title	Methods	Factor														
			Number	1	2	3	4	5	6	7	8	9	10	11	12	13	14
Lee and Pradhan (2006)	Landslide hazard mapping at Selangor, Malaysia using frequency ratio and logistic regression models	FR and LR	10	✓	✓	✓	✓	✓	✓	✓	✓	✓	✓	✓	✓	✓	✓
Lee and Sambath (2006)	Landslide susceptibility mapping in the Damrei Romel area, Cambodia using frequency ratio and logistic regression models	FR and LR	7	✓	✓	✓	✓	✓	✓	✓	✓	✓	✓	✓	✓	✓	✓
Poudyal et al. (2010)	Landslide susceptibility maps comparing frequency ratio and artificial neural networks: a case study from the Nepal Himalaya	FR, ANN	10	✓	✓	✓	✓	✓	✓	✓	✓	✓	✓	✓	✓	✓	✓
Youssef et al. (2014)	Landslide susceptibility mapping at Al-Hasher area, Jizan (Saudi Arabia) using GIS-based frequency ratio and index of entropy models	FR and IoE	10	✓	✓	✓	✓	✓	✓	✓	✓	✓	✓	✓	✓	✓	✓
Rasyid et al. (2016)	Performance of frequency ratio and logistic regression model in creating GIS based landslides susceptibility map at Lompobattang Mountain, Indonesia	FR and LR	8	✓	✓	✓	✓	✓	✓	✓	✓	✓	✓	✓	✓	✓	✓
Solaimani et al. (2012)	Landslide susceptibility mapping based on frequency ratio and logistic regression models	FR and LR	9	✓	✓	✓	✓	✓	✓	✓	✓	✓	✓	✓	✓	✓	✓

Author (year)	Title	Methods	Factor														
			Number	1	2	3	4	5	6	7	8	9	10	11	12	13	14
Shahabi et al. (2014)	Landslide susceptibility mapping at central Zab basin, Iran: A comparison between analytical hierarchy process, frequency ratio and logistic regression models	AHP, FR and LR	8	✓	✓	✓	✓	✓	✓	✓	✓	✓	✓	✓	✓	✓	✓
Marsala et al. (2019)	Landslide Susceptibility Assessment of Mauritius Island (Indian Ocean)	Photogeology, GFM	7	✓	✓	✓	✓	✓	✓	✓	✓	✓	✓	✓	✓	✓	✓
Dao et al. (2020)	A spatially explicit deep learning neural network model for the prediction of landslide susceptibility	ANN	7	✓	✓	✓	✓	✓	✓	✓	✓	✓	✓	✓	✓	✓	✓
Abbaszadeh Shahri et al. (2019)	Landslide susceptibility hazard map in southwest Sweden using artificial neural network	ANN	7	✓	✓	✓	✓	✓	✓	✓	✓	✓	✓	✓	✓	✓	✓
Nohani et al. (2019)	Landslide Susceptibility Mapping Using Different GIS-Based Bivariate Models	FR, SE, WoE, EBF	10	✓	✓	✓	✓	✓	✓	✓	✓	✓	✓	✓	✓	✓	✓
Wu et al. (2016)	Landslide susceptibility assessment using frequency ratio, statistical index and certainty factor models for the Gangu County, China	FR, SI, CF	11	✓	✓	✓	✓	✓	✓	✓	✓	✓	✓	✓	✓	✓	✓

Author (year)	Title	Methods	Factor															
			1	2	3	4	5	6	7	8	9	10	11	12	13	14		
Devkota et al. (2012)	Landslide susceptibility mapping using certainty factor, index of entropy and logistic regression models in GIS and their comparison at Mugling–Narayanghat road section in Nepal Himalaya	CF, IoE, LR	✓	✓	✓	✓	✓	✓	✓	✓	✓	✓	✓	✓	✓	✓	✓	✓
Persichillo et al. (2016)	Shallow landslides susceptibility assessment in different environments	GAM	✓	✓	✓	✓	✓	✓	✓	✓	✓	✓	✓	✓	✓	✓	✓	✓
Srivastava et al. (2010)	Fuzzy gamma based geomatic modelling for landslide hazard susceptibility in a part of Tons River valley, northwest Himalaya, India	FGBG	✓	✓	✓	✓	✓	✓	✓	✓	✓	✓	✓	✓	✓	✓	✓	✓
Abedini and Tulabi (2018)	Assessing LNRF, FR, and AHP models in landslide susceptibility mapping index: a comparative study of Nojjan watershed in Lorestan province, Iran	LNRF, FR, AHP	✓	✓	✓	✓	✓	✓	✓	✓	✓	✓	✓	✓	✓	✓	✓	✓
Meena et al. (2019)	A Comparative Study of Statistics-Based Landslide Susceptibility Models: A Case Study of the Region Affected by the Gorkha Earthquake in Nepal	AHP, FR, HSMCE	✓	✓	✓	✓	✓	✓	✓	✓	✓	✓	✓	✓	✓	✓	✓	✓
Wicaksono et al. (2020)	Landslide susceptibility map of Bogor Area using analytical hierarchy process	AHP	✓	✓	✓	✓	✓	✓	✓	✓	✓	✓	✓	✓	✓	✓	✓	✓

Author (year)	Title	Methods	Factor														
			Number	1	2	3	4	5	6	7	8	9	10	11	12	13	14
Mondal and Maiti (2014)	Integrating the Analytical Hierarchy Process (AHP) and the frequency ratio (FR) model in landslide susceptibility mapping of Shiv-khola watershed, Darjeeling Himalaya	AHP, FR, WLC	9	✓	✓	✓	✓	✓	✓	✓	✓	✓	✓	✓	✓	✓	✓
Poudyal et al. (2010)	Landslide susceptibility maps comparing frequency ratio and artificial neural networks: a case study from the Nepal Himalaya	FR, ANN	9	✓	✓	✓	✓	✓	✓	✓	✓	✓	✓	✓	✓	✓	✓
Lee and Pradhan (2006)	Landslide hazard mapping at Selangor, Malaysia using frequency ratio and logistic regression models	FR and LR	7	✓	✓	✓	✓	✓	✓	✓	✓	✓	✓	✓	✓	✓	✓
Zhang et al. (2020)	Optimizing the frequency ratio method for landslide susceptibility assessment: A case study of the Caiyuan Basin in the southeast mountainous area of China	FR	6	✓	✓	✓	✓	✓	✓	✓	✓	✓	✓	✓	✓	✓	✓
Sur et al. (2020)	Landslide susceptibility assessment in a lesser Himalayan Road corridor (India) applying fuzzy AHP technique and earth-observation data	Fuzzy AHP	12	✓	✓	✓	✓	✓	✓	✓	✓	✓	✓	✓	✓	✓	✓
Valencia Ortiz and Martínez-Graña (2018)	A neural network model applied to landslide susceptibility analysis (Capitanejo, Colombia)	Neural Network	8	✓	✓	✓	✓	✓	✓	✓	✓	✓	✓	✓	✓	✓	✓

Author (year)	Title	Methods	Factor															
			1	2	3	4	5	6	7	8	9	10	11	12	13	14		
Mind'je et al. (2019)	Landslide susceptibility and influencing factors analysis in Rwanda	FR	✓	✓	✓	✓	✓	✓	✓	✓	✓	✓	✓	✓	✓	✓	✓	✓
Le et al. (2021)	Developing a Landslide Susceptibility Map Using the Analytic Hierarchical Process in Ta Van and Hau Thao Communes, Sapa, Vietnam	AHP	✓	✓	✓	✓	✓	✓	✓	✓	✓	✓	✓	✓	✓	✓	✓	✓
Intarawichian and Dasananda (2010)	Analytical hierarchy process for landslide susceptibility mapping in lower mae chaem watershed, northern Thailand	AHP	✓	✓	✓	✓	✓	✓	✓	✓	✓	✓	✓	✓	✓	✓	✓	✓
El Jazouli et al. (2019)	GIS-multicriteria evaluation using AHP for landslide susceptibility mapping in Oum Er Rbia high basin (Morocco)	AHP	✓	✓	✓	✓	✓	✓	✓	✓	✓	✓	✓	✓	✓	✓	✓	✓
Yalcin et al. (2011)	A GIS-based comparative study of frequency ratio, analytical hierarchy process, bivariate statistics and logistics regression methods for landslide susceptibility mapping in Trabzon, NE Turkey	FR, AHP, BS, LR	✓	✓	✓	✓	✓	✓	✓	✓	✓	✓	✓	✓	✓	✓	✓	✓
Acharya and Lee (2018)	Landslide Susceptibility Mapping using Relative Frequency and Predictor Rate along Araniko Highway	RF and PR	✓	✓	✓	✓	✓	✓	✓	✓	✓	✓	✓	✓	✓	✓	✓	✓

Author (year)	Title	Methods	Factor														
			Number	1	2	3	4	5	6	7	8	9	10	11	12	13	14
Muavhi et al. (2021)	Mapping groundwater potential zones using relative frequency ratio, analytic hierarchy process and their hybrid models: case of Nzhelele-Makhado area in South Africa	RF, PR, AHP	7	✓	✓	✓	✓	✓	✓	✓	✓	✓	✓	✓	✓	✓	✓
Tan et al. (2020)	GIS-based flood hazard mapping using relative frequency ratio method: A case study of Panjkora River Basin, eastern Hindu Kush, Pakistan	RF and PR	6	✓	✓		✓	✓									✓
Sangeeta and Maheshwari (2018)	Earthquake-Induced Landslide Hazard Assessment of Chamoli District, Uttarakhand Using Relative Frequency Ratio Method	RF and PR	5	✓		✓											✓
Ahmed and Dewan (2017)	Application of Bivariate and Multivariate Statistical Techniques in Landslide Susceptibility Modeling in Chittagong City Corporation, Bangladesh	WoE and MR	8	✓	✓	✓	✓	✓	✓	✓	✓	✓	✓	✓	✓	✓	✓
Utilization Times				52	46	45	44	43	37	32	31	26	25	19	15	13	11
Utilization Frequency (%)				100	88	87	85	83	71	62	60	50	48	37	29	25	21

2.8.1 Slope Angle

Slope angle is a LCF which is related to landslides directly and is commonly used in constructing LSMs (Marsala et al., 2019; Wu et al., 2016). The interaction of slope angle with material characteristics including permeability, friction angle, and cohesion is slope stability/instability (Youssef et al., 2014). The slope gradient also directly influences soil moisture, soil formation, and erosion potential. If the materials are soil or weak rocks, it is thought that a larger slope angle correlates to increased shear stress and a higher failure likelihood (Shano et al., 2021). In theory, as the slope rises, shear stress increases, making the structure more prone to failure (Nohani et al., 2019; Sur et al., 2020), nevertheless, in almost vertical conditions, landslides are scarce or absent (Abbaszadeh Shahri et al., 2019).

2.8.2 Distance to Rivers

Water is one of the most important components in the triggering of landslides; it may exacerbate the occurrence of landslides by eroding slopes or soaking the toe material unit, resulting in a rise in water level. Areas with a shorter distance to rivers have comparatively more likelihood of landslide initiation than areas located far-off (El Jazouli et al., 2019; Nohani et al., 2019; Sur et al., 2020; Wu et al., 2016; Youssef et al., 2014).

2.8.3 Slope Aspect

The azimuthal orientation of the slope face is indicated by the term Aspect (0 to 360°). The link between slope aspect and landslides occurrence has been analyzed for long, but no consensus has been found on how they are related (Youssef et al., 2014), however, it has been accepted as a possible conditioning factor (Abbaszadeh Shahri et al., 2019). The meteorological phenomena such as rainfall direction, sunshine amount, drying winds, as well as hydrological processes such as evapotranspiration and then, influences soil thickness and moisture and vegetation coverage are all related to slope aspect which can instigate landslides, so it has an important role in conditioning landslide occurrence (Abedini & Tulabi, 2018; Dao et al., 2020; Marsala et al., 2019; Nohani et al., 2019; Shano et al., 2021; Sur et al., 2020; Youssef et al., 2014).

2.8.4 Lithology

Lithology is also frequently used in LSA studies. Different lithological units have various compositions, permeability, and structures, which affect the slope material strength. According to the literature, landslides frequently take place in the presence of a rock stratum with low shear strength and permeability, in other words, stronger rocks can resist dragging forces better than weaker rocks, and have less risk of landslide occurrence, and vice versa (Abedini & Tulabi, 2018; Le et al., 2021; Marsala et al., 2019; Nohani et al., 2019; Sur et al., 2020; Wu et al., 2016).

2.8.5 Land Use and Land Cover (LULC)

LULC represents both natural processes and human-induced activities that promote slope instability, either directly or indirectly. The conversion of agricultural and forest land to residential areas, forest to agriculture, and the reduction of the unethical or involuntary slope for infrastructure building are all examples of land-use change. Landslides are less common in forested areas than in barren areas, and vegetated land with a robust root system can stabilize slopes through mechanical and hydrological processes. However, landslides may occur in vegetation ground cover with strong and large root systems as well (El Jazouli et al., 2019; Le et al., 2021; Nohani et al., 2019; Sur et al., 2020).

2.8.6 Distance to Faults

Lineament factors such as faults, folds, shear zoned have a direct influence on the distribution of landslides, which mainly affect co-seismic landslides by cracking stones and creating instability, a distance close to the geological faults often leads to high landslide susceptibility (Abedini & Tulabi, 2018; El Jazouli et al., 2019; Le et al., 2021; Nohani et al., 2019; Shano et al., 2021; Wu et al., 2016; Youssef et al., 2014).

2.8.7 Distance to Roads

The distance to roads is a major anthropogenic parameter affecting landslide occurrence. Utilizing additional hydrologic load change, slope excavation, and deforestation, the building of communication networks including roads and railways, often leads to the destabilization of slopes and changes the natural equilibrium condition of soil and rock in hilly terrain. The lack of toe support can be caused by roads built on slopes, the loss of support leads to increase the strain behind

the slope and facilitate developing tension cracks. Furthermore, the closer the locations are to the road system, the greater the risk of landslides (Le et al., 2021; Nohani et al., 2019; Sur et al., 2020; Wu et al., 2016; Youssef et al., 2014).

2.8.8 Curvature

Curvature is defined as the rate at which the slope gradient or slope aspect changes, generally in one direction. Positive curvature value reveals convexity and negative value characterize slope concavity. In other words, the positive value represents for ridges and negative one defines valleys, while values around zero indicate flat surfaces. curvature affects erosion and groundwater accumulation, as well as gravitational stresses and surface run-off on shallow failure surfaces, thus it has a dominant influence on slope instability (Abbaszadeh Shahri et al., 2019; Marsala et al., 2019; Shano et al., 2021; Youssef et al., 2014).

2.8.9 Elevation

The elevation is frequently used as a LCF for LSA. It does not directly affect landslide activity, but its indirect influences are various (Le et al., 2021; Wu et al., 2016). For example, some researchers believe that elevation may be correlated to fluctuations of rainfall and the distribution of vegetation types (Shano et al., 2021; Sur et al., 2020). Others argue that changing altitude has a significant impact on soil erosion and slope mass movement, allowing for more precise control of runoff direction and drainage efficiency (Abedini & Tulabi, 2018). All these geomorphological, tectonic, and biological processes, as well as anthropogenic activities, can cause slope instability and contribute to spatial landscape variability (Abbaszadeh Shahri et al., 2019; Nohani et al., 2019; Sur et al., 2020). Therefore, elevation can be considered an important LCF.

2.8.10 Precipitation

According to statistics, over 90% of the landslides and debris flow were triggered by high-intensity rainfall, thus it is a significant landslide initiation factor (Marsala et al., 2019; Wu et al., 2016; Yanhui Zhu et al., 2018). Slope stability is affected by rainfall due to surface overflow and pore water pressure on the unstable slope. Its quantity, intensity, magnitude and return period are important parameters to landslide possibility and destructiveness, thus has been adopted by researchers in big

or small study areas, either through historical studies or through physical models (Le et al., 2021; Sur et al., 2020; Van Westen et al., 2003).

2.8.11 Normalized Difference Vegetation Index (NDVI)

The normalized difference vegetation index (NDVI) is a quantitative measure of vegetation growth and biomass based on surface reflectance. NDVI value is calculated using the formula $NDVI = (IR - R)/(IR + R)$, where, the IR and R bands are the infrared and red bands of the electromagnetic spectrum of satellite photographs, of which values near to -1 represents that the bare earth surface short of vegetation, while a value near to +1 represents a higher and healthier vegetation cover. The vegetation roots contribute to stabilizing the hill slope and reducing landslides occurrence. As the bases of deep tree roots do not change along with seasons, the analysis of temporal NDVI is needless, concerning temporal changes in vegetation such as recent deforestation is beyond the scope of this study (Abbaszadeh Shahri et al., 2019; Nohani et al., 2019; Sur et al., 2020; Wu et al., 2016; Youssef et al., 2014).

2.8.12 Soil Texture

Soil type and its corresponding thickness are widely used as a LCF in LSA, since it is mostly exposed to weathering, which may influence land permeability and other geotechnical parameters. For example, soil characteristics such as clay content, texture, organic matter content, structure, and permeability in the mountainous areas can be the potential slip factors that lead to slope failure resulting in landslides (Abbaszadeh Shahri et al., 2019; Marsala et al., 2019; Sur et al., 2020).

2.8.13 Topographic Wetness Index (TWI)

The topographic wetness index (TWI) is an important factor obtained from the digital elevation model (DEM) that depicts geotechnical wetness and is a steady-state wetness index represents topography influence. When a large catchment area is coupled with a low slope gradient, TWI affects soil moisture and soil depth, as well as groundwater conditions (Devkota et al., 2012; Fang et al., 2020; Kumar & Anbalagan, 2016; Poudyal et al., 2010; Pourghasemi et al., 2012; Sur et al., 2020; Wicaksono et al., 2020).

2.8.14 Stream Power Index (SPI)

The stream power index (SPI) measures how corrosive a terrain's streams are. The slope gradient and the streams' erosive power reveal a positive correlation. SPI has been adopted by many researchers in LSA (Devkota et al., 2012; Fang et al., 2020; Kumar & Anbalagan, 2016; Poudyal et al., 2010; Pourghasemi et al., 2012; Sur et al., 2020; Wicaksono et al., 2020).

2.8.15 Rubber Plantation Density (RPD)

According to literature, Xishuangbanna has the highest rubber plantations density among China and South Asia (as is shown in **Figure 6**) (Zhu et al., 2014), the area of monoculture rubber plantations has increased by more than 12 times from 1976 to 2015 and accounts for 22% of the total land cover in 2010 in Xishuangbanna, which has led to prominent degradation of the local ecology (Cao et al., 2017; Hemati et al., 2020; Min et al., 2019; Zhang et al., 2019). Thus, it is quite reasonable and in timely demand to take the RPD into account in LSA in the study area.

2.9 Geographic Information System (GIS) and Remote Sensing (RS) in Landslide Susceptibility Assessment (LSA)

Over the past two decades, in India, Japan, Vietnam, Malaysia, Thailand, Iran, Turkey, Romania, China, Nepal, and many other parts of the world, almost all methods are used to assess the landslide susceptibility and predict landslides spatial distributions, are based on GIS concepts. It's a simple and effective spatial data collection, management, and manipulation tool (Abbaszadeh Shahri et al., 2019; Dao et al., 2020; Poudyal et al., 2010; Zhang et al., 2020). Moreover, by combining remotely sensed (RS) data with GIS, studies using various methods and approaches have been made easier by expanding the ability to handle and analyze landslide data for large areas, and refining LSA in the future (Marsala et al., 2019; Mind'je et al., 2019).

The GIS environment, in particular, is commonly employed in models for producing single factor layers, computing different LCFs, assigning weights, data integration, and generating LSMs (Marsala et al., 2019). The realization of the LSA objectives has been greatly enhanced by the introduction of the GIS technique.

When constructing a GIS database in LSA, two basic requirements must be followed:

- a) The data must be homogeneous, with the same work-scale and geographic projection system;
- b) The database must be organized into basic single thematic layers, each containing homogeneous data (Aleotti & Chowdhury, 1999).

2.10 Frequency Ratio (FR) Model

The Frequency Ratio (FR) model is based on the geographical distribution of landslides in respect to each LCF, which is particularly applicable for larger areas and notably performs better accuracy than other methods in mapping landslide susceptibility classifications in every single layer. Additionally, it has the advantage of simplicity and understandability, it is not necessary to select model parameters and to determine the reasonable non-landslides area for FR. The FR model not only generates LSMs but also takes into account the sensitivity of landslide failure to certain landslide-related factors. Even though numerous complex machine learning (ML) approaches have been proposed, this method is still frequently utilized by researchers and practitioners. Furthermore, the principles' simplicity and ease of implementation in a GIS environment make it an approach for LSM that is both user-friendly and effective, thus is considered as one of the most widely used approaches for preparing LSMs (Milevski et al., 2019; Shano et al., 2021; Zhang et al., 2020). The FR is the proportion of landslides in a certain factor's classification as a percentage of all landslides, and the area of that classification as a percentage of the overall research region (Shahabi et al., 2014). The FR approach, a variation of the probabilistic technique, is based on observable links between the distribution of historical landslide sites and each of the landslide conditioning factors and is used to uncover the association between them (Nohani et al., 2019; Wu et al., 2016).

According to the basis of the FR method, the single LCF layer is to be overlapped with the past landslide event points layer, then two attributes of each factor need to be considered, namely the quantity of area in the zone (classification of each factor) and the number of landslides in the same zone, of which, for some researchers, the area of landslides has been adopted as the representation of the

number of landslides in the zone, however, some others have adopted the number of landslide points in the zone instead based on the actual data availability (Hidayat et al., 2019; Sangeeta & Maheshwari, 2018), the theory of the latter is based on **Equation 1**.

$$\begin{aligned}
 FR_i &= \frac{\text{The number of landslide points frequency in class } i}{\text{The area frequency of class } i} \\
 &= \\
 &= \frac{\text{Number of landslide points in class } i / \text{Total number of landslide points}}{\text{Area of class } i / \text{Total area}} \\
 &= \frac{L(i) / \sum_i^n L(i)}{S(i) / \sum_i^n S(i)} \tag{1}
 \end{aligned}$$

Where, FR_i is the frequency ratio value of class i of a selected factor.

In the relationship analysis, a FR value of 1 is an average value, if a FR value is equal to 1 means that the classification has a landslides density proportionally to the size of the classification in the map, while if the value greater than 1 means a higher correlation, a FR value of less than 1 means a lower correlation area vice versa, normally, the original FR values are decimals.

To meet the input principle of the new value data type of the raster reclassify function (**Figure 1**) of ArcGIS that “The newValue must be an integer” (Esri, 2016), all the original FR values have the need of being converted to integers.

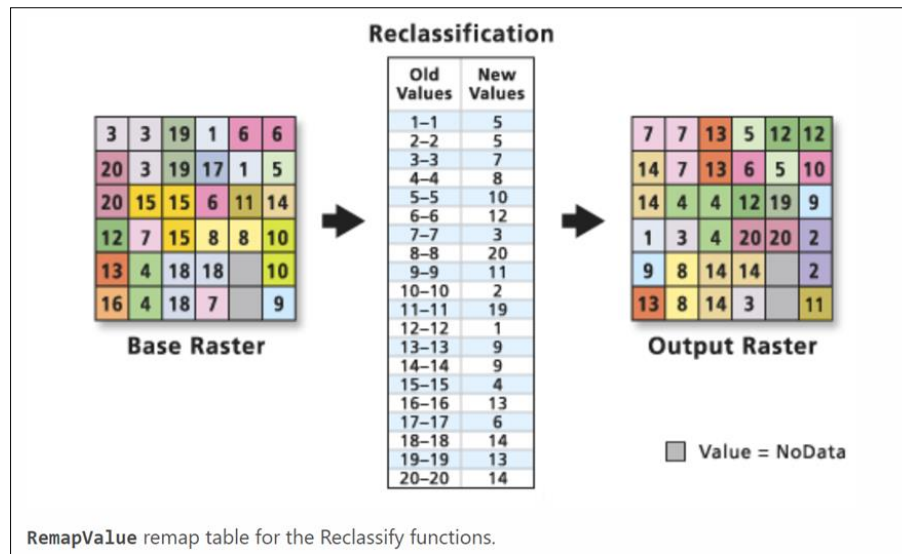


Figure 1 The Illustration of Reclassify Function of ArcGIS

Source: ESRI, 2022

2.11 Relative Frequency (RF) and Predictor Rate (PR)

Some researchers (Acharya & Lee, 2018; Rabby & Li, 2020; Sangeeta & Maheshwari, 2018), adopted the conversion method of normalizing the FR value into a range of probability values [0,1] using the equation of $\frac{FR}{\sum FR}$ to get the relative frequency (RF) value for each classification of every factor, then convert the RF values into integers by multiplying by 100 using **Equation 2**.

$$RF = Round \left(\frac{FR}{\sum FR} * 100 \right) \quad (2)$$

where, RF is the normalized relative frequency value of each class of every factor. After normalization, however, the RF value still has the drawback of considering all LCFs as equally important and having an equal weight value of 1, which is unrealistic in the real situation (Acharya & Lee, 2018; Tan et al., 2020).

Finally, the weight value for each factor namely predictor rate (PR) is derived from **Equation 3**.

$$PR = \frac{(RF_{max} - RF_{min})}{(RF_{max} - RF_{min})_{min}} \quad (3)$$

Where, PR is the predictor rate (weight) value of each factor, RF_{max} and RF_{min} are the maximum and minimum RF of each selected factor, respectively. $(RF_{max} - RF_{min})_{min}$ is the minimum $(RF_{max} - RF_{min})$ value of all factors.

2.12 Landslide Susceptibility Index (LSI)

To generate the final LSM for the area, the landslide susceptibility index (LSI) needs to be defined, it is calculated using **Equation 4**.

$$LSI = \sum(RF * PR) \quad (4)$$

The higher the LSI value, the more susceptible the area is to landslides. The lower the LSI value, on the other hand, the lower the susceptibility to landslides.

2.13 Receiver Operating Characteristic (ROC) Curve and Area Under the Curve (AUC)

A LSM is superior only after the result is validated to check how well the model predicts the landslides in the study area (Mind'je et al., 2019). According to previous research, most of the validation work has been done by assessing AUC value of the ROC method (Intarawichian & Dasananda, 2011; Le et al., 2021; Pourghasemi et al., 2013; Wu et al., 2016; Youssef et al., 2014; Zhang et al., 2016). The ROC curve may be used to assess the quality of both probabilistic and deterministic detection systems, as well as forecasting systems (Youssef et al., 2014). Therefore, the final landslide susceptibility productions of the study are to be validated using the AUC. The software package Arc-SDM (Brown et al., 2017), which, as the name suggests, is a free of charge extension of ESRI's ArcGIS is adopted to generate the AUC.

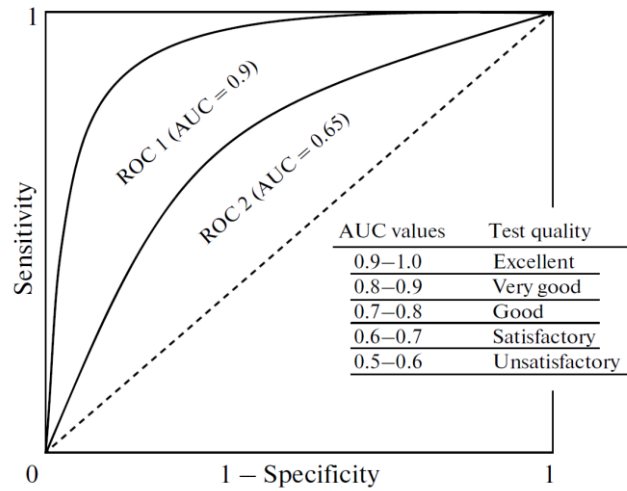


Figure 2 An Example of ROC Curves with Good (AUC = 0.9) and Satisfactory (AUC = 0.65) Results of Specificity and Sensitivity

Source: Trifonova et al., 2014

The AUC is based on a graph of 'sensitivity' and '1-specificity,' which is calculated for a variety of thresholds. In the AUC method, the number of pixels correctly predicted by the model is displayed versus the number of pixels incorrectly predicted (Mind'je et al., 2019). The model's sensitivity (the fraction of existing landslide pixels accurately predicted by the model) is displayed versus 1-specificity (the percentage of predicted landslide pixels over the total study area) in the ROC curve. The AUC evaluates a probabilistic model's ability to reliably predict the existence or absence of landslides (Youssef et al., 2014). In generally, the higher the AUC value, the better the model (Le et al., 2021; Wu et al., 2016). The AUC value of 1 represents a perfect prediction. However, in the real situation, as is shown in **Figure 2**. The quantitative-qualitative relationship between AUC and prediction accuracy is classified as follows: 0.9-1 means excellent; 0.8-0.9 means very good; 0.7–0.8 means good; 0.6–0.7 means average; and 0.5–0.6 means poor (Pourghasemi et al., 2013). In other words, the better the prediction, the steeper the slope of the curve. An AUC of

0.9, for example, suggests a very good model in which 90% of the landslides fall in the 10% zone with the highest susceptibility (Zhang et al., 2016).

2.14 Decision Support System

According to Mohd et al. (2014), a DSS is a collection of tools and procedures that work together to manage a system. Making judgments in a dynamic and rapidly changing world is difficult because many factors are involved, including the decision-maker, conflicts of interest, the importance of the decision, and the various criteria involved in the problem. In the face of a complex, uncertain, and contradicting situations, DSSs have been widely used (de Lima et al., 2019).

Decision support can be defined as the aid for, substantiation, and confirmation of an act or result of deciding. The following requirements should be met by DSSs:

- Proposed to solve problems with a semi-structured framework;
- Analytical models can be combined with traditional data and retrieval functions;
- Easy to use and accessible for decision-makers with not much computer experience
- Flexible and adaptive to various decision-making approaches (Yatsalo & Sullivan, 2012).

The typical framework of a DSS is characterized by including:

- Capabilities in analytical modeling;
- Systems for database management;
- Display of graphical contents;
- Tools for reporting;
- Knowledge of decision-makers (Oliveira et al., 2012).

2.15 Spatial Decision Support System

Similar to DSS, SDSS is intended to solve semi-structured spatial problems, it was evolved from the DSS by including the geospatial content. SDSSs also provide functions and tools for spatial/geographic data processing and analysis, in addition to

the aforementioned features of DSSs. As a result, SDSS aids decision-making in terms of spatial alternatives analysis by merging GIS functionalities with DSS tools for stakeholders (Yatsalo & Sullivan, 2012). In some cases, the data are stored in the form of tables in a database, of which, their links with locations cannot be visualized. GIS allows people to visualize spatial data by linking attribute information from tables to a geographic location (Sreekanth et al., 2021). SDSSs are typically designed to give a decision-making environment that allows for the flexible analysis of both geographical and attribute components (Mansourian et al., 2011). The SDSS aided in decision making and is helpful in planning, monitoring, evaluating the delivery, evacuation, and coverage of interventions, site selection, and accountability that have a strong geographical component (Wangdi et al., 2016). SDSSs have been used in a variety of fields, including flood risk management, earthquake disasters, infrastructure investment, and public education (de Lima et al., 2019). SDSSs can be used in disaster response to identify the best places for rescue crews, plan evacuation routes, and assign evacuees to shelters (Nyimbili & Erden, 2017).

A SDSS combines GIS capabilities including geographical data management and cartographic display with analytical modeling, a customizable user interface, and complicated spatial data structures. A SDSS is a framework for integrating:

- Spatial and analytical modeling ability;
- Handling of spatial and non-spatial data;
- Domain expertise;
- Capabilities of spatial display;
- Capabilities for reporting (Sugumaran & Sugumaran, 2007).

2.16 Web-based Spatial Decision Support System

Web-based SDSS has been suggested as a useful tool for participatory/collaborative/group spatial planning and decision-making (Jelokhani-Niaraki, 2018). As a result of the collaborative nature of many decision-making problems, a participatory decision-making process is becoming increasingly important for resolving conflicts and reducing uncertainty in spatial planning and decision-making by facilitating information/knowledge exchange as well as software and model sharing. The Internet can be considered a preferred medium for communication

between the public and urban planners when large numbers of citizens and a diverse range of stakeholders are required for decision-making (Mansourian et al., 2011). The challenge of exchanging spatial data in real-time has a new dimension with the recent adoption of web services for various GIS applications (Sreekanth et al., 2021). Web technologies open up new options for using SDSS in a participatory environment, allowing the traditional SDSS to shift from a closed, place-based (time and location fixed), and synchronous process to an open, asynchronous, dispersed, and active process (Jelokhani-Niaraki, 2018). What the users need to access to a WebSDSS is only a web browser that is installed originally on any PCs or mobile devices (e.g., PDA, smart phones). This revolution leads to a shift in decision-making from individual data browsing, analysis, and management to collective participation and communication on scientific and social decision-making issues (Mohd et al., 2014).

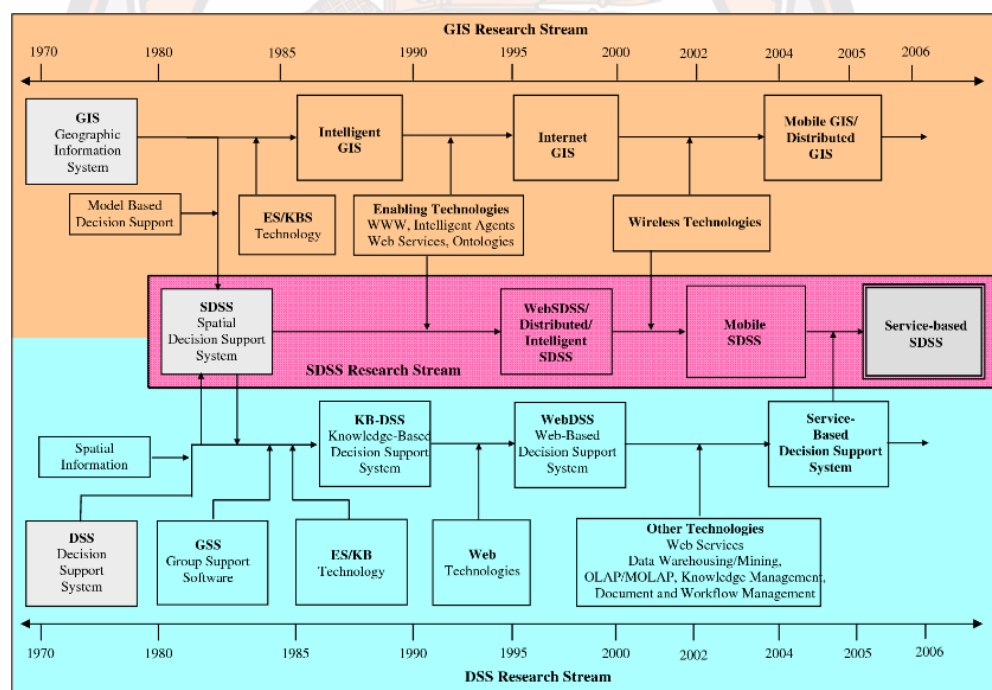
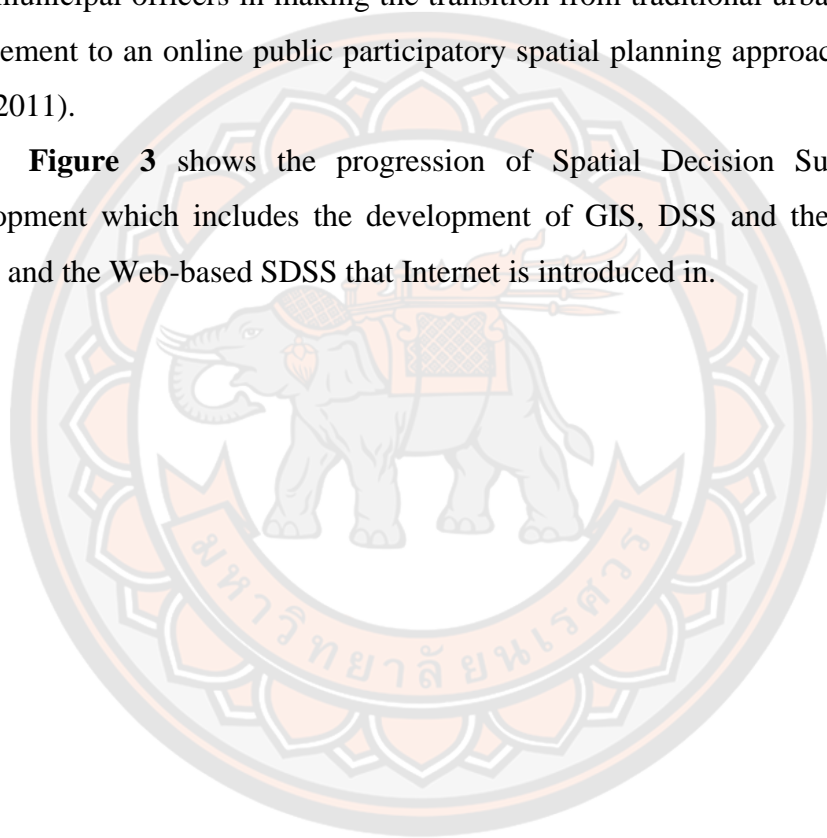


Figure 3 The Progression of Spatial Decision Support Systems Development

Source: Sugumaran & Sugumaran, 2007

Web-based SDSSs have many advantages compared with stand-alone desktop systems such as platform independency, cutting down costs, reduction of maintenance problems, ease of use, data sharing among the users worldwide, supporting group discussion, and an increase in public access and decision-making participants (Yatsalo & Sullivan, 2012). Furthermore, as is customary, a large number of people and permission applicants must visit the municipality offices to submit their applications and track their progress. As a result, the creation of a WebSDSS can assist municipal officers in making the transition from traditional urban planning and management to an online public participatory spatial planning approach (Mansourian et al., 2011).

Figure 3 shows the progression of Spatial Decision Support Systems Development which includes the development of GIS, DSS and their combination SDSS, and the Web-based SDSS that Internet is introduced in.



CHAPTER III

METHODOLOGY

3.1 Introduction

3.1.1 Overall Research Methodology

The purpose of this study is to assess the landslides susceptible areas and degree with the adoption of the PR model which is the derivative of the FR model, and the aid of GIS in Xishuangbanna Dai Prefecture, Yunnan Province, the People's Republic of China, then develop a Web-based SDSS using the landslide susceptibility maps. This chapter explains the research methodology including the study area, data preparation, methods for processing and analyzing the data, and the results verification and development of the proposed platform. The overall research methodology is shown in **Figure 4**.

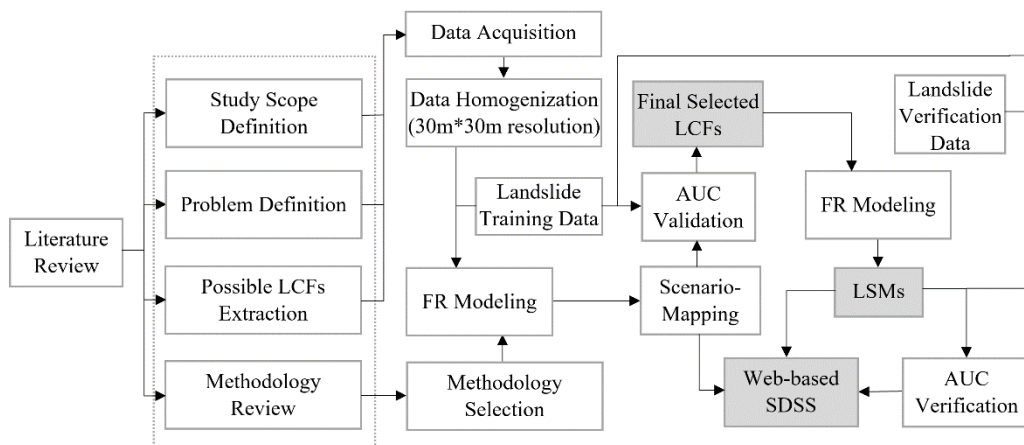


Figure 4 The Overall Research Methodology

3.2 Study Area

Xishuangbanna Prefecture, Yunnan Province, China, lies at (21°10'-22°40'N, 99°55' -101°50' E), the harsh topography, fault lines, monsoon rains, and anthropogenic activity on unstable slopes make it one of the places that is prone to

landslides. The administrative region includes one county-level city-Jinghong and two counties-Menghai and Mengla, borders Myanmar to the southwest and Lao People's Democratic Republic (Lao PDR) to the south (Cao et al., 2017) (**Figure 5**). The region features a mountain-valley topology, with the Hengduan Mountains running north-south, and mountains and hills cover around 95 percent of the area. The Lancang River (upper Mekong River) runs through the middle of Xishuangbanna, with more than 20 major tributaries, resulting in several river valleys and minor basins (Li et al., 2008). Xishuangbanna covers a total area of about 19,120 km². According to the ASTER GDEM, the elevation ranges from 390 to 2,428 meters above sea level. The annual precipitation from 1,324 mm to 2,355 mm derived from 0.5°×0.5° Grid Dataset of Daily Precipitation over China (V2.0) of National Meteorological Science Data Center. The climate is tropical monsoon, with a dry season from November - April and a wet season from May - October. The average annual temperature is 20-22.5 °C, over 90% of the precipitation in the rainy season (Xiao et al., 2019). Only 0.2 percent of China's geographical area is covered by Xishuangbanna, yet it contains 16 percent of the country's vascular flora, 22 percent of animals, and 36 percent of birds (JianhouZhang & MinCao, 1995).

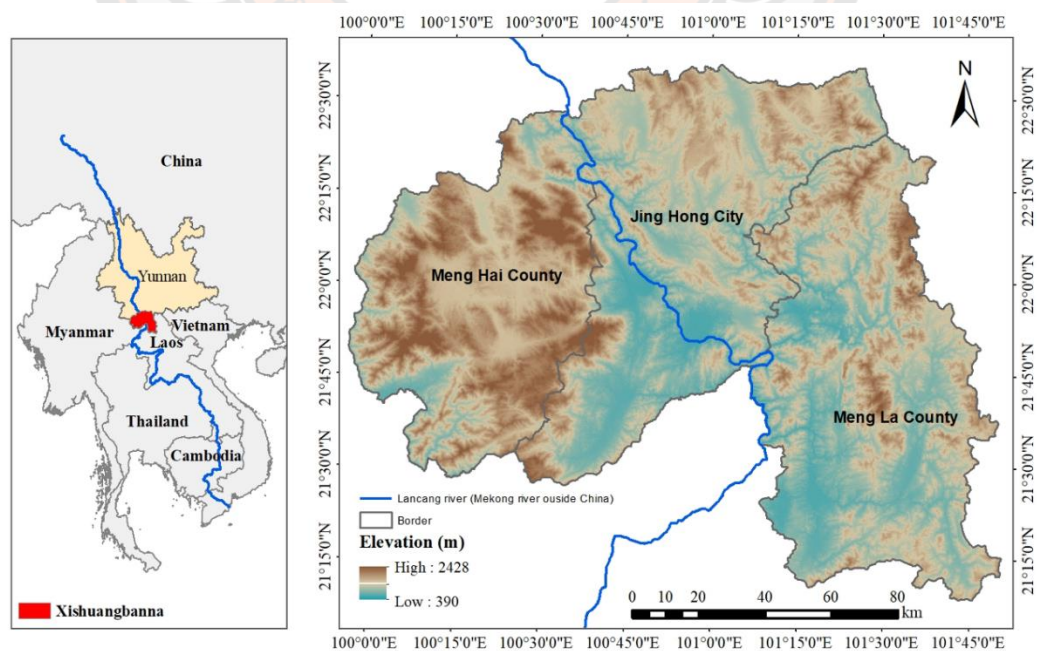


Figure 5 Study Area

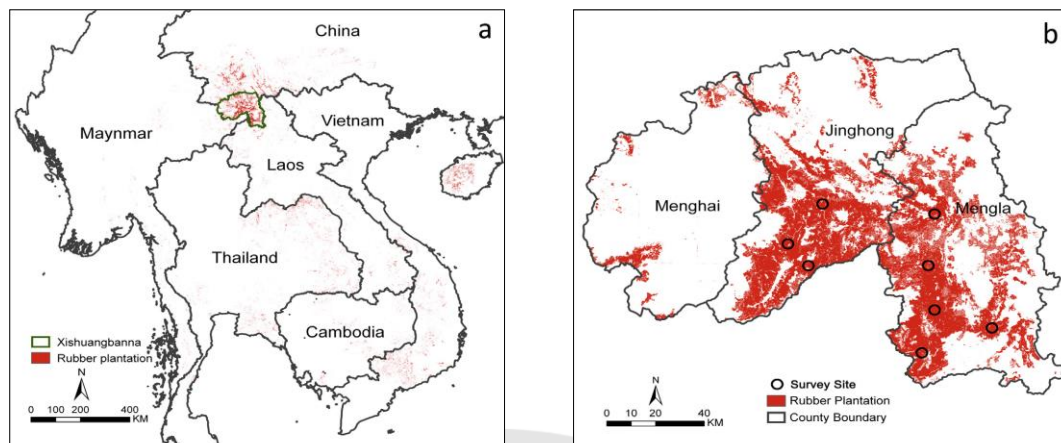


Figure 6 The Southeast Asia Rubber Plantation Zone (a), and the Xishuangbanna Rubber Plantation Zone (b)

Source: Zhu et al., 2014

Since the release of reform and opening-up (1978) policy of the Chinese government, Xishuangbanna has experienced rapid urbanization and significant changes in land use (Cao et al., 2017), the spread of monoculture rubber plantations accounts for the primary liability (Xu et al., 2014), the area of monoculture rubber plantations has increased to 22% (424,000 ha) of the total land cover in 2010 (Hemati et al., 2020; Zhang et al., 2019), and increased by more than 12-times from 1976 to 2015 (Cao et al., 2017), which has resulted in broad land-use change and led to prominent degradation of the local environment (Min et al., 2019). China is a net importer of rubber, accounting for 30% of all rubber consumption worldwide (Sarathchandra et al., 2021). Xishuangbanna is one of the hot spots with rich biodiversity, but with the increasing demand for rubber and other economic crops, the region has resulted in severe deforestation and has become China's second-largest natural rubber-planting base (Li et al., 2008), though, as shown in **Figure 6**, The rubber trees are planted in a 2 m x 10 m grid, resulting in 500 trees per hectare in Xishuangbanna, which is the highest concentration of rubber plantations in China and South Asia (Zhu et al., 2014). Rubber plantations have limited carbon storage

compared to the natural forest ecosystems they are replacing; therefore, their rapid development could have serious consequences. Furthermore, in recent decades, Xishuangbanna has experienced massive urbanization, with the urban population and GDP per capita growing from roughly 50 thousand and 347 RMB in 1978 to 483 thousand and 26,507 RMB in 2014 (Cao et al., 2017).

3.2 Data Preparation

In all versions of LSM, the construction of a landslide inventory map has been regarded as the most important and initial phase. Landslides are thought to be influenced by LCFs, and future landslides will take place under the same circumstances as earlier landslides (Abedini & Tulabi, 2018; Lee & Talib, 2005; Nohani et al., 2019; Rasyid et al., 2016; Youssef et al., 2014). As a result, the landslide inventory map is crucial for determining the quantitative spatial correlations between relevant causative factors and landslide sites. These maps may also be used to forecast future landslides using historical landslide data.

In addition, collecting all available data as well as the construction of a spatial database in the study area are also indispensable. This need for accurate data collection and preservation in databases is widely recognized, but choosing those different factors is surely one of the most difficult tasks. There are no common criteria or rules for this, as a result, the local environment of the study area and the data availability must be considered while selecting criteria. Some researchers claim that data collection and processing costs account for 70-80% of the total, including review and updating (Aleotti & Chowdhury, 1999; Marsala et al., 2019).

According to the time range statistics from the literature review (**Table 3**), of the 52 previous studies, only Pradhan (2010) has used the same time range of landslide inventory and precipitation data. Sur et al. (2020), Youssef et al. (2014), Shahabi et al. (2014), Mind'je et al. (2019), and Intarawichian and Dasananda (2011) used a very big data difference regarding the aforementioned time range. For other studies, the time range is not complete or has not been provided. Some have not considered the precipitation as a landslide conditioning factor for their study area. Zhang et al. (2016) decided not to use the precipitation data because it has been proved that not corresponding to the past landslide distribution. Due to the limitation

of the data availability, the LSA in this study does not consider the impact of climate change. Instead, a long-term trend of the landslide distribution density and annual precipitation extracted from a long-term time range precipitation data of the study are considered.

Table 3 Time Range Statistics of Data Adopted from Literature Review

Author (year)	Landslide inventory data time range	Landslide inventory data duration	Precipitation data time range	Precipitation data duration	Remarks
Pradhan (2010)	1981 - 2004	23 years	1981-2004	23 years	Landsat image in April 2004 was used
Sur et al. (2020)	2001 - 2017	16 years	1947 - 2017	60 years	
Youssef et al. (2014)	2005 - 2015	10 years	1960 - 2013	53 years	
Shahabi et al. (2014)	2008 - 2011	3 years	1980 - 2010	30 years	
Mind'je et al. (2019)	June - September 2018	3 months	1990 - 2017	27 years	
Intarawichian and Dasananda (2011)	2003 - 2007	4 years	2000 - 2010	10 years	
Meena et al. (2019)	April - June 2015	2 months	Not specified	Not specified	
Pirasteh and Li (2017)	2009 - 2016	7 years	Not used	Not used	
Hung et al. (2015)	2010 - 2011	1 year	Not used	Not used	
Zhang et al. (2020)	June, 2010	1 month	Not used	Not used	
Rasyid et al. (2016)	2004 - 2014	10 years	Not used	Not used	
Huang et al. (2018)	2015	1 years	Not used	Not used	Landsat image on July 03, 2013, was used
Zhang et al. (2016)	Up to 2014	Not specified	Not used	Not used	Precipitation not corresponding

3.2.1 Landslide Inventory

Landslide inventory is the detailed record of the location and features of historical landslides (Hervás, 2013). In LSM, some researchers argue that, of all the data maps, the landslide inventory map (LIM) is the most important since it provides information into the location of historical landslide occurrences and also their failure processes (Persichillo et al., 2016; Zhang et al., 2020). Besides, a LIM has been frequently used for validating the accuracy of the model (Milevski et al., 2019). In the form of points or polygons, the LIM depicts the spatial distribution of landslides (Arabameri et al., 2020). In this study, the landslides inventory is prepared in points based on its availability. There are currently no standard processes for selecting training and testing samples; nonetheless, the training and testing samples should be distinct from one another. According to previous studies, 70:30 ratio and random sampling techniques are the most employed approaches (Laila Fayez et al., 2018; Mahalingam et al., 2016; Pourghasemi et al., 2013), hence, a 70:30 ratio was chosen by using the random sampling method in this study.

214 landslide inventory points data derived from Resource and Environment Science and Data Center of China (RESDC) (<http://www.resdc.cn>) has been adopted in this study, of which, Jinghong city, Menghai, and Mengla county accounts for 52, 92, and 70, respectively. The landslide inventory has been randomly divided into two parts, i.e., 150 points (70%) as the training and the remaining 64 points (30%) as the verification datasets, see the statistical number (sample) in **Table 4**.

Table 4 The Landslide Inventory and the Randomly Divided Training, Verification Datasets

Region	Landslide inventory points	Training points (70%)	Verification points (30%)
Xishuangbanna	214	150	64
Jinghong	52	34	18
Menghai	92	67	25
Mengla	70	49	21

3.2.2 Landslide Conditioning Factor Sources

As an essential part of both the generation of single factor maps and the final landslide susceptibility maps, the data sources are required and prepared as shown in **Table 5**. The Advanced Spaceborne Thermal Emission and Reflection Radiometer (ASTER) Global Digital Elevation Model Version 3 (GDEM 003) was released on August 5, 2019, while the first version of the ASTER GDEM, released in June 2009. The improved GDEM V3 adds additional stereo-pairs, improving coverage and reducing the occurrence of artifacts, which shows significant improvements over the previous release. The refined production algorithm provides improved spatial resolution, increased horizontal and vertical accuracy. Thus, GDEM V3 was selected as the digital elevation model (DEM) of the study. All types of original data formats need to be unitized into the same cell size resolution raster data type using ArcGIS, in this study, an accuracy of $30\text{m} \times 30\text{m}$ is selected, and all data layers are projected into the reference coordinate system of WGS84_3_degree_Gauss_Kruger_CM_102E.

Table 5 Data Type and Sources

Layer	Format	Resolution	Data source
Elevation	.tif	$30\text{m} \times 30\text{m}$	ASTER GDEM V3 (https://earthexplorer.usgs.gov/)
Slope angle	.tif	$30\text{m} \times 30\text{m}$	
Slope aspect	.tif	$30\text{m} \times 30\text{m}$	
Curvature	.tif	$30\text{m} \times 30\text{m}$	
TWI	.tif	$30\text{m} \times 30\text{m}$	
SPI	.tif	$30\text{m} \times 30\text{m}$	
Distance to rivers	.shp (polyline)	-	Water Bureau of Xishuangbanna Prefecture
Distance to roads	.shp (polyline)	-	OpenStreetMap (https://www.openstreetmap.org/)
Distance to faults	.jpg	-	Seismic Active Fault Survey Data Center of China (http://www.activefault-datacenter.cn/)
Precipitation	.txt	$0.5^\circ \times 0.5^\circ$	Meteorological Science Data Center of China (http://data.cma.cn/)
NDVI	.tif	$30\text{m} \times 30\text{m}$	Landsat 8 OLI/TIRS Level-2 Data Products (https://earthexplorer.usgs.gov/)
LULC	.tif	$30\text{m} \times 30\text{m}$	National Geomatics Center of China (NGCC) (http://www.globallandcover.com/)

Layer	Format	Resolution	Data source
Lithology	.jpg	-	OSGeo China Center (https://www.osgeo.cn/)
Soil texture	.shp (polygon)	-	Chinese Soil Database (http://vdb3.soil.csdb.cn/)
RPD	.tif	30m × 30m	(Need to study)

3.3 Method

The LSA process in the current study uses FR methods, combined with GIS as well as RS techniques. Two assumptions of principal are employed in the study, one is that the landslides conditioning factors (LCFs) for future landslides will stay the same as they were in the past (Milevski et al., 2019). Another possibility is that future landslides will occur in the same environmental conditions as previous ones (Abedini & Tulabi, 2018; Nohani et al., 2019; Youssef et al., 2014). Consequently, analysis of the spatial variation of landslides inventory in the area, as well as the classification of each LCF layer and the relationships between them provide important information in predicting future landslides. Rather than landslide hazard assessment (LHA), a landslide susceptibility assessment (LSA) is to be done in this study which considers only the spatial likelihood of future landslides occurrence. All the spatial source data preparation, storage, homogenizing, and the calculation of landslide susceptibility index (Index), the mapping of landslide susceptibility is conducted by using ArcGIS. The verification of the results is done by using the ROC which evaluates the quality by analyzing the area under the curve (AUC) values, the ArcGIS add-in namely Arc-SDM is adopted for calculation of AUC values. The overall methodology can be divided into 3 parts including the identification of landslide conditioning factors (LCFs) for the study area, landslide susceptibility mapping (LSM) with adopting the selected LCFs, and design and development of Web-based Spatial Decision Support System for Landslide in Xishuangbanna, China, using the outcomes of the LSA.

3.3.1 Landslide Conditioning Factor Identification

The objective of the study is to assess the area prone to landslides for the study area by the means of LSM, however, the precondition is all the LCF layers are getting readily prepared before inputting them into the model. Based on the local

peculiarities of the study area, for LSA, at least three aspects of factors must be input in GIS analysis: topography, land use, and lithology (Milevski et al., 2019). However, for the LCFs, there are no predefined criteria for selection (Sur et al., 2020). For this study 14 LCFs are preliminarily picked based on the 52 pieces of literature (**Table 2**), which are mainly related to geological (Soil texture, Distance to faults, and Lithology), hydrological (Distance to rivers and Precipitation), geomorphological (Slope angle, Curvature, Slope aspect, Elevation, TWI, and SPI), and anthropogenic factors (LULC, NDVI, Distance to roads) that can lead to slope instabilities (Meena et al., 2019). Though, the rationality and helpfulness of each factor in LSA for the study area need to be identified. The identification process is designed as following steps:

a) Generating 1 LSM using FR model with inputting all the 14 LCF layers and the landslide training dataset, then calculate the AUC value for generated LSM;

b) Generating 14 LSMs using FR model by adopting one-at-a-time sensitivity analysis method (remove each of the 14 LCF layers in turn from the whole), then calculate the AUC value for each single factor map by inputting the landslide training dataset;

c) Based on the theory that at least three aspects of factors including topography, lithology, and land use must be input in GIS analysis for LSM (Milevski et al., 2019), the slope angle, lithology, and LULC are selected as the minimum factor group to generate the LSM, together with inputting the landslide training dataset using FR model, then calculate its AUC value;

d) Based on the minimum factor group, each of the other 11 LCFs will be added into the group in turn, adopting one-at-a-time sensitivity analysis method and using the FR model to generate the 11 LSMs, together with inputting the landslide training dataset, then calculate the AUC values for each LSM;

e) Analyze the AUC values of all generated LSMs to determine whether the participation of each factor helps to increase the AUC value. Only if the factor shows a prominent positive effect in improving the AUC value, this factor will be kept as a member of the final LCF group for the study area. Conversely, if the factor plays a negative role or has no prominent effect on the AUC value, this factor will be removed from the final LCF group.

Finally, the identified LCF group will be set as the effective landslide conditioning factors for this study. See the workflow of the identification process in **Figure 7**.

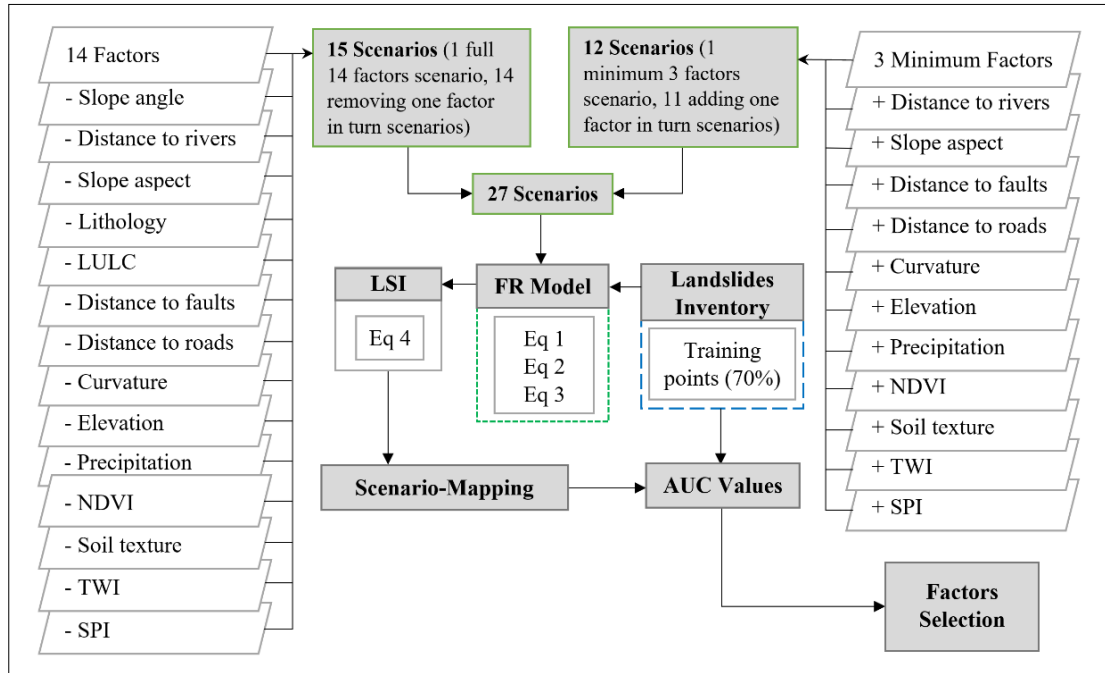


Figure 7 Landslide Conditioning Factors (LCFs) Identification Workflow

3.3.2 Landslide Susceptibility Mapping

The general LSM process of the study is shown in **Figure 8**, of which, landslide inventory dataset is used in both LSM processes of 27 individual scenarios and the final identified factor case as the necessary input data for calculating FR value and AUC value, while landslide inventory verification dataset is only used to verify the final landslide susceptibility map.

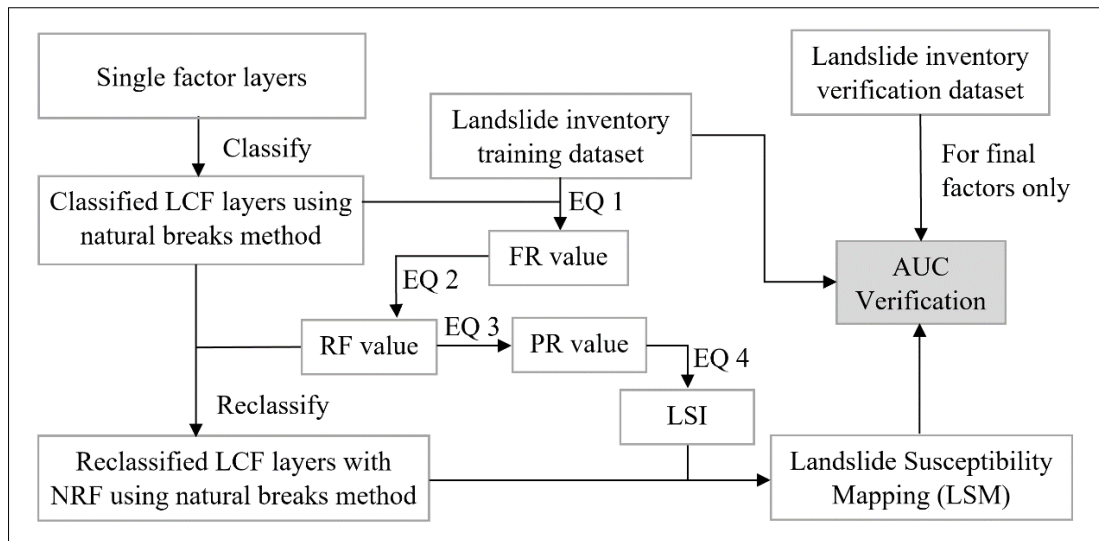


Figure 8 General Landslide Susceptibility Mapping (LSM) Process of the Study

3.3.2.1 Factor Classification

Each of the LCFs must be classified into categorical susceptibility classifications for visual interpretation of LSMs. Quantiles, equal intervals, standard deviations, and natural breaks are some of the classification methods available (Youssef et al., 2014). However, there is also no widely accepted consensus on the optimal method for categorizing each factor into subclasses. The most commonly utilized techniques are natural breaks and quantile categorization (Milevski et al., 2019). Natural breaks is an approach for determining the appropriate organization of values into distinct groups that has been widely employed, particularly by planners (Rasyid et al., 2016). The variance between categories is maximized, while the variance within classifications is minimized, using this method. In this study, each LCF is to be subdivided into different classifications using the natural breaks classification method, to adapt to the variety of data sources and scale differences, and to effectively illustrate its role in the occurrence mechanism of landslides, except for the one that has unique classifications itself.

3.3.2.2 Landslide Susceptibility Mapping with Identified Factors

The detailed process of LSM after getting the identified LCFs is shown in **Figure 9**, and the process (all steps have proceeded in ArcGIS) is as follows:

- a) Classify all the identified LCFs (including RPD) layers using the natural breaks method;
- b) Generating LSMs using FR model with all the classified LCF layers, as well as the landslide training dataset, then calculate the FR value for each classification of each LCF using **Equation 1**, then convert the FR values to RF values using **Equation 2**;
- c) Reclassify all the LCFs layers by assigning the corresponding calculated RF value for each classification of each LCF;
- d) Calculate the PR value for each LCF using **Equation 3**;
- e) Calculate the LSI using **Equation 4**;
- f) Generating the final LSMs in ArcGIS with the LSI values.

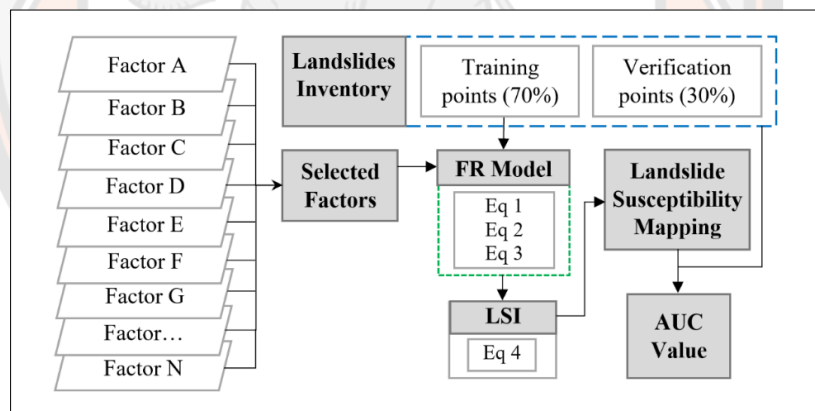


Figure 9 Final Landslide Susceptibility Mapping Workflow

3.3.2.3 Frequency Ratio (FR) Calculation

The FR value is calculated by using **Equation 1** (defined in **Chapter II**).

3.3.2.4 Relative Frequency (RF) Calculation

The RF value is calculated by using **Equation 2** (defined in **Chapter II**).

3.3.2.5 Predictor rate (PR) Calculation

The PR value is calculated by using **Equation 3** (defined in **Chapter II**).

3.3.2.6 Landslide Susceptibility Map (LSM) Generation

Before generating the LSM, LSI needs to be calculated first, which is calculated by using **Equation 4** (see in **Chapter II**). Then the LSI value for interpretation with the assistance of ArcGIS function, namely “Raster Calculator” was used to produce all the final LSMs.

3.3.3.7 Mapping Results Verification

The LSMs constructed by FR model are to be verified by comparing the AUC values of the final LSMs with inputting the landslide inventory data. The AUC approach is used to evaluate the prediction quality of the model. The AUC value of inputting the landslide inventory training dataset and the verification dataset represent the success rate and prediction rate of the model respectively, and the results are to be plotted in the form of a graphic.

3.3.3 Design of Web-based Spatial Decision Support System

Figure 10 shows the design of the proposed Web-based SDSS for Landslide in Xishuangbanna, China, which aims to present the outcomes of the study. There are in total 14 landslide conditioning factors which are obtained from the literature review at first. By analyzing the corresponding relationship between landslide inventory training data and each factor, Finally, several factors will be kept as the dominant landslide conditioning factors for Xishuangbanna, China.

Hypertext Markup Language (HTML) is a typical choice for the development of websites, web pages and web-based applications. Business stakeholders, project management and program developers prefer HTML over other alternative program development options due to its advantageous characteristics. A few of the notable advantages of HTML are ‘it is lightweight in structure’, ‘it is easy to learn and use’, ‘it is an open-source program that can be used for free of cost’, ‘it is supported in all kinds of browsers’, ‘effortless to create and edit’, ‘easy to integrate with other programming languages’, ‘allows to accommodate changes at any time as required for the requirements’, etc. (Goyal, 2022). As a static language, however, one of the limitations of the HTML is it cannot produce dynamic output alone, while

Hypertext Preprocessor (PHP) can make up the shortage which is initially designed to create dynamic web pages. Moreover, PHP also has other advantages including “great synergy with HTML”, “many available specialists”, “a large base of reference and educational materials”, “better loading speed of websites”, “more options for database connectivity”, “a large collection of open-source addons”, “inexpensive website hosting”, “excellent flexibility and combinability”, “various benefits provided by cloud solutions”. PHP allows connection to almost any type of database but the most common one is MySQL, because it is free and effective (Roznovsky, 2022). Baidu Map JavaScript API is a set of application programming interface written by JavaScript language which can help users build a rich and interactive map application on the website. It supports PC and mobile browser-based map application development and supports HTML5 features of map development. Moreover, it is free of charge, the utilization times of the interface are unlimited (Baidu, 2022). Considering the advantages described above, HTML, PHP, MySQL, and Baidu Map JavaScript API are selected as the programming language and tools for the development of the proposed Web-based SDSS for current study.

The system can reappear the process of our landslide susceptibility assessment for Xishuangbanna and help decision-makers to identify the landslide susceptibility level of a specific location, which can be used as effective decision-making supporting tool, as well as providing a contemplable way of making better use of the conventional LSA outcomes for future researchers. As is shown in **Figure 10**, the system is designed to include the following 5 modules:

- a) General - Consists of location identification, program introduction, data type and resource, methodology, and about us pages;
- b) Single Layer Maps - Present landslide inventory distribution on each of the landslide conditioning factor classification maps;
- c) Remove Factor Scenarios - Present factor weight & AUC value of the case of adopting all 14 factors, and the cases of removing one factor from the 14 factors in turn;
- d) Add Factor Scenarios - Present factor weight & AUC value of the case of adopting 3 minimum factors (Slope Angle, Lithology and Land Use & Land Cover (LULC)), and the cases of adding one factor into the 3 factors in turn;

e) Final Results - Present AUC value compare of both cases of removing and adding factor except for the obligatory 3 minimum factors (Slope Angle, Lithology and LULC), factor weight value for the final 7 factors, the final Landslide Susceptibility Mapping result, the result for township level and the susceptibility statistic data of each township.

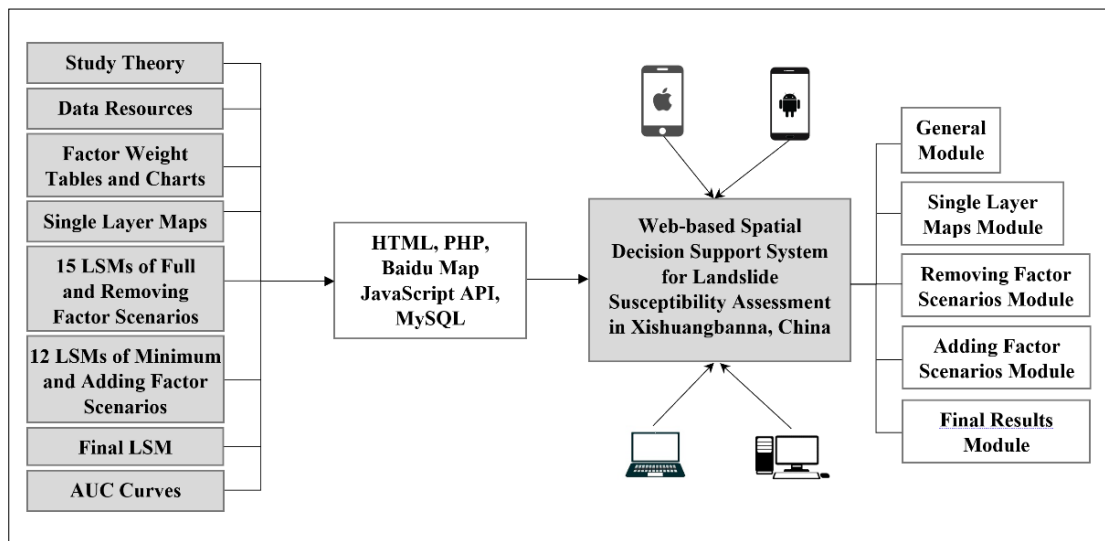


Figure 10 Design of Web-based SDSS for LSA in Xishuangbanna, China

CHAPTER IV

RESULTS AND DISCUSSION

In this chapter, the results and discussion under the topic of Landslide Susceptibility Assessment and Development of the Web-based Spatial Decision Support System for Landslide in Xishuangbanna, China, concerning the research objectives, set in **Chapter I** is illustrated, which is produced using ArcGIS and Microsoft Excel.

4.1 Results

4.1.1 Factor Classification Results

4.1.1.1 Slope Angle

As the most frequently used LCF in LSA, the slope angle is selected in this study and the map data was obtained from the ASTER GDEM with resolution $30\text{ m} \times 30\text{ m}$ and the values are divided into 7 classifications adopting the natural breaks classification method: $0 - 8^\circ$, $8 - 14^\circ$, $14 - 20^\circ$, $20 - 26^\circ$, $26 - 32^\circ$, $32 - 38^\circ$, and $> 38^\circ$. The landslide inventory distribution in each classification and the area percentage of each classification is shown in **Table 5**, and the classification overlapping map with landslide inventory can be seen in **Figure 13 (a)**.

4.1.1.2 Distance to River

The Lancang River is the biggest river in the study area, but there are also a huge number of smaller rivers and their branches. The distance to rivers was considered in the current study. To analyze the impact of rivers on the slopes, five river buffer types were devised, which are $0\text{ m} - 50\text{ m}$, $50\text{ m} - 100\text{ m}$, $100\text{ m} - 150\text{ m}$, $150\text{ m} - 200\text{ m}$, and $> 200\text{ m}$. The landslide inventory distribution in each classification and the area percentage of each classification is shown in **Table 5**, and the classification overlapping map with landslide inventory is shown in **Figure 13 (b)**.

4.1.1.3 Slope Aspect

In LSA, the slope aspect is considered as a possible conditioning factor and is adopted in the study and also generated from ASTER GDEM under nine directional classifications, using the natural breaks classification method, i.e., flat (-

1°), north (337.5° - 360°, 0° - 22.5°), northeast (22.5° - 67.5°), east (67.5° - 112.5°), southeast (112.5° - 157.5°), south (157.5° - 202.5°), southwest (202.5° - 247.5°), west (247.5° - 292.5°), and northwest (292.5° - 337.5°). The landslide inventory distribution in each classification and the area percentage of each classification are shown in **Table 5**, and the classification overlapping map with landslide inventory is shown in **Figure 13 (c)**.

4.1.1.4 Lithology

The lithology map was digitalized from the image file which is a non-georeferenced map obtained from OSGeo China Center. Since the map is in Chinese language and the petrographic classification is also in the Chinese method, to avoid inaccurate translation, in the current study, the original 16 classification units are depicted as Group A - Group P. The landslide inventory distribution in each classification and the area percentage of each classification is shown in **Table 5**, and the classification overlapping map with landslide inventory is shown in **Figure 13 (d)**.

4.1.1.5 Land Use and Land Cover (LULC)

The land use source data was obtained from the National Geomatics Center of China, which has 7 classifications in the study area, which are Cultivated Land, Forest, Grass Land, Shrubland, Wetland, Water Body. The landslide inventory distribution in each classification and the area percentage of each classification are shown in **Table 5**, and the classification overlapping map with landslide inventory can be seen in **Figure 13 (e)**.

4.1.1.6 Distance to Fault

Because there are geological faults in the study area, we must consider the distance to faults when conducting LSA. The faults buffer classifications were defined as < 500 m, 1000 m - 2000 m, 2000 m - 3000 m, 3000 m - 4000 m, and > 4000 m. The landslide inventory distribution in each classification and the area percentage of each classification are shown in **Table 5**, and the classification overlapping map with landslide inventory can be seen in **Figure 13 (f)**.

4.1.1.7 Distance to Road

The study area has experienced rapid urbanization, including the expansion of the transport network, so it is reasonable to take the road system into account for LSA. Five different buffer zones were generated using ArcGIS: < 50 m,

50 m - 100 m, 100 m - 150 m, 150 m - 200 m, and > 200 m. The landslide inventory distribution in each classification and the area percentage of each classification are shown in **Table 5**, and the classification overlapping map with landslide inventory can be seen in **Figure 14 (a)**.

4.1.1.8 Curvature

The curvature value is used to assess the landslide susceptibility in the study area, which represents the morphology of the topography. The curvature map is also generated from ASTER GDEM and is divided into 3 categories adopting the natural breaks classification method, which are Concave (-1 to -0.01), Flat (-0.01 to 0.01), and Convex (0.01 to 1). The landslide inventory distribution in each classification and the area percentage of each classification is shown in **Table 5**, and the classification overlapping map with landslide inventory can be seen in **Figure 14 (b)**.

4.1.1.9 Elevation

The elevation map is derived from the ASTER GDEM with resolution 30 × 30 m ranges from 390 m to 2428 m in the study area, of which, about 95% is mountains and hills area, thus the elevation plays an significant role in LSA. Its values were classified into seven classifications using the natural breaks classification method, which are < 1450 m, 1450 - 1580 m, 1580 - 1720 m, 1720 - 1840 m, 1840 - 1970 m, 1970 - 2140 m, and > 2140 m. The landslide inventory distribution in each classification and the area percentage of each classification are shown in **Table 5**, and the classification overlapping map with landslide inventory is shown in **Figure 14 (c)**.

4.1.1.10 Precipitation

As a tropical rainforest area, there is abundant rainfall for the study area, of which the annual precipitation data derived from Meteorological Science Data Center of China (2001 - 2020) are processed and converted into map form using both Microsoft Excel and ArcGIS, the values range from 1324 mm to 2355 mm. The precipitation map is classified into seven classifications using the natural breaks classification method, < 1450 mm, 1450 mm - 1580 mm, 1580 mm - 1720 mm, 1720 mm - 1840 mm, 1840 mm - 1970 mm, 1970 mm - 2140 mm, and > 2140 mm. The landslide inventory distribution in each classification and the area percentage of each

classification are shown in **Table 5**, and the classification overlapping map with landslide inventory can be seen in **Figure 14 (d)**.

4.1.1.11 Normalized Difference Vegetation Index (NDVI)

In this study, the NDVI was obtained from the satellite images using the Raster Calculator tool in ArcGIS, and it is also considered in preparing LSMs. The NDVI values vary from 0.18 to 0.34, and NDVI map is classified into five classifications using natural breaks classification method: < 0.18 , $0.18 - 0.24$, $0.24 - 0.29$, $0.29 - 0.34$, and > 0.34 . The landslide inventory distribution in each classification and the area percentage of each classification are shown in **Table 5**, and the classification overlapping map with landslide inventory is shown in **Figure 14 (e)**.

4.1.1.12 Soil Texture

The soil type data is obtained from the Chinese Soil Database, which has the composition percentage of clay, sand, and silt. It was converted into 5 new classifications using the United States Department of Agriculture (USDA) Textural Soil Classification method, the reference classification criteria are shown in **Figure 11**. The new classifications are Clay (C), Sandy Clay Loam (SCL), Sandy Loam (SL), Clay Loam (CL), Sandy Silt Loam (SZL). The landslide inventory distribution in each classification and the area percentage of each classification are shown in **Table 5**, and the classification overlapping map with landslide inventory is shown in **Figure 14 (f)**.

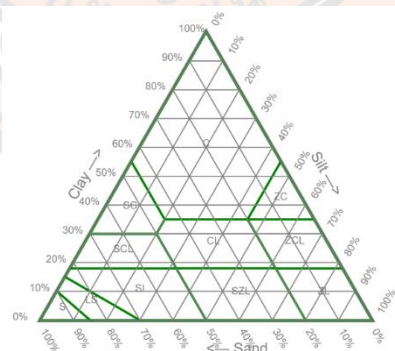


Figure 11 USDA Soil Texture Triangle

Source: University, 2022

4.1.1.13 Topographic Wetness Index (TWI)

The topographic wetness index (TWI) is calculated from the ASTER GDEM, using the equation defined by (Beven & Kirkby, 1979):

$$TWI = \ln \left(\frac{\alpha}{\tan \beta} \right) \quad (5)$$

Where, the α is the cumulative upslope area draining through a point (per unit contour length), and $\tan \beta$ is the slope angle at the point. The *TWI* was classified into 5 classifications using the natural breaks classification method: < 4.87, 4.87 - 5.95, 5.95 - 7.35, 7.35 - 9.19, > 9.19. The landslide inventory distribution in each classification and the area percentage of each classification are shown in **Table 5**, and the classification overlapping map with landslide inventory is shown in **Figure 15 (a)**.

4.1.1.14 Stream Power Index (SPI)

The stream power index (SPI) is calculated from the ASTER GDEM, using the equation defined by (Moore et al., 1991):

$$SPI = As * \tan b \quad (6)$$

Where, the *As* is the specific catchment volume, and *b* is the local slope gradient measured in degrees. it is categorized into 5 classifications adopting the natural breaks classification method: < 604, 604 – 2,719, 2719 – 7,250, 7,250 – 16,615, > 16,615. The landslide inventory distribution in each classification and the area percentage of each classification are shown in **Table 5**, and the classification overlapping map with landslide inventory can be seen in **Figure 15 (b)**.

4.1.1.15 Rubber Plantation Density (RPD)

When comparing the landslide inventory mapping result (**Figure 12 (a)**) and the RPD map (**Figure 12 (b)**), there is no corresponding relationship was found between RPD and landslide occurrence. According to **Figure 12 (b)**, rubber is mainly planted in the lower elevation areas, while **Figure 12 (a)** shows higher elevation areas have more density of landslide inventory. Furthermore, other LCFs

like LULC and NDVI can also reflect some of the characteristics of RPD, thus, RPD is excluded as the final LCF for the study area in this study.

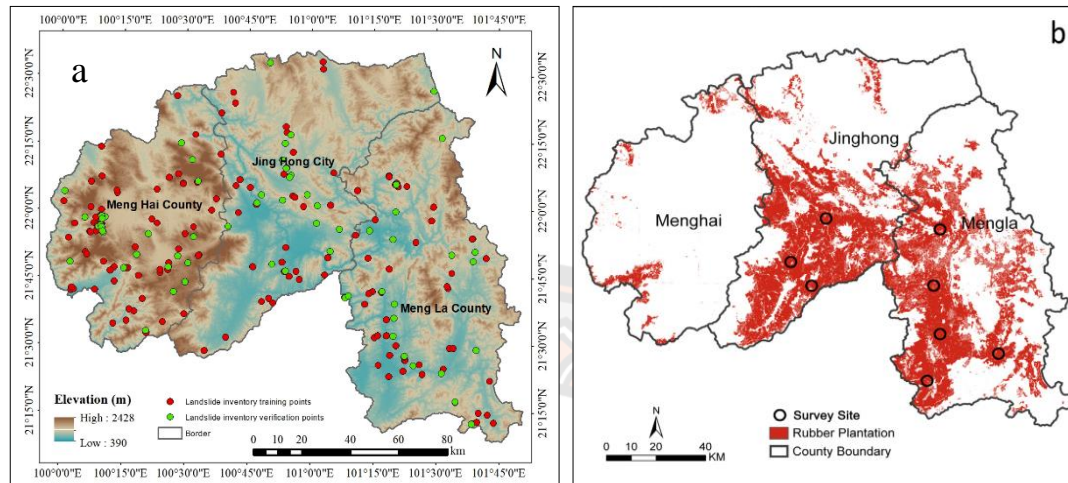


Figure 12 Landslide Inventory Mapping Result (a), and the Rubber Plantation Zone Map (b) (Zhu et al., 2014) in Xishuangbanna

Table 5 Landslide Inventory Distribution in Each Classification and the Area Percentage of Each Classification of LCFs

Factor Name	Classification	Landslide Number	Landslide Percentage	Cell Number	Cell Percentage
Slope Angle	0 - 8°	25	16.67%	2941342	13.84%
	0 - 14°	33	22.00%	4388988	20.65%
	14 - 20°	43	28.67%	5093316	23.97%
	20 - 26°	30	20.00%	4367099	20.55%
	26 - 32°	14	9.33%	2696373	12.69%
	32 - 38°	5	3.33%	1214940	5.72%
	>38°	0	0.00%	549441	2.59%
	Total		150		21251499
Distance to River	0 - 50 m	7	4.67%	762667	3.59%
	50 - 100 m	11	7.33%	727464	3.42%
	100 - 150 m	12	8.00%	704566	3.32%
	150 - 200 m	9	6.00%	696511	3.28%
	>200 m	111	74.00%	18360291	86.40%

Factor Name	Classification	Landslide Number	Landslide Percentage	Cell Number	Cell Percentage
	Total	150		21251499	
Slope Aspect	Flat (-1)	0	0.00%	2198	0.01%
	North (0-22.5)	7	4.67%	1406262	6.62%
	Northeast (22.5-67.5)	24	16.00%	2718311	12.79%
	East (67.5-112.5)	22	14.67%	2443558	11.50%
	Southeast (112.5-157.5)	15	10.00%	2640620	12.43%
	South (157.5-202.5)	28	18.67%	2725823	12.83%
	Southwest (202.5-247.5)	18	12.00%	2744525	12.91%
	West (247.5-292.5)	11	7.33%	2500976	11.77%
	Northwest (292.5-337.5)	17	11.33%	2721415	12.81%
	North (337.5-360)	8	5.33%	1347811	6.34%
		Total	150		21251499
Lithology	Group A	2	1.33%	131953	0.62%
	Group B	0	0.00%	261852	1.23%
	Group C	0	0.00%	75795	0.36%
	Group D	26	17.33%	1793320	8.44%
	Group E	31	20.67%	3886269	18.29%
	Group F	4	2.67%	366959	1.73%
	Group G	1	0.67%	456903	2.15%
	Group H	23	15.33%	3128825	14.72%
	Group I	2	1.33%	229426	1.08%
	Group J	22	14.67%	1976289	9.30%
	Group K	1	0.67%	318798	1.50%
	Group L	2	1.33%	67910	0.32%
	Group M	5	3.33%	986135	4.64%
	Group N	13	8.67%	5378662	25.31%
	Group O	3	2.00%	492355	2.32%
	Group P	15	10.00%	1700048	8.00%
	Total	150		21251499	
LULC	Cultivated Land	67	44.67%	6451623	30.36%
	Forest	23	15.33%	12789079	60.18%
	Grass Land	19	12.67%	1481998	6.97%
	Shrubland	2	1.33%	170810	0.80%
	Wetland	0	0.00%	145	0.00%
	Water Body	0	0.00%	92733	0.44%

Factor Name	Classification	Landslide Number	Landslide Percentage	Cell Number	Cell Percentage
	Artificial Surfaces	39	26.00%	265111	1.25%
	Total	150		21251499	
Distance to Fault	< 500 m	3	2.00%	224543	1.06%
	500 - 1000 m	6	4.00%	231876	1.09%
	1000 - 2000 m	4	2.67%	485537	2.28%
	2000 - 3000 m	2	1.33%	518667	2.44%
	3000 - 4000 m	1	0.67%	534888	2.52%
	>4000 m	134	89.33%	19255988	90.61%
	Total	150		21251499	
Distance to Road	0 - 50 m	23	15.33%	464644	2.19%
	50 - 100 m	10	6.67%	396250	1.86%
	100 - 150 m	9	6.00%	359069	1.69%
	150 - 200 m	4	2.67%	334974	1.58%
	>200 m	104	69.33%	19696562	92.68%
	Total	150		21251499	
Curvature	Concave	70	46.67%	10348291	48.69%
	Flat	8	5.33%	719618	3.39%
	Convex	72	48.00%	10183590	47.92%
	Total	150		21251499	
Elevation	< 760 m	40	26.67%	3069266	14.44%
	760 - 940 m	33	22.00%	3869986	18.21%
	940 - 1110 m	19	12.67%	4310576	20.28%
	1110 - 1280 m	18	12.00%	4380191	20.61%
	1280 - 1470 m	11	7.33%	2911115	13.70%
	1470 - 1710 m	19	12.67%	1871642	8.81%
	> 1710 m	10	6.67%	838723	3.95%
	Total	150		21251499	
Precipitation	<1450 mm	25	16.67%	2916117	13.72%
	1450 - 1580 mm	64	42.67%	7294495	34.32%
	1580 - 1720 mm	12	8.00%	3251553	15.30%
	1720 - 1840 mm	28	18.67%	3196994	15.04%
	1840 - 1970 mm	7	4.67%	2092719	9.85%
	1970 - 2140 mm	10	6.67%	1694585	7.97%
	>2140 mm	4	2.67%	805036	3.79%
	Total	150		21251499	
NDVI	<0.18	28	18.67%	1029888	4.85%
	0.18 - 0.24	50	33.33%	2509425	11.81%
	0.24 - 0.29	38	25.33%	5335626	25.11%
	0.29 - 0.34	23	15.33%	7852472	36.95%

Factor Name	Classification	Landslide Number	Landslide Percentage	Cell Number	Cell Percentage
	>0.34	11	7.33%	4524088	21.29%
	SUM	150		21251499	
Soil Texture	Clay	80	53.33%	14163039	66.64%
	Sandy Clay Loam	10	6.67%	1543497	7.26%
	Sandy Loam	9	6.00%	1367611	6.44%
	Clay Loam	51	34.00%	4127426	19.42%
	Sandy Silt Loam	0	0.00%	49926	0.23%
	Total	150		21251499	
TWI	<4.87	36	24.00%	5964104	28.06%
	4.87 - 5.95	51	34.00%	7813447	36.77%
	5.95 - 7.35	29	19.33%	4554354	21.43%
	7.35 - 9.19	23	15.33%	2041958	9.61%
	>9.19	11	7.33%	877636	4.13%
	Total	150		21251499	
SPI	<604	141	94.00%	20541781	96.66%
	604 - 2719	9	6.00%	600703	2.83%
	2719 - 7250	0	0.00%	91739	0.43%
	7250 - 16615	0	0.00%	15396	0.07%
	>16615	0	0.00%	1880	0.01%
	Total	150		21251499	

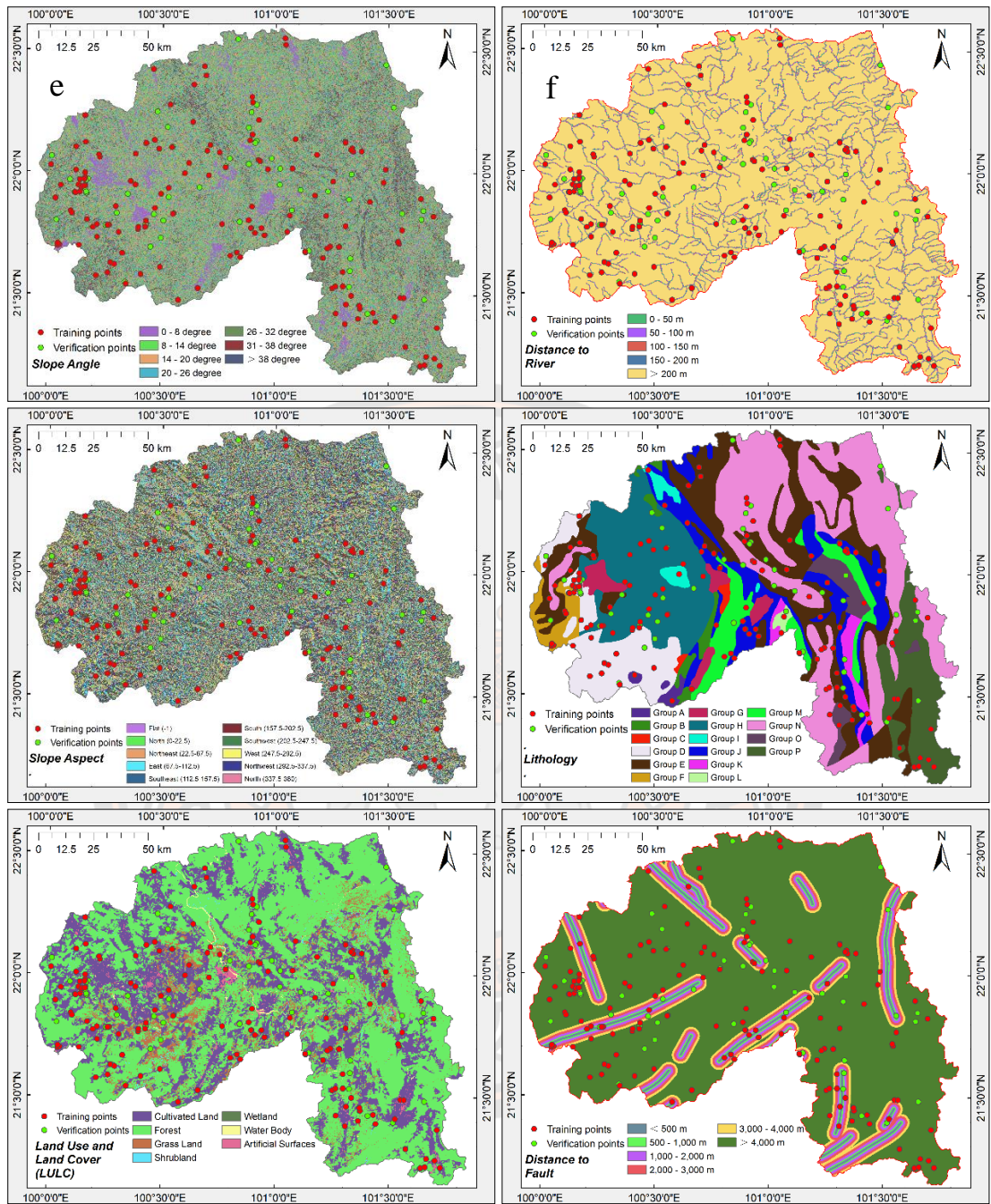


Figure 13 Maps of Landslide Inventory Distribution in the Classification of Slope Angle (a), Distance to River (b), Slope Aspect (c), Lithology (d), Land Use and Land Cover (LULC) (e), and Distance to Fault (f)

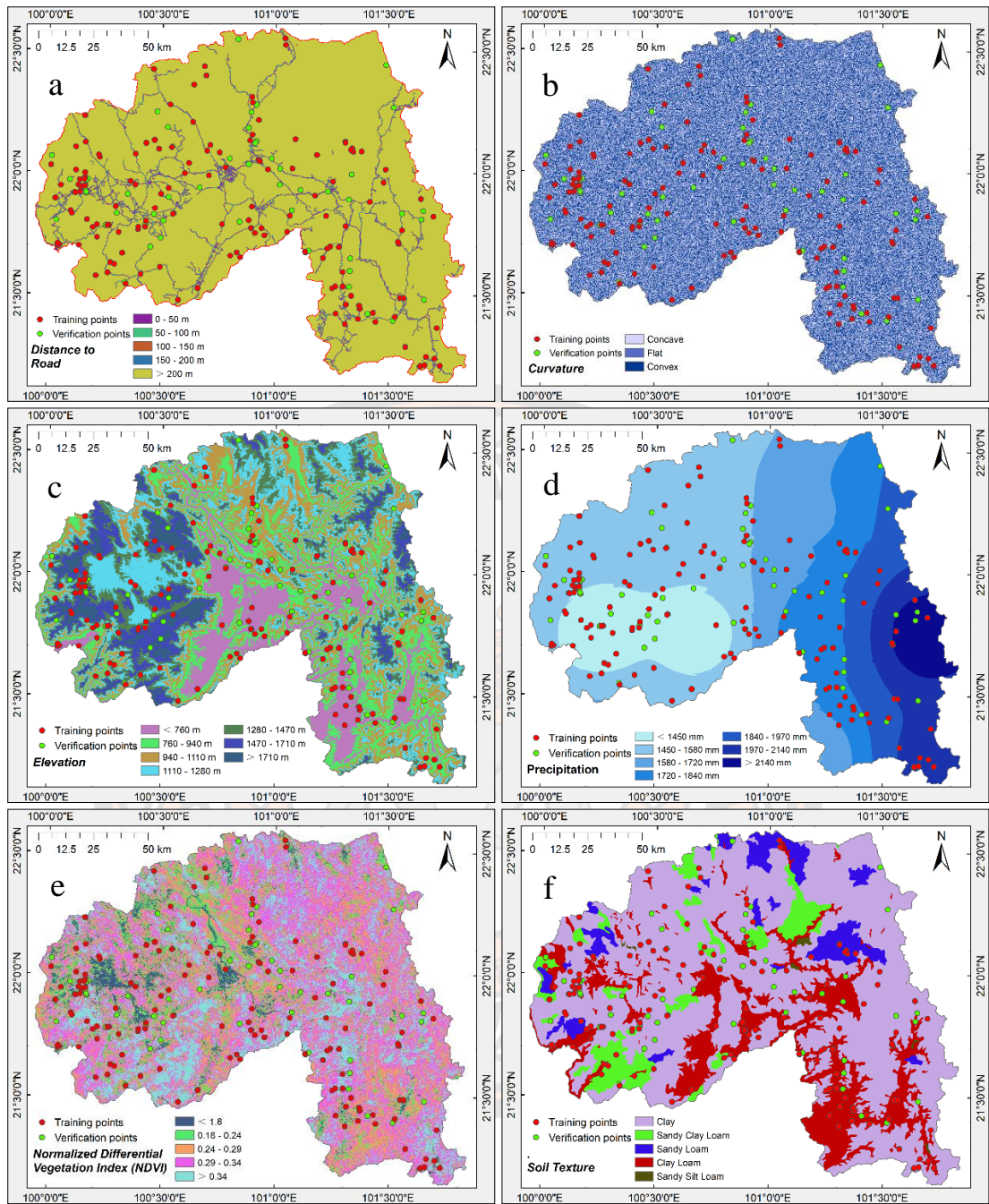


Figure 14 Maps of Landslide Inventory Distribution in the Classification of Distance to Road (a), Curvature (b), Elevation (c), Precipitation (d), Normalized Differential Vegetation Index (NDVI) (e), and Soil Texture (f).

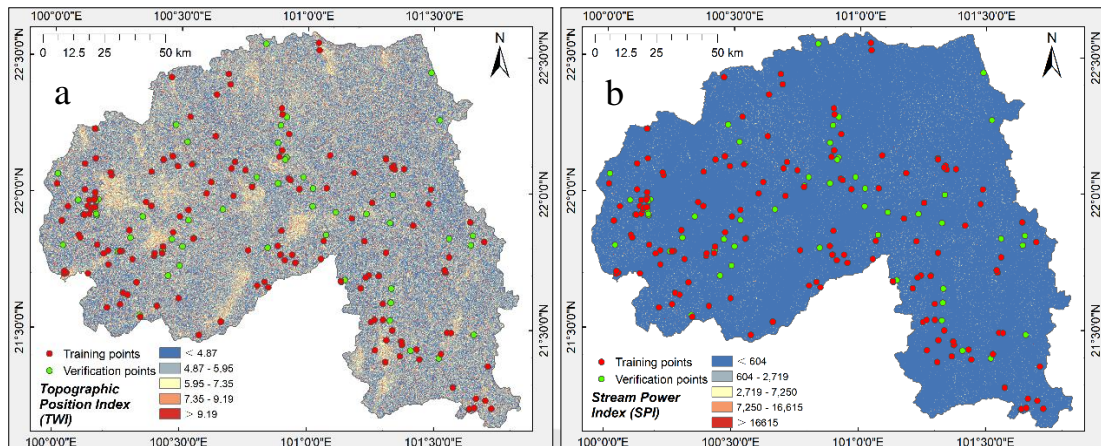


Figure 15 Maps of Landslide Inventory Distribution in the Classification of Topographic Position Index (TWI) (a) and Stream Power Index (b)

4.1.2 Frequency Ratio (FR), Relative Frequency (RF), and Predictor Rate (PR) Value Calculation Results

4.1.2.1 Frequency Ratio Value Results

Based on the data of landslide inventory training points distribution percentage in each classification, and the area percentage of each classification of each factor, using **Equation 1** which is defined in **Chapter II**, the FR value of each classification of each factor is calculated using ArcGIS, the calculation results are shown in **Table 6**. As is described in **Chapter II**, A FR value of 1 indicates that this classification has a landslide density proportional to the area of the classification in the map; a value greater than 1 reveals a higher correlation, while a value smaller than 1 reveals a lower correlation region and vice versa.

4.1.2.2 Relative Frequency Value Results

Based on the FR values above, the FR value of each classification of each factor is normalized into RF values using **Equation 2** which is defined in **Chapter II**, the normalization results can be seen in **Table 6**.

Figure 16 illustrates the landslide number and the curve of its percentage in each classification of each factor, the curve of area percentage of each classification, and the RF value of the corresponding classification of each factor.

Figure 19-21 shows the Maps of Relative Frequency (RF) value for each classification of each factor, relatively.

4.1.2.3 Predictor Rate Value Results

Based on the RF values above, the PR value of each factor can be calculated using **Equation 3** which is defined in **Chapter II**, the PR calculation results are shown in **Table 6**.

Furthermore, according to the methodology of the study set in **CHAPTER III**, besides the case of all 14 factors are adopted, there are also other 14 cases that remove one factor in turn from the whole, as well as the case of adopting the minimum 3 factors (Slope Angle, Lithology and LULC) group, and the other 11 cases of adding other 11 factors into the minimum factor group in turn. The PR values may vary when different factors are adopted according to **Equation 3** which is defined in **Chapter II**. The PR values of all cases are shown in **Table 7** and **Table 8**, and the bar charts of PR values of adopting all 14 factors and removing one factor in turn cases can be seen in **Figure 22**, and that of adopting 3 minimum factors and adding one factor in turn cases can be seen in **Figure 23**.

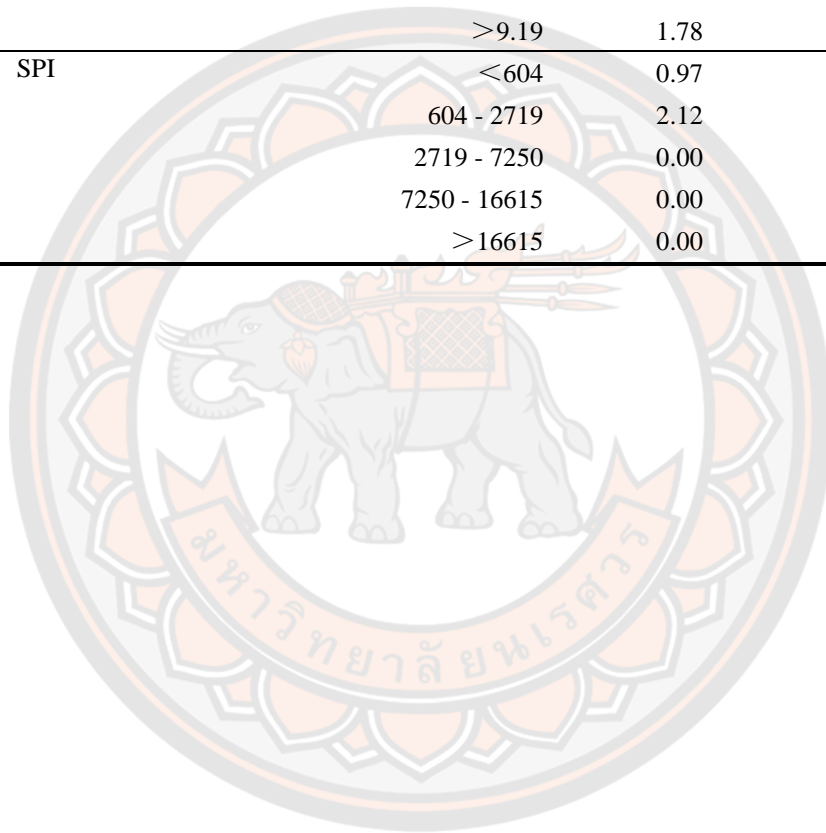
According to **Equation 3** which is defined in **Chapter II**, the minimum value of $(RF_{max} - RF_{min})$ of all LCFs has a deterministic role on the PR value of each LCF. The minimum value of $(RF_{max} - RF_{min})$ for the case of adopting all 14 LCFs is that of Precipitation, which means the cases that as long as Precipitation is adopted, the PR value of each LCF remains the same as the case of all 14 LCFs are adopted. For the only case that when Precipitation is absent, the PR value of each LCF also can be seen in **Table 7**. For the cases of adding one LCF into the 3 minimum LCFs in turn, only if the case of the added LCF has the less value of $(RF_{max} - RF_{min})$ than Slope Angle, Lithology, and LULC, the PR value of each LCF will be different with the case of when only the 3 minimum LCFs are adopted. The PR values of each adding LCF case can be seen in **Table 8**.

Table 6 Frequency Ratio and Relative Frequency Value for Each Classification of Each Factor, and Predictor Rate Value for Each Factor

Factor Name	Classification	FR Value	RF Value	PR Value
Slope Angle	0 - 8°	1.20	21	1.70
	0 - 14°	1.07	19	
	14 - 20°	1.20	21	
	20 - 26°	0.97	17	
	26 - 32°	0.74	13	
	32 - 38°	0.58	10	
	> 38°	0.00	0	
Distance to River	0 - 50 m	1.30	15	1.48
	50 - 100 m	2.14	25	
	100 - 150 m	2.41	28	
	150 - 200 m	1.83	21	
	> 200 m	0.86	10	
Slope Aspect	Flat (-1)	0.00	0	1.35
	North (0-22.5)	0.71	8	
	Northeast (22.5-67.5)	1.25	14	
	East (67.5-112.5)	1.28	15	
	Southeast (112.5-157.5)	0.80	9	
	South (157.5-202.5)	1.46	17	
	Southwest (202.5-247.5)	0.93	11	
	West (247.5-292.5)	0.62	7	
	Northwest (292.5-337.5)	0.89	10	
	North (337.5-360)	0.84	10	
Lithology	Group A	2.15	11	1.80
	Group B	0.00	0	
	Group C	0.00	0	
	Group D	2.05	11	
	Group E	1.13	6	
	Group F	1.54	8	
	Group G	0.31	2	
	Group H	1.04	6	
	Group I	1.24	7	
	Group J	1.58	8	
	Group K	0.44	2	
	Group L	4.17	22	
	Group M	0.72	4	
	Group N	0.34	2	
Group O	0.86	5		

Factor Name	Classification	FR Value	RF Value	PR Value
	Group P	1.25	7	
LULC	Cultivated Land	1.47	6	6.49
	Forest	0.25	1	
	Grass Land	1.82	7	
	Shrubland	1.66	6	
	Wetland	0.00	0	
	Water Body	0.00	0	
	Artificial Surfaces	20.84	80	
Distance to Fault	< 500 m	1.89	22	3.24
	500 - 1000 m	3.67	43	
	1000 - 2000 m	1.17	14	
	2000 - 3000 m	0.55	6	
	3000 - 4000 m	0.26	3	
	> 4000 m	0.99	12	
Distance to Road	0 - 50 m	7.01	42	3.06
	50 - 100 m	3.58	22	
	100 - 150 m	3.55	21	
	150 - 200 m	1.69	10	
	>200 m	0.75	5	
Curvature	Concave	0.96	27	1.41
	Flat	1.58	45	
	Convex	1.00	28	
Elevation	< 760 m	1.85	23	1.34
	760 - 940 m	1.21	15	
	940 - 1110 m	0.62	8	
	1110 - 1280 m	0.58	7	
	1280 - 1470 m	0.54	7	
	1470 - 1710 m	1.44	18	
	> 1710 m	1.69	21	
Precipitation	<1450 mm	1.21	19	1.00
	1450 - 1580 mm	1.24	20	
	1580 - 1720 mm	0.52	8	
	1720 - 1840 mm	1.24	20	
	1840 - 1970 mm	0.47	8	
	1970 - 2140 mm	0.84	13	
	>2140 mm	0.70	11	
NDVI	<0.18	3.85	46	3.37
	0.18 - 0.24	2.82	33	
	0.24 - 0.29	1.01	12	
	0.29 - 0.34	0.41	5	
	>0.34	0.34	4	

Factor Name	Classification	FR Value	RF Value	PR Value
Soil Texture	Clay	0.80	18	3.23
	Sandy Clay Loam	0.92	21	
	Sandy Loam	0.93	21	
	Clay Loam	1.75	40	
	Sandy Silt Loam	0.00	0	
TWI	<4.87	0.86	14	1.23
	4.87 - 5.95	0.92	15	
	5.95 - 7.35	0.90	15	
	7.35 - 9.19	1.60	26	
	>9.19	1.78	29	
SPI	<604	0.97	31	5.56
	604 - 2719	2.12	69	
	2719 - 7250	0.00	0	
	7250 - 16615	0.00	0	
	>16615	0.00	0	



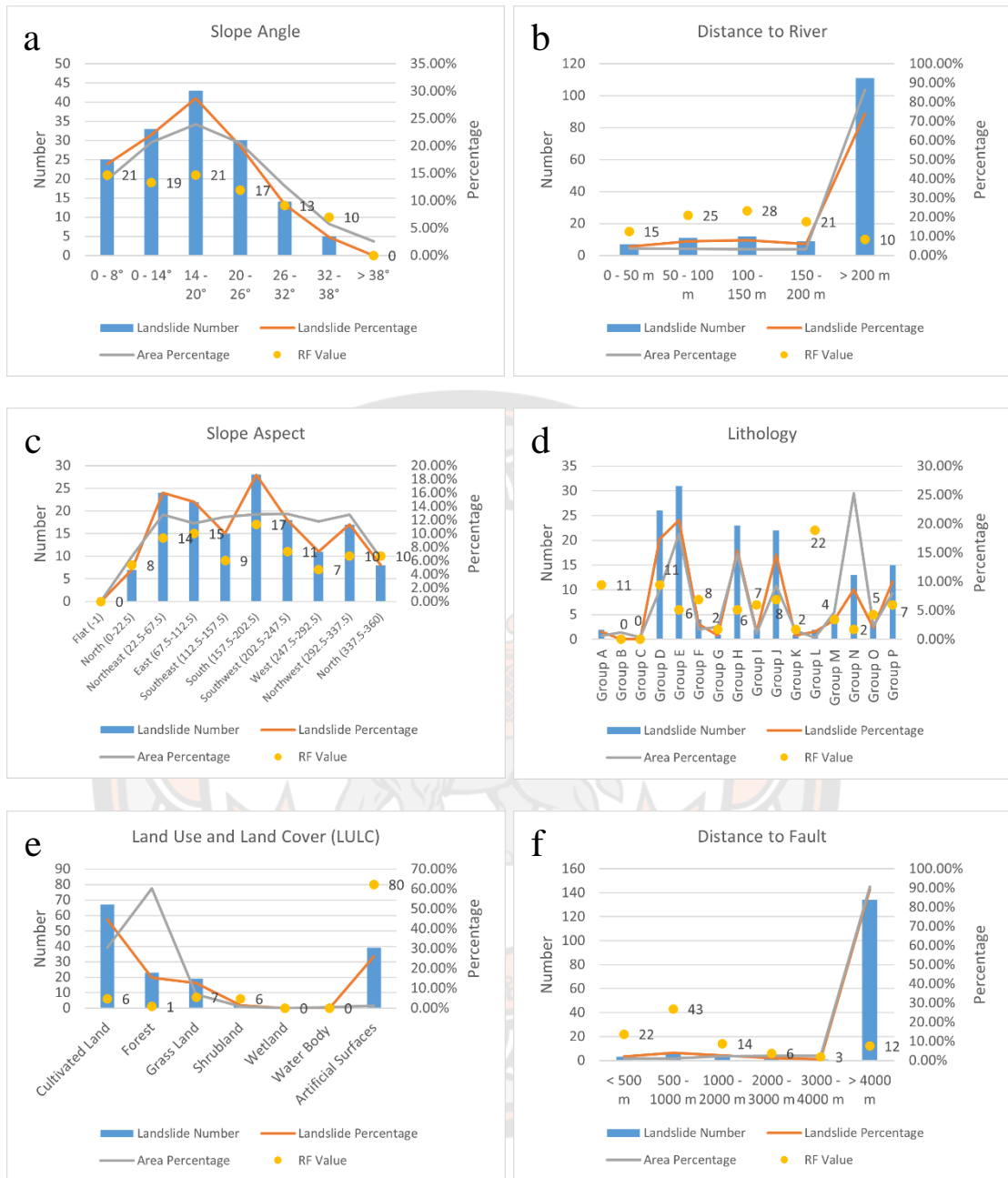


Figure 16 Landslide Number and Percentage in Each Classification, Area Percentage and RF Value of Each Classification of Slope Angle (a), Distance to River (b), Slope Aspect, Lithology (c), LULC, and Distance to Fault (d)

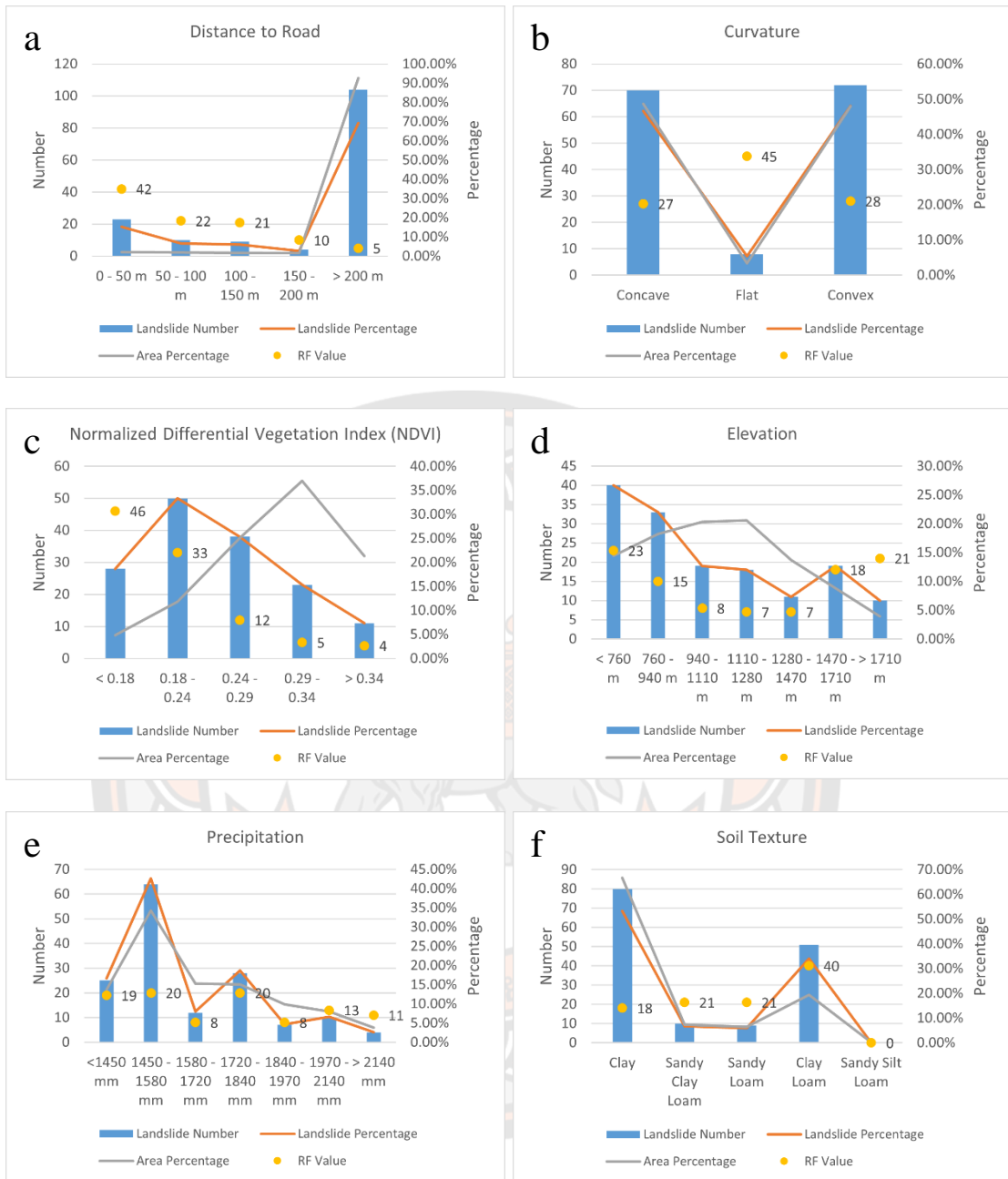


Figure 17 Landslide Number and Percentage in Each Classification, Area Percentage, and RF Value of Each Classification of Distance to Road (a), Curvature (b), NDVI (c), Elevation (d), Precipitation (e), and Soil Texture (f)

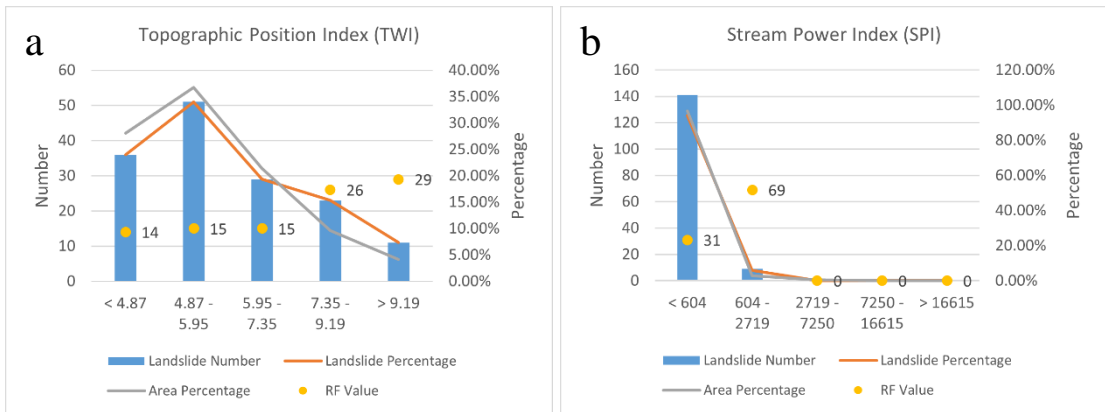


Figure 18. Landslide Number and Percentage in Each Classification, Area Percentage, and RF Value of Each Classification of TWI (a) and SPI (b)

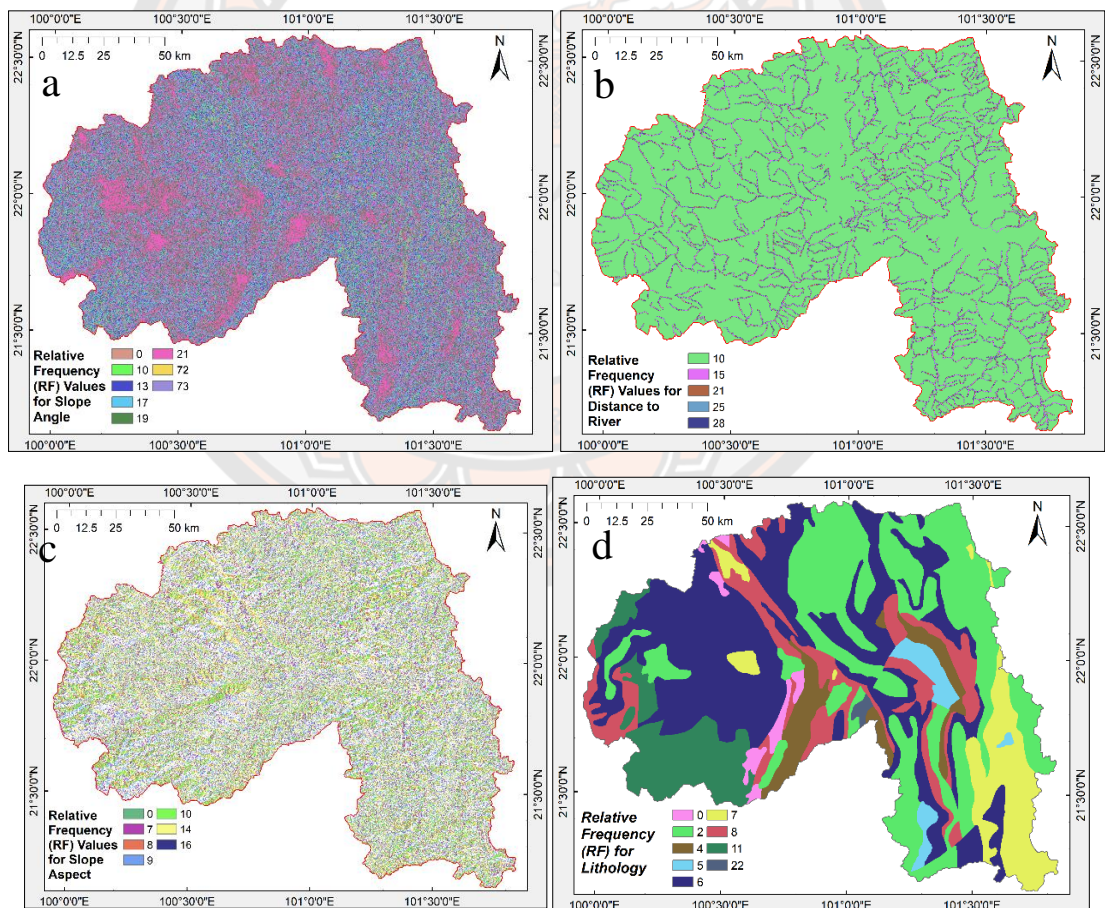


Figure 19 Maps of Relative Frequency (RF) Value for Each Classification of Slope Angle (a), Distance to River (b), Slope Aspect (c), and Lithology (d)

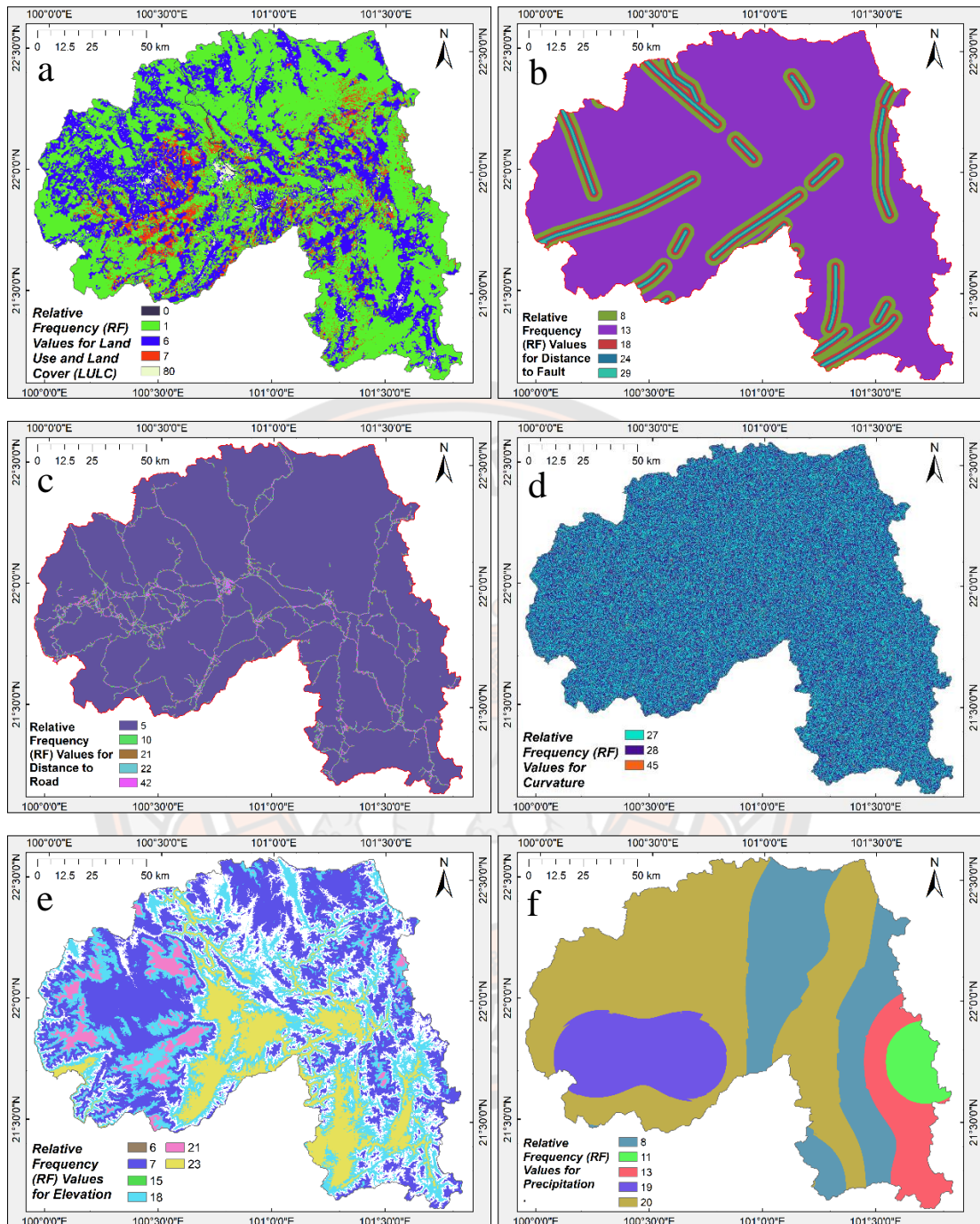


Figure 20 Single Layer Maps of Relative Frequency (RF) Value for Each Classification of LULC (a), Distance to Fault (b), Distance to Road, Curvature (c), Elevation (e), and Precipitation (f)

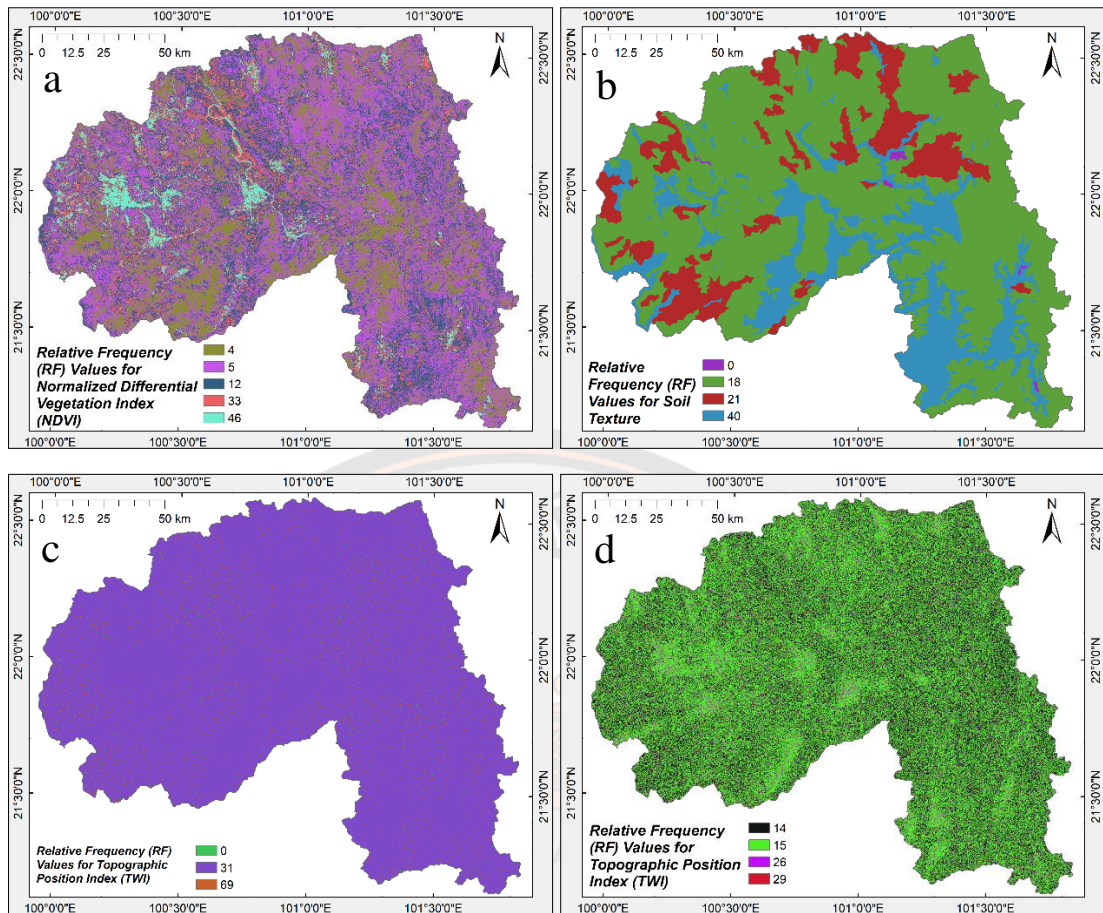


Figure 21 Single Layer Maps of Relative Frequency (RF) Value for Each Classification (a) of NDVI (b), Soil Texture (c), TWI, and SPI (d)

Table 7 Predictor Rate Value (PRV) Results of All 14 Input Factors and Removing One Factor in Turn

Input	PRV of	Slope Angle	Distance to River	Slope Aspect	Lithology	LULC	Distance to fault	Distance to road	Curvature	Elevation	Precipitation	NDVI	Soil Texture	TWI	SPI
14 Factors		1.70	1.48	1.35	1.80	6.49	3.24	3.06	1.41	1.34	1.00	3.37	3.22	1.23	5.56
Remove Slope Angle			1.48	1.35	1.80	6.49	3.24	3.06	1.41	1.34	1.00	3.37	3.22	1.23	5.56
Remove Distance to River		1.70		1.35	1.80	6.49	3.24	3.06	1.41	1.34	1.00	3.37	3.22	1.23	5.56
Remove Slope Aspect		1.70	1.48		1.80	6.49	3.24	3.06	1.41	1.34	1.00	3.37	3.22	1.23	5.56
Remove Lithology		1.70	1.48	1.35		6.49	3.24	3.06	1.41	1.34	1.00	3.37	3.22	1.23	5.56
Remove LULC		1.70	1.48	1.35	1.80		3.24	3.06	1.41	1.34	1.00	3.37	3.22	1.23	5.56
Remove Distance to fault		1.70	1.48	1.35	1.80	6.49		3.06	1.41	1.34	1.00	3.37	3.22	1.23	5.56
Remove Distance to road		1.70	1.48	1.35	1.80	6.49	3.24		1.41	1.34	1.00	3.37	3.22	1.23	5.56
Remove Curvature		1.70	1.48	1.35	1.80	6.49	3.24	3.06		1.34	1.00	3.37	3.22	1.23	5.56
Remove Elevation		1.70	1.48	1.35	1.80	6.49	3.24	3.06	1.41		1.00	3.37	3.22	1.23	5.56
Remove Precipitation		1.70	1.48	1.35	1.80	6.49	3.24	3.06	1.41	1.00		3.37	3.22	1.23	5.56
Remove NDVI		1.70	1.48	1.35	1.80	6.49	3.24	3.06	1.41	1.34	1.00		3.22	1.23	5.56
Remove Soil Texture		1.70	1.48	1.35	1.80	6.49	3.24	3.06	1.41	1.34	1.00	3.37		1.23	5.56
Remove TWI		1.70	1.48	1.35	1.80	6.49	3.24	3.06	1.41	1.34	1.00	3.37	3.22		5.56
Remove SPI		1.70	1.48	1.35	1.80	6.49	3.24	3.06	1.41	1.34	1.00	3.37	3.22	1.23	

Table 8 Predictor Rate Value (PRV) Results of Minimum 3 Input Factors and Adding One Factor in Turn

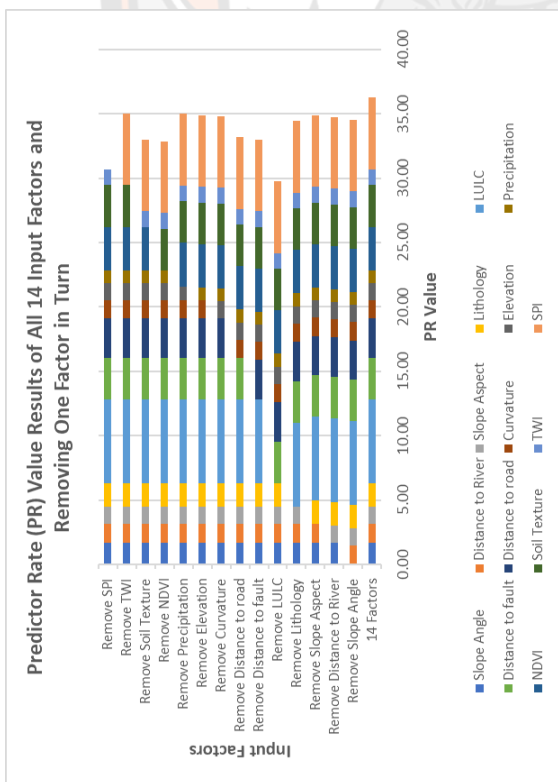
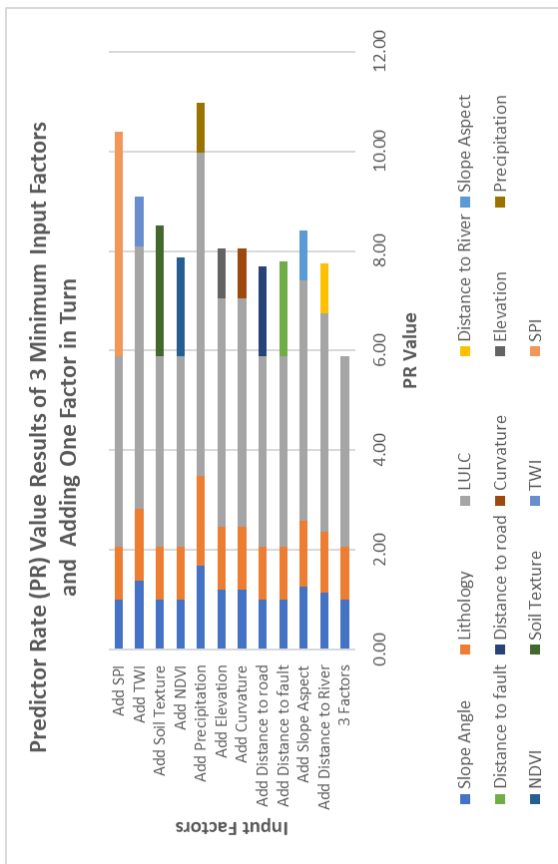


Figure 22 Predictor Rate value (PRV) Results of Inputting All 14 Factors and Removing One Factor in Turn

Figure 23 Predictor Rate value (PRV) Results of Inputting 3 Minimum Factors and Removing One Factor in Turn

4.1.3 Landslide Susceptibility Mapping (LSM) and AUC Results

4.1.3.1 Landslide Susceptibility Mapping (LSM) Results for Cases of Inputting All 14 Factors and Removing Factor in Turn

Based on the RF values of each classification of each LCF and the PR value for each LCF of all designed cases, the LSI of each case is calculated using **Equation 2** which is defined in **Chapter II**, Then LSM is conducted using ArcGIS based on each LSI. LSM results of cases of inputting all 14 factors, removing Slope Angle, removing Distance to River, and removing Slope Aspect from the 14 factors are shown in **Figure 24**.

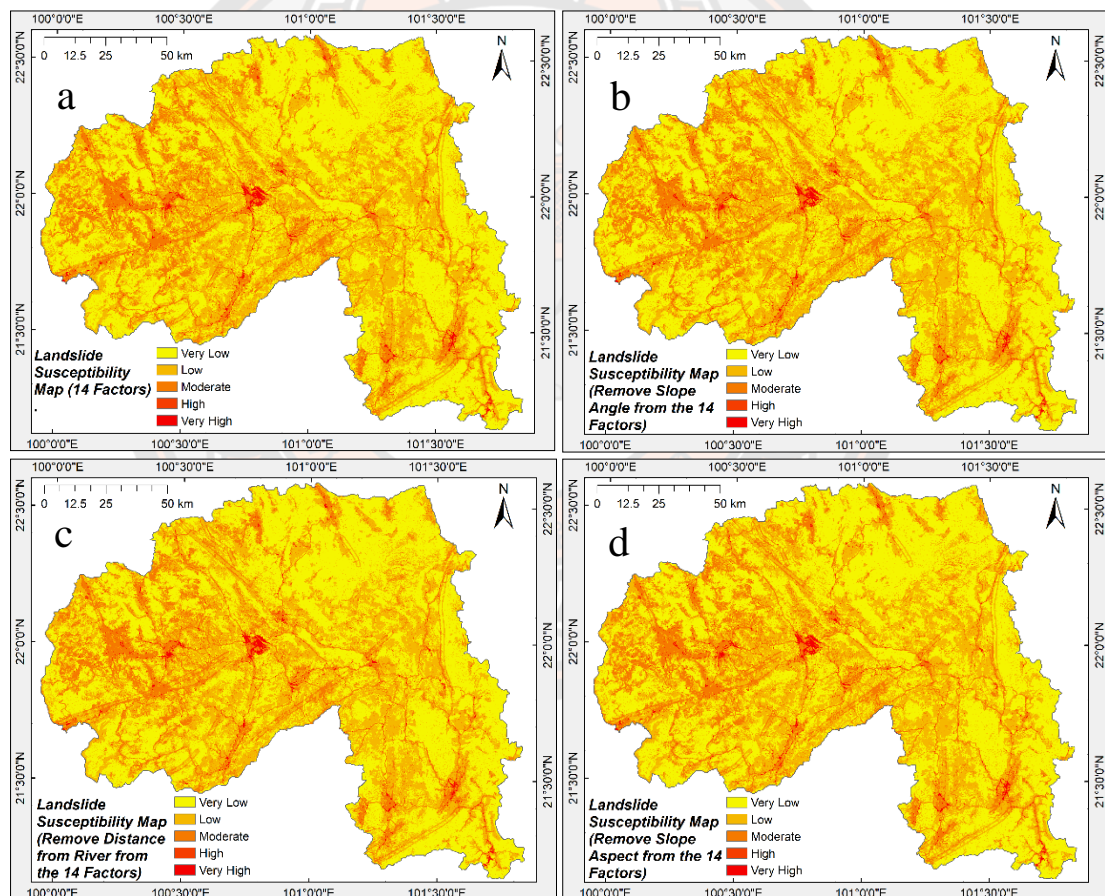


Figure 24 Landslide Susceptibility Mapping (LSM) Results for the Case of Inputting All 14 Factors (a), Removing Slope Angle (b), Removing Distance to River (c), and Removing Slope Aspect (d) from the 14 Factors

The LSM results of cases of removing Lithology, removing LULC, removing Distance to Fault, removing Distance to Road, removing Curvature, and removing Elevation from the 14 factors are shown in **Figure 25**.

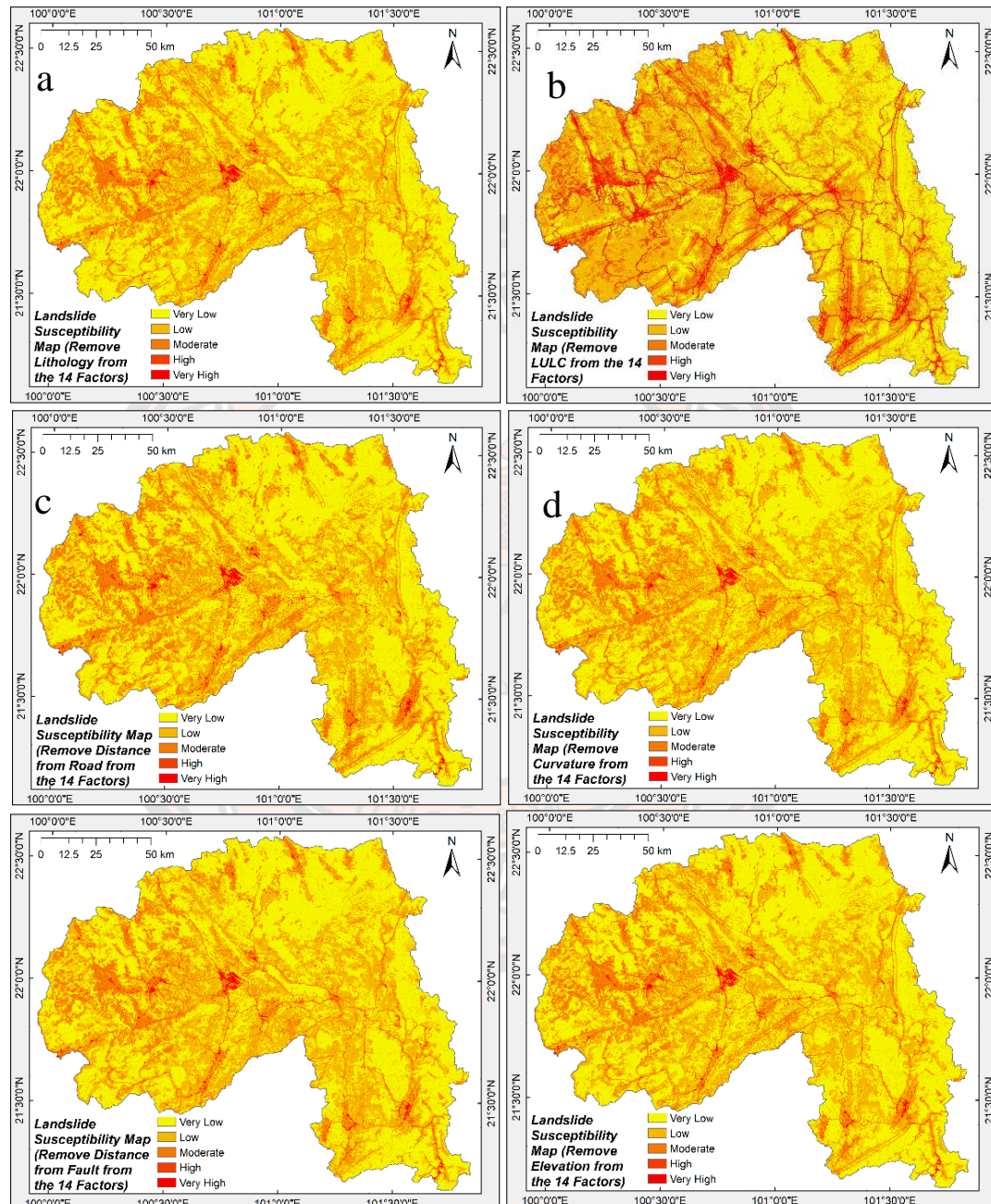


Figure 25 Landslide Susceptibility Mapping (LSM) Results for the Case of Removing Lithology (a), Removing LULC (b) Removing Distance to Fault (c), Removing Distance to Road (d), Removing Curvature (e), and Removing Elevation (f) from the 14 Factors

The LSM results of cases of removing Precipitation, removing NDVI, removing Soil Texture, removing TWI, and removing SPI from the 14 factors are shown in **Figure 26**.

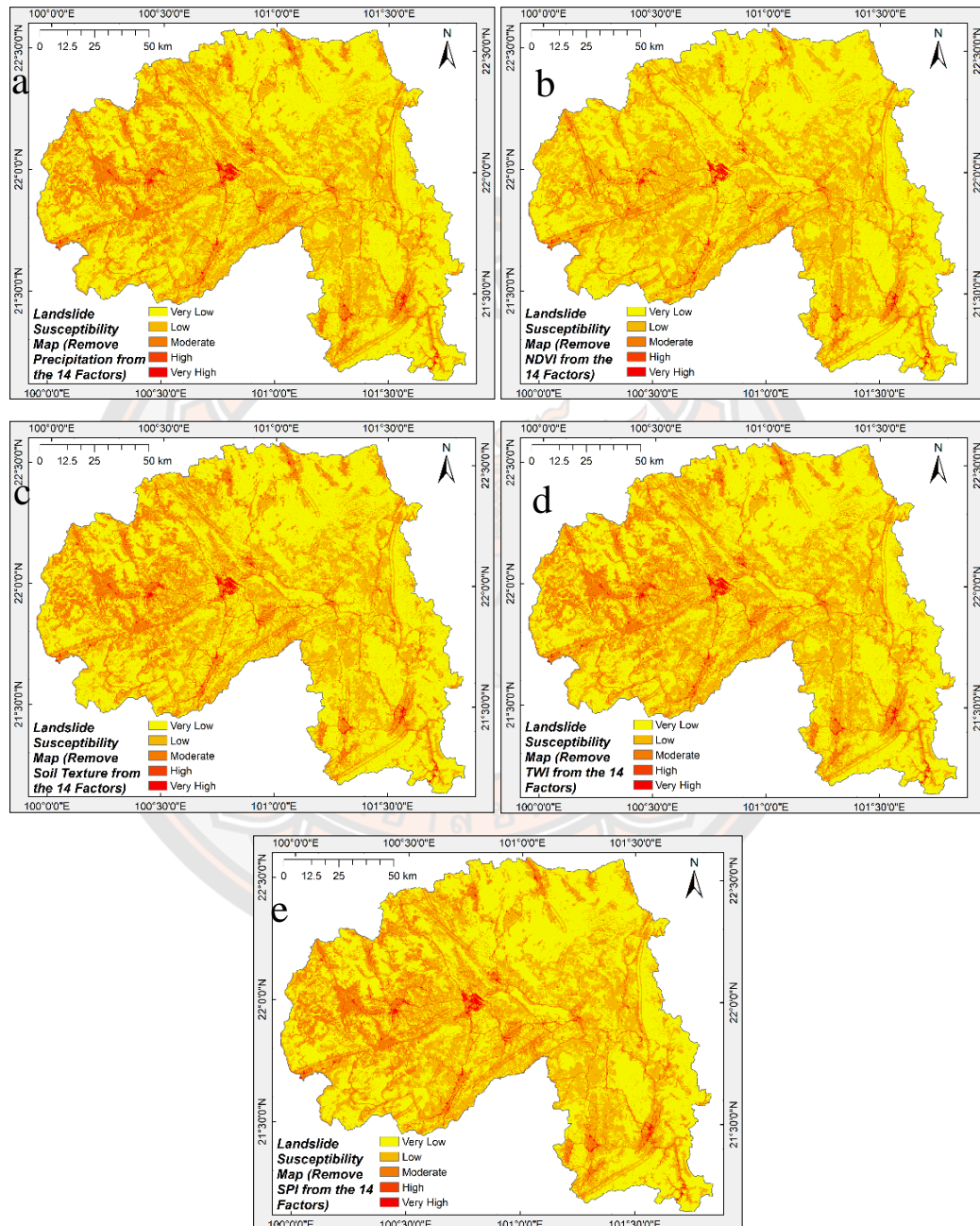


Figure 26 Landslide Susceptibility Mapping (LSM) Results for the Case of Removing Precipitation (a), Removing NDVI (b), Removing Soil Texture (c), Removing TWI (d), and Removing SPI (e) from the 14 Factors

The area percentage of very low, low, moderate, high, very high, and high landslide susceptibility levels of inputting all 14-factor case and removing factor cases, and their area percentage variation of High and Very High level is shown in **Table 9**.

In this study, we focus on the variation of High and Very High levels between cases of removing one LCF in turn from the whole and the case of adopting all 14 LCFs. The case of removing LULC shows a significant variation with area percentage of High-level landslide susceptibility increased 6.79% and Very High-level increased 2.01%, the case of removing Distance to Road shows the second significant variation with area percentage of High-level landslide susceptibility decreased 0.38% and Very High-level increased 0.38%, while cases of removing Slope Angle, removing Distance to River, removing Slope Aspect, removing Lithology, removing Distance to Fault, removing Elevation, removing NDVI, removing Soil Texture, and removing SPI have only slight area percentage variation of High and Very High-level landslide susceptibility, with variation values ranging from 0.01% to 0.04%. Cases of removing Curvature, removing Precipitation, and removing TWI show no area percentage variation for High and Very High-level landslide susceptibility.

Table 9 The Area Percentage of Each Landslide Susceptibility Level of Inputting all 14-Factor Case and Removing Factor Cases, and the Area Percentage Variation of High and Very High Level

	Very Low	Low	Moderate	High	Very High	“High” Variation	“Very High” Variation
14 Factors	47.50%	36.75%	14.34%	0.66%	0.58%	0.00%	0.00%
Remove Slope Angle	47.67%	36.72%	14.37%	0.64%	0.60%	-0.02%	0.02%
Remove Distance to River	47.97%	36.77%	14.02%	0.62%	0.62%	-0.04%	0.04%
Remove Slope Aspect	47.85%	36.66%	14.25%	0.64%	0.60%	-0.02%	0.02%
Remove Lithology	48.32%	36.25%	14.19%	0.63%	0.61%	-0.03%	0.03%
Remove Curvature	47.67%	36.79%	14.30%	0.66%	0.58%	0.00%	0.00%
Remove LULC	36.24%	35.86%	17.86%	7.45%	2.59%	6.79%	2.01%

	Very Low	Low	Moderate	High	Very High	“High” Variation	“Very High” Variation
Remove Distance to Fault	47.51%	37.54%	13.71%	0.63%	0.61%	-0.03%	0.03%
Remove Distance to Road	47.93%	33.00%	17.84%	0.28%	0.96%	-0.38%	0.38%
Remove Elevation	49.37%	35.55%	13.84%	0.64%	0.59%	-0.02%	0.01%
Remove Precipitation	48.15%	36.73%	13.88%	0.66%	0.58%	0.00%	0.00%
Remove NDVI	51.88%	39.69%	7.20%	0.68%	0.56%	0.02%	-0.02%
Remove Soil Texture	50.10%	33.57%	15.08%	0.63%	0.61%	-0.03%	0.03%
Remove SPI	48.53%	36.87%	13.51%	0.64%	0.60%	-0.02%	0.02%
Remove TWI	47.80%	36.75%	14.21%	0.66%	0.58%	0.00%	0.00%

4.1.3.2 Area Under the Curve (AUC) values for Cases of Inputting All 14 Factors and Removing Factor in Turn

The AUC values for cases of inputting all 14 LCFs and removing one LCF in turn are shown in **Table 10**, and the curve chart of each case can be seen in **Figure 27 - 29**. **Figure 30** shows the Area Under the Curve (AUC) value compared between the case of inputting all 14 LCFs and the cases of removing 14 factors in turn.

Table 10 Area Under the Curve (AUC) Values for Cases of Inputting All 14 LCFs and Removing One LCF in Turn

Input	AUC value	AUC variation
14 Factors	85.40%	0.00%
Remove Slope Angle	85.40%	0.00%
Remove Distance to River	85.30%	-0.10%
Remove Slope Aspect	85.30%	-0.10%
Remove Lithology	84.50%	-0.90%
Remove LULC	80.50%	-4.90%
Remove Distance to Fault	85.10%	-0.30%
Remove Distance to Road	84.50%	-0.90%
Remove Curvature	85.30%	-0.10%
Remove Elevation	85.10%	-0.30%
Remove Precipitation	85.30%	-0.10%
Remove NDVI	84.70%	-0.70%
Remove Soil Texture	85.20%	-0.20%
Remove TWI	85.40%	0.00%
Remove SPI	86.30%	0.90%

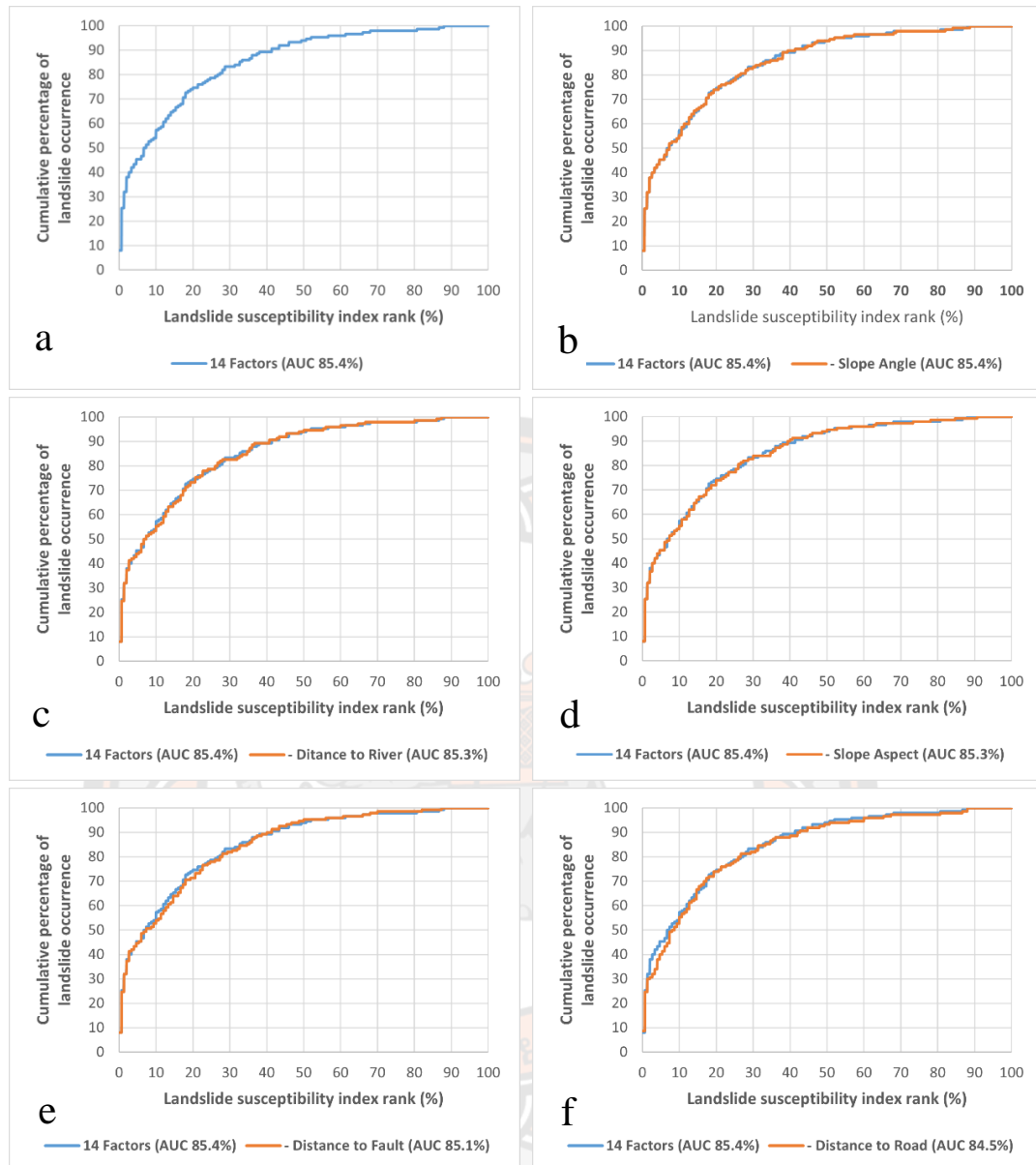


Figure 27 AUC Results for Cases of Inputting All 14 LCFs (a), Removing Slope Angle (b), Removing Distance to River (c), Removing Slope Aspect (d), Removing Lithology (e), and Removing LULC (f) from the 14 LCFs

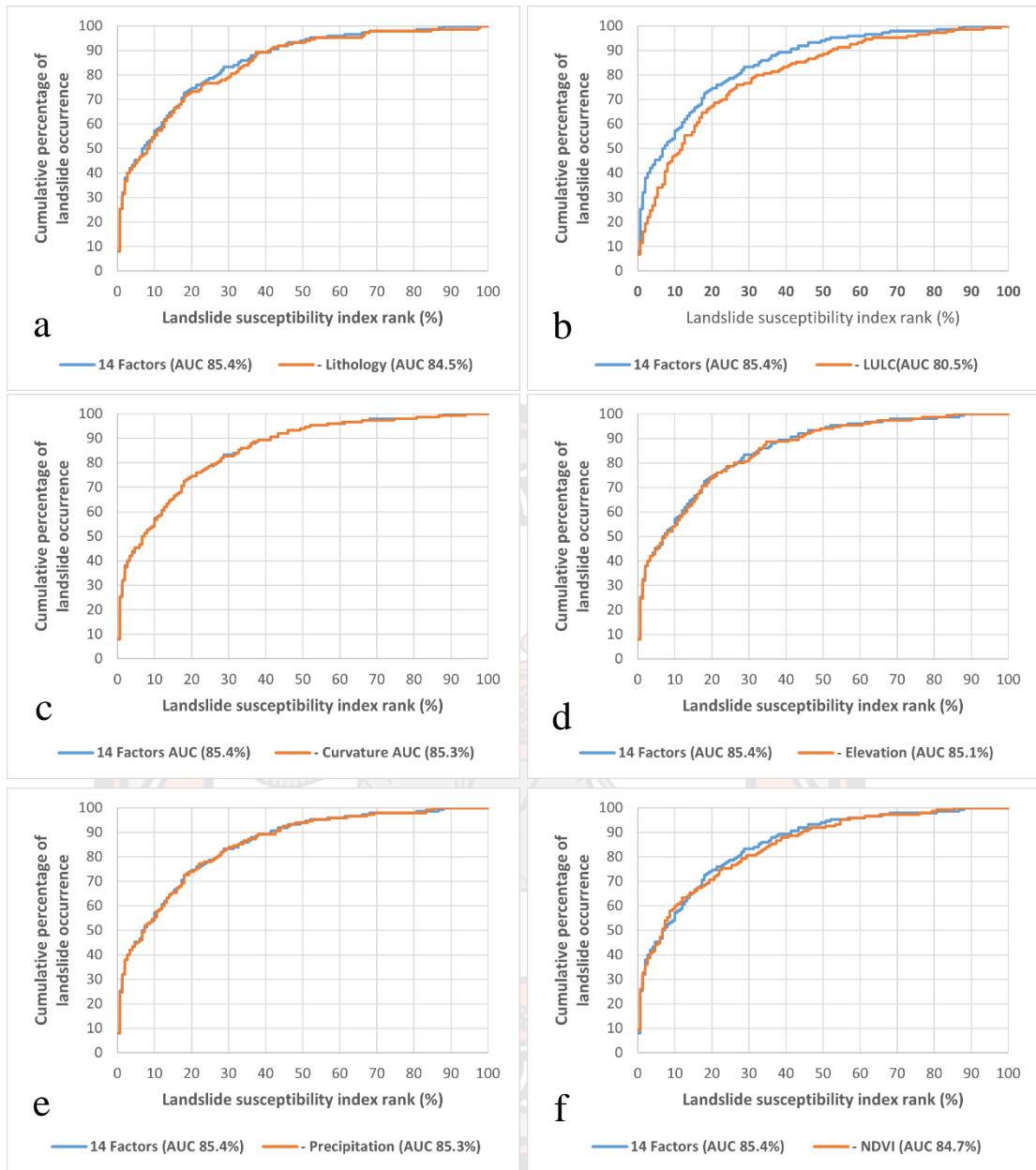


Figure 28 AUC Results for the Case of Removing Distance to Fault (a), Removing Distance to Road (b), Removing Curvature (c), Removing Elevation (d), Removing Precipitation (e), and Removing NDVI (f) from the 14 LCFs

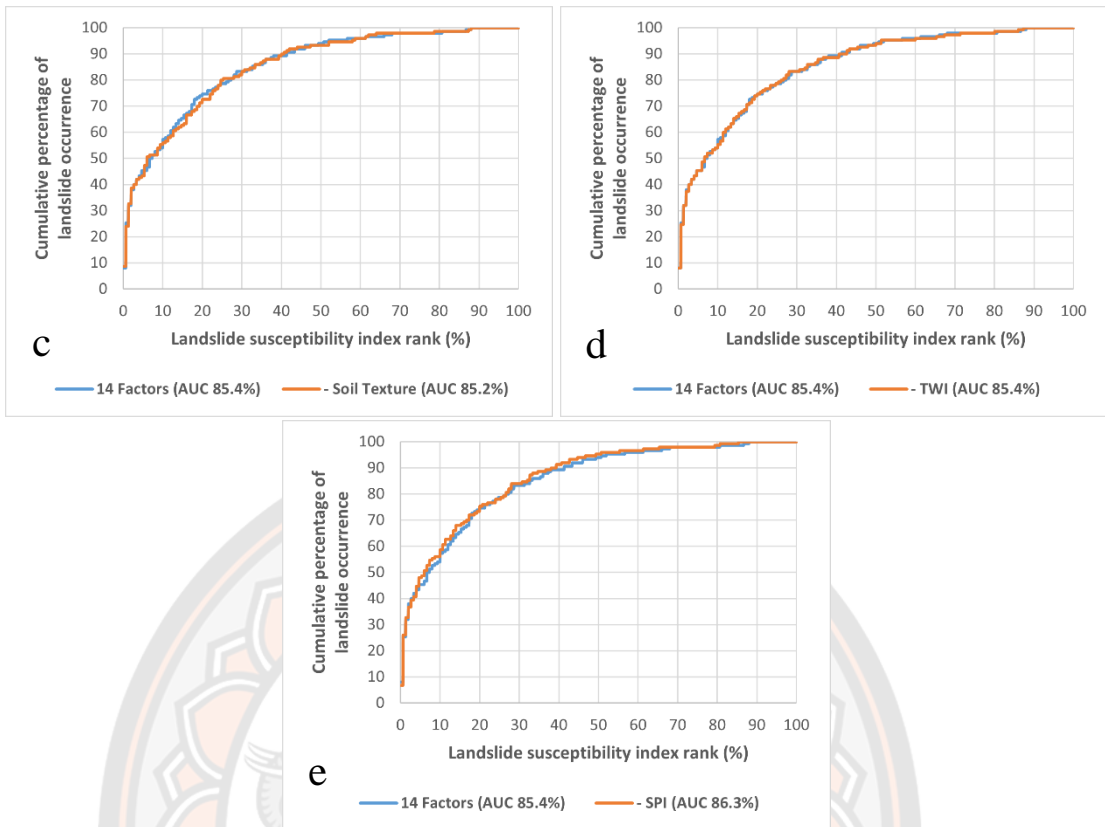


Figure 29 AUC Results for the Case of Removing Soil Texture (a), Removing TWI (b), and Removing SPI (c) from the 14 LCFs.

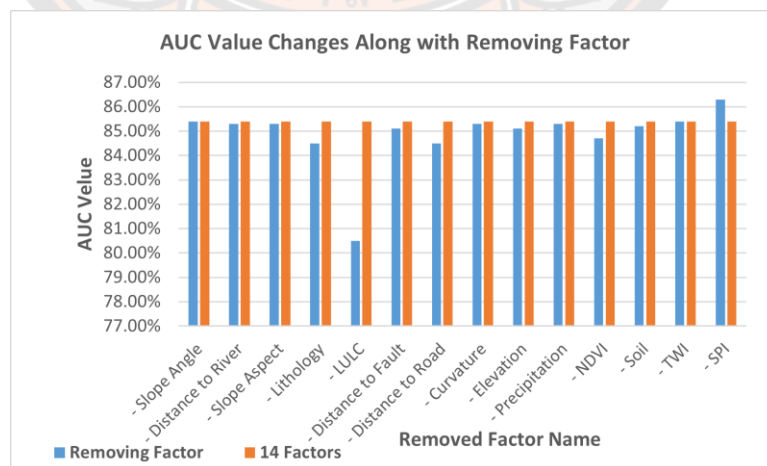


Figure 30 Area Under the Curve (AUC) Value Comparison Between the Case of Inputting All 14 LCFs and Cases of Removing Other 14 Factors in Turn

Generally, the greater the AUC value, the better the prediction quality of the LSM model. According to the AUC variation values between cases of removing one LCF and cases of adopting all 14 LCFs, removing LULC causes the AUC value of the LSM to decrease by 4.9%, which is the highest AUC value change of the cases of removing factor. It means LULC has a significant role in improving the LSM model. The cases of removing Lithology and removing Distance to Road have the second-highest AUC variation value which equals to 0.9%, the case of removing NDVI has the third-highest AUC variation value of 0.7%, the case of removing elevation has an AUC variation value of 0.3%, the case of removing Soil Texture has an AUC variation value of 0.2%, the cases of removing Distance to River, removing Slope Aspect, removing Curvature, and removing Precipitation have an AUC variation value of 0.1%. Cases of removing Slope Angle and removing TWI do not cause the AUC value change. When removing SPI from the 14 LCFs, the AUC value increased 0.9%, which means SPI has a negative effect in improving the LSM model quality.

4.1.3.3 Landslide Susceptibility Mapping (LSM) Results for Cases of Inputting 3 Minimum Factors and Adding Factor in Turn

LSM results of cases of inputting 3 minimum factors (slope angle, lithology, and LULC) only, adding Distance to River, adding Slope Aspect, adding Distance to Fault, adding Distance to Road, and adding Curvature into the 3-factor group are shown in **Figure 31**.

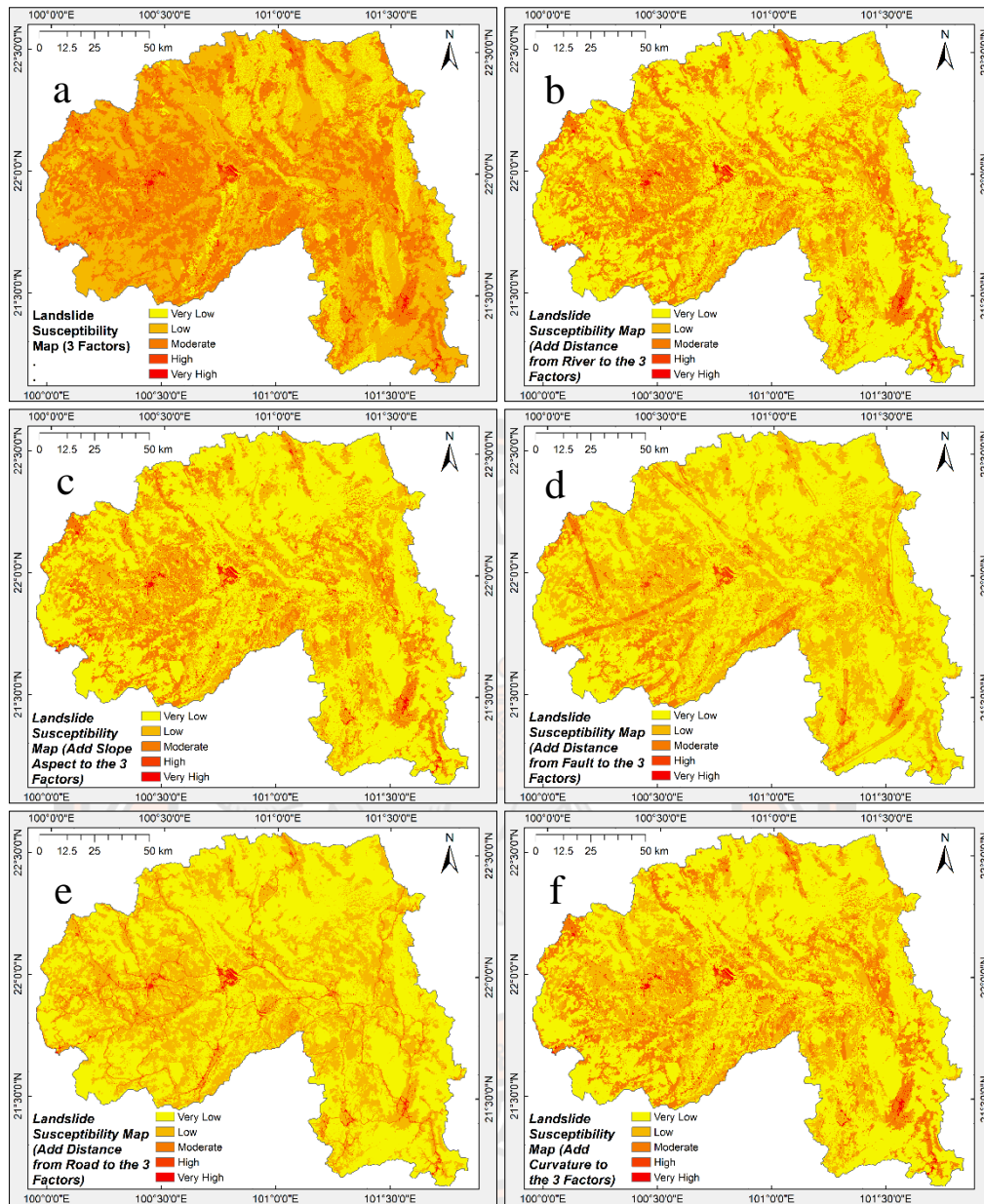


Figure 31 Landslide Susceptibility Mapping (LSM) Results for the Case of Inputting 3 Minimum Factors (a), Adding Distance to River Into the 3-Factor Group (b), Adding Slope Aspect (c), Adding Distance to Fault (d), Adding Distance to Road (e), and Adding Curvature (f) to the 3-Factor Group

LSM results of cases of adding Elevation, adding Precipitation, adding NDVI, adding Soil Texture, adding Curvature, adding Elevation, adding Precipitation, adding TWI, and adding SPI into the 3-factor group are shown in **Figure 32**.

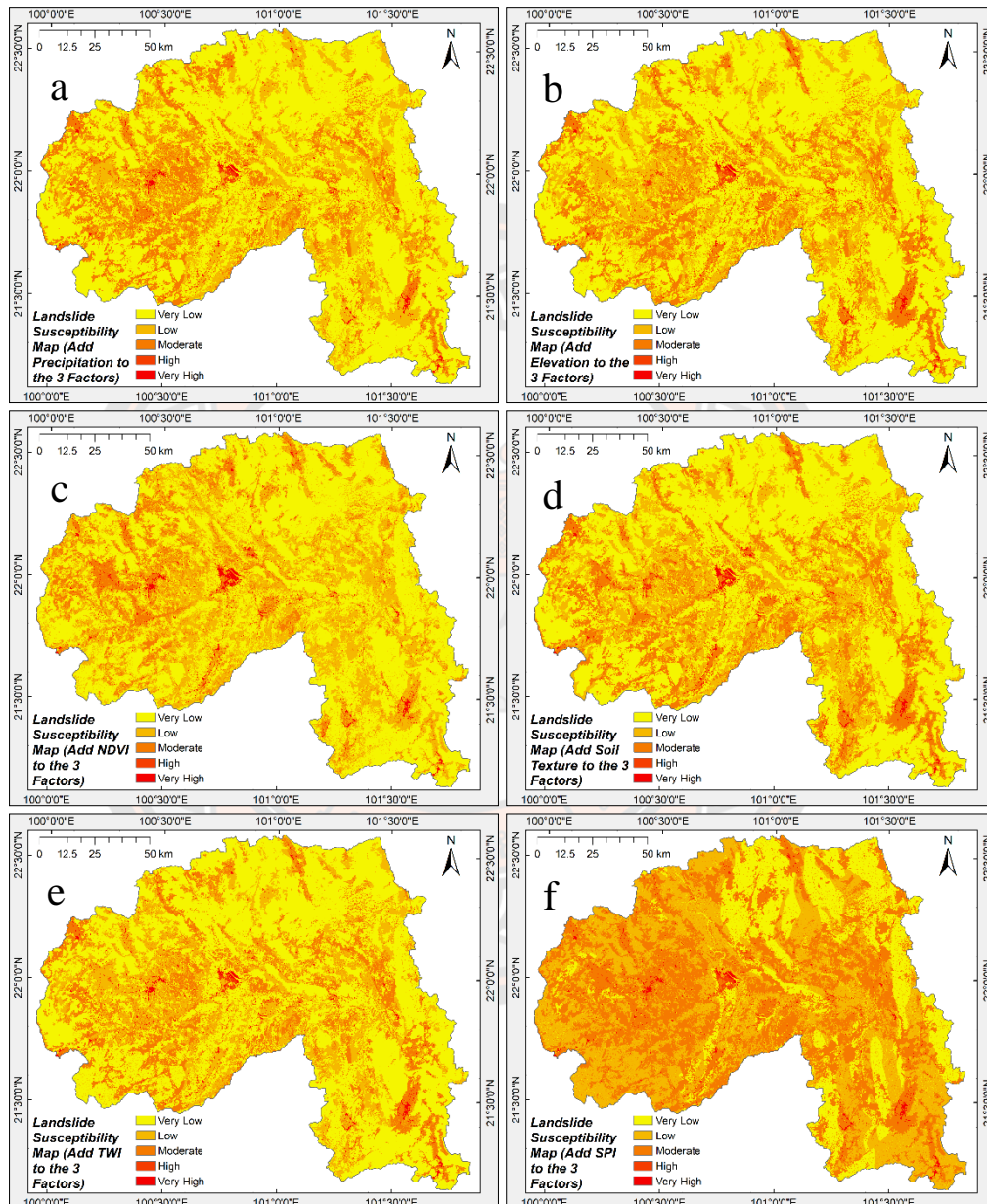


Figure 32 Landslide Susceptibility Mapping (LSM) Results for the Case of Adding Elevation (a), Adding Precipitation (b), Adding NDVI (c), Adding Soil Texture (d), Adding SPI (e), and Adding TWI (f) to the 3-Factor Group

The area percentage of very low, low, moderate, high, very high, and high landslide susceptibility level of inputting 3 minimum factors case and adding factor cases, and their area percentage variation of High and Very High level is shown in **Table 11**.

In this study, we focus on the variation of High and Very High levels between cases of adding one LCF in turn to the 3 minimum factors and the case of adopting 3 minimum LCFs (slope angle, lithology, and LULC) only. The cases of adding Distance to fault shows the most significant variation with area percentage of High-level landslide susceptibility increased 0.80% and Very High-level decreased 0.8%, the case of adding Distance to Road shows the second significant variation with area percentage of High-level landslide susceptibility increased 0.48% and Very High-level decreased 0.48%, the cases of adding Elevation and adding NDVI also show a prominent variation with the area percentage of the former increased 0.23% in High and decreased 0.23% in Very High landslide susceptibility level, the later decreased 0.24% in High and increased 0.23% in Very High landslide susceptibility level. While cases of adding Slope Aspect, adding Precipitation, adding Soil Texture, adding TWI, and adding SPI have only slight area percentage variation of High and Very High-level landslide susceptibility, with variation values less than 0.10%. Cases of adding Distance to River, adding Curvature have no area percentage variation for High and Very High-level landslide susceptibility.

Table 11 The Area Percentage of Each Landslide Susceptibility Level of Inputting 3 Minimum Factors (Slope Angle, Lithology, and LULC) Case and Adding Factor Cases, and Their Area Percentage Variation of High and Very High Level

	Very Low	Low	Moderate	High	Very High	“High” Variation	“Very High” Variation
3 Factors	15.70%	44.79%	38.27%	0.40%	0.84%	0.00%	0.00%
Add Distance to River	59.91%	14.89%	23.97%	0.40%	0.84%	0.00%	0.00%
Add Slope Aspect	60.50%	19.98%	18.30%	0.31%	0.93%	-0.09%	0.09%
Add Curvature	60.43%	20.42%	17.92%	0.40%	0.84%	0.00%	0.00%
Add Distance to Fault	58.38%	32.01%	8.37%	1.20%	0.04%	0.80%	-0.80%
Add Distance to Road	58.62%	36.05%	4.09%	0.88%	0.36%	0.48%	-0.48%
Add Elevation	59.48%	18.17%	21.12%	0.63%	0.61%	0.23%	-0.23%

	Very Low	Low	Moderate	High	Very High	“High” Variation	“Very High” Variation
Add Precipitation	60.48%	19.42%	18.86%	0.41%	0.83%	0.01%	-0.01%
Add NDVI	54.88%	32.61%	11.27%	0.16%	1.07%	-0.24%	0.23%
Add Soil Texture	55.34%	22.57%	20.87%	0.46%	0.78%	0.06%	-0.06%
Add SPI	22.33%	36.45%	39.83%	0.40%	0.83%	0.00%	-0.01%
Add TWI	60.05%	19.75%	18.96%	0.37%	0.87%	-0.03%	0.03%

4.1.3.4 Area Under the Curve (AUC) Values for Cases of Inputting 3 Minimum Factors and Adding Factor in Turn

The AUC values for cases of inputting 3 minimum factors and adding other 11 factors in turn, are shown in **Table 12**, and the plots of each case can be seen in **Figure 33 - 34**. **Figure 35** shows the Area Under the Curve (AUC) value comparison between the case of inputting 3 minimum LCFs and the case of adding other 11 factors in turn.

Table 12 Area Under the Curve (AUC) Values for Cases of Inputting All 14 Factors and Removing Factors in Turn

Input	AUC value	AUC variation
3 Factors	82.70%	0.00%
Add Distance to River	82.90%	0.20%
Add Slope Aspect	82.90%	0.20%
Add Distance to Fault	83.40%	0.70%
Add Distance to Road	84.50%	1.80%
Add Curvature	83.00%	0.30%
Add Elevation	83.60%	0.90%
Add Precipitation	83.00%	0.30%
Add NDVI	83.70%	1.00%
Add Soil Texture	83.00%	0.30%
Add TWI	82.90%	0.20%
Add SPI	81.60%	-1.10%

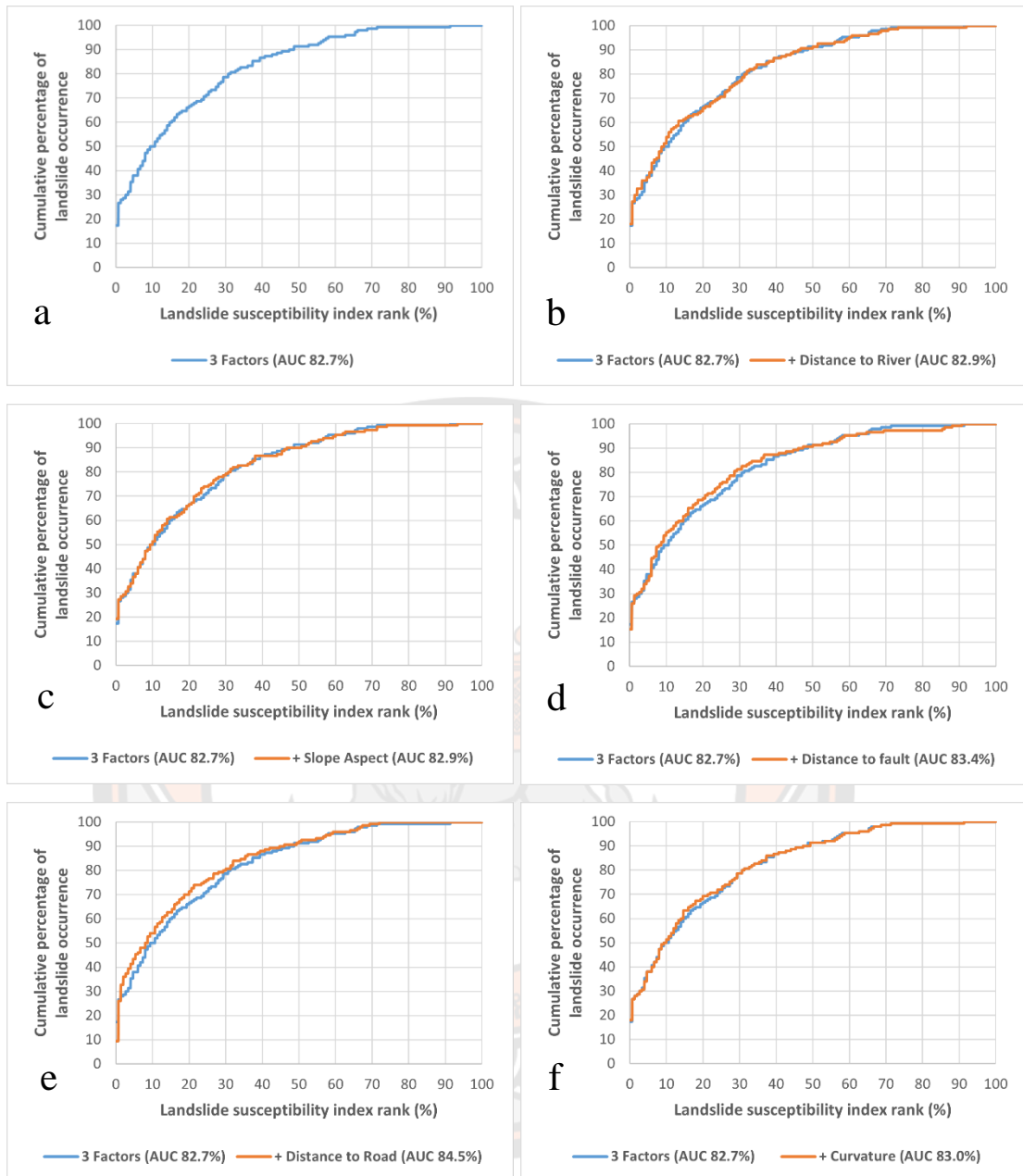


Figure 33 AUC Results for the Case of Inputting 3 Minimum LCFs (a), Adding Distance to River (b), Adding Slope Aspect (c), Adding Distance to Fault (d), Adding Distance to Road (e), and Adding Curvature (f) to the 3 Minimum LCFs.

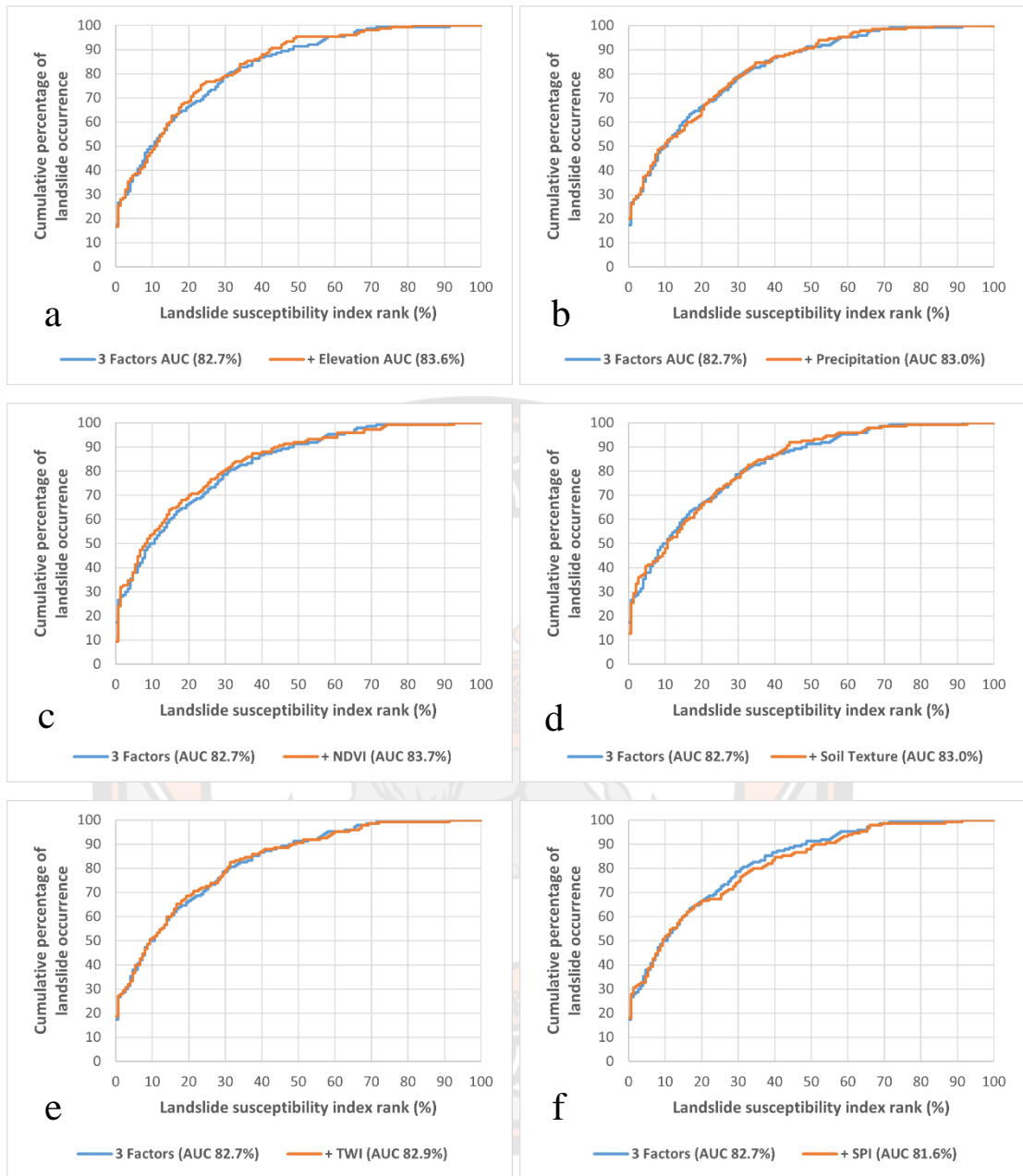


Figure 34 AUC Results for the Case of Adding Elevation (a), Adding Precipitation (b), Adding NDVI (c), Adding Soil Texture (d), Adding TWI (e), and Adding SPI (f) to the 3 Minimum LCFs

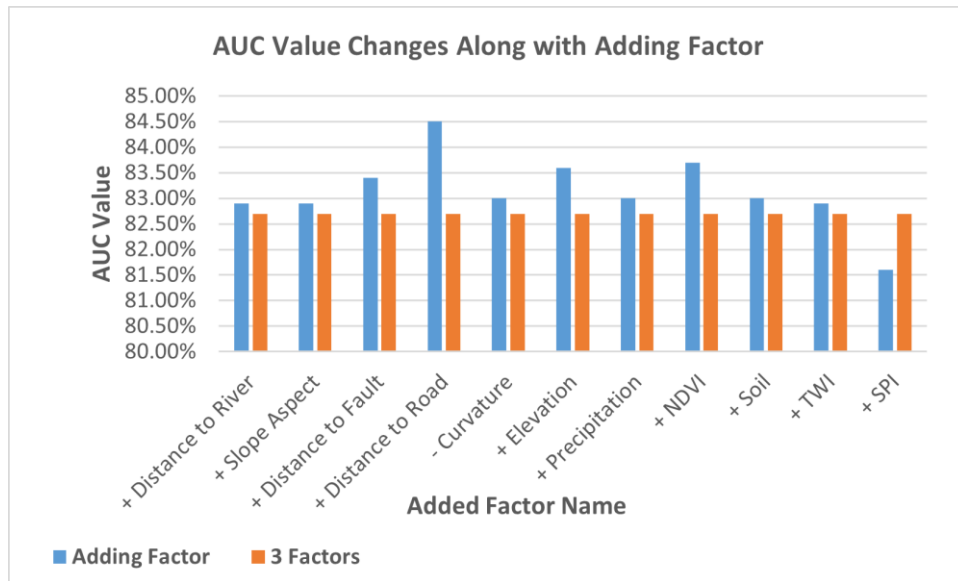


Figure 35 AUC Value Comparison Between the Case of Inputting 3 Minimum LCFs and Case of Adding Other 11 Factors in Turn

According to the AUC variation values between cases of adding the 11 LCFs in turn, and the case of adopting 3 minimum LCFs only, adding Distance to Road causes the AUC value of the LSM to increase by 1.8%, which is the highest AUC value change of the cases of removing factor. It means Distance to Road has a significant role in improving the prediction quality of the LSM model. The cases of adding NDVI, adding Elevation, and adding Distance to Fault have the second-highest AUC variation value of 1.00%, 0.90%, and 0.70%, respectively. Moreover, the cases of adding Distance to River, adding Slope Aspect, adding Curvature, adding Precipitation, and adding TWI cause only AUC value variation less than or equal to 0.3%. The cases of removing Slope Angle and removing TWI do not cause the AUC value change. When adding SPI to the 3 minimum LCFs, the AUC value decreased 1.10%, which means SPI has a negative effect in improving the LSM model quality, which is consistent with the case of removing SPI from the 14 LCFs.

4.1.3.5 Area Under the Curve (AUC) Value Variation for Both Removing and Adding Single Factor Cases

Based on the principle that at least 3 aspects of factors must be input in GIS analysis, including lithology, topography, and land use for LSA (Milevski et al.,

2019), Slope Angle, Lithology and LULC are confirmed to be included as the final LCFs. **Figure 36** shows the Area Under the Curve (AUC) value variation of other 11 LCFs of both removing and adding Distance to River, Aspect, Fault, Distance to Road, Curvature, Elevation, Precipitation, NDVI, Soil Texture, TWI, and SPI.

According to **Figure 36**, the AUC value decreased when SPI is involved and increased when SPI is absent, which means SPI shows a negative effect in improving the prediction quality of the LSM model. TWI does not cause an AUC value change when it is removed from the participating LCFs. Other processes of both when the LCF is included or excluded, all show positive effects in improving the prediction quality of the LSM model. Of which, Distance to Road, NDVI, Elevation, and Distance to Fault cause the greatest AUC values to change in both factor involved and absent cases, which causing the AUC value variation greater than or equal to 0.3%, while other LCFs cause up to 0.2% of that in factor absent cases and causing the AUC value variation greater than or equal to 0.7%, while other LCFs cause up to 0.3% in factor involved cases.

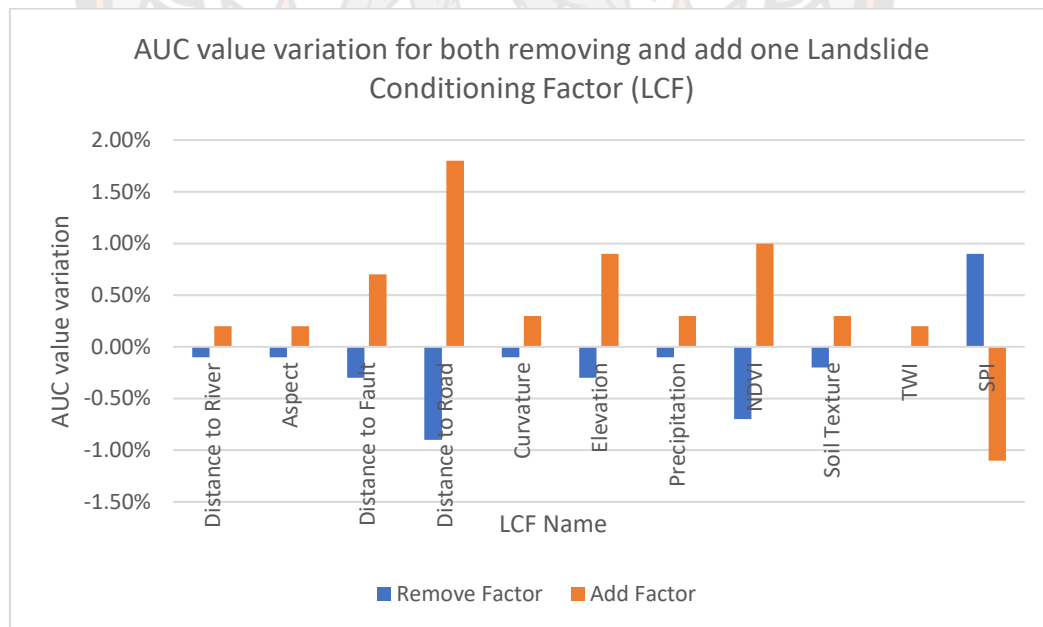


Figure 36 AUC Value Variation of Both Removing and Adding Distance to River, Aspect, Fault, Distance to Road, Curvature, Elevation, Precipitation, NDVI, Soil Texture, TWI, and SPI

4.1.4 Results of Final Factors Selection and Predictor Rate (PR) Value, and Final Landslide Susceptibility Mapping Results

4.1.4.1 Final Factors Selection Results

Based on the above analysis, 7 LCFs including Slope Angle, Lithology, LULC, Distance to Road, NDVI, Elevation, and Distance to Fault are selected as the final LCFs for the study area.

4.1.4.2 Predictor Rate (PR) Value for Final Factors

The PR values of the final 7 LCFs including Slope Angle, Lithology, LULC, Distance to Road, NDVI, Elevation, and Distance to Fault are calculated with the same process in **Section 4.1.2.3** and the PR calculation results are shown in **Table 13**, and the corresponding bar chart can be seen in **Figure 37**. PR value represents the weighting value of LCFs, according to the PR values, LULC shows the greatest importance and Elevation shows the least importance on affecting the landslide occurrence using the FR modeling method, for the study area.

Table 13 Predict Rate (PR) Values for Final 7 LCFs

LCF name	PR value
LULC	4.84
NDVI	2.51
Distance to Fault	2.41
Distance to Road	2.28
Lithology	1.34
Slope Angle	1.26
Elevation	1.00

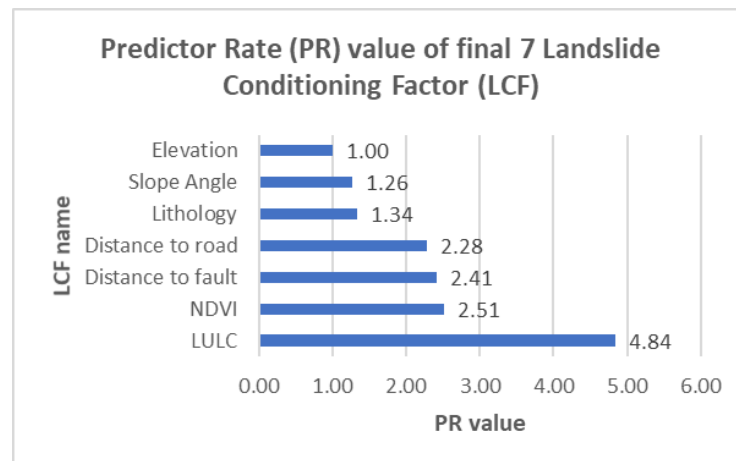


Figure 37 PR Value for Final 7 Landslide Conditioning Factors (LCFs)

4.1.4.3 Landslide Susceptibility Mapping (LSM) Results with Final Landslide Conditioning Factors (LCFs)

Based on the RF values of each classification (remain the same as in **Table 6**) of each LCF and the PR value for each LCF from **Table 13**, the Landslide Susceptibility Index (LSI) of inputting the 7 final LCFs is calculated using **Equation 2** which is defined in **Chapter II**, Then LSM is conducted using ArcGIS based on the LSI. The final LSM result for county-level and the 5-level of landslide susceptibility proportion including Very Low, Low, Moderate, High, and Very High levels are shown in **Figure 38 (a)** and **(b)** respectively. The proportion of landslide susceptibility for county-level and township-level administrative division can be seen in **Table 14** and **Table 15** respectively, the area bar chart of each landslide susceptibility level for county-level administrative division can be seen in **Figure 38 (c)**. The final LSM result for township-level and the 5-level of landslide susceptibility proportion including Very Low, Low, Moderate, High, and Very High can be seen in **Figure 39**. The area bar chart of each landslide susceptibility level for township-level administrative division can be seen in **Figure 40**.

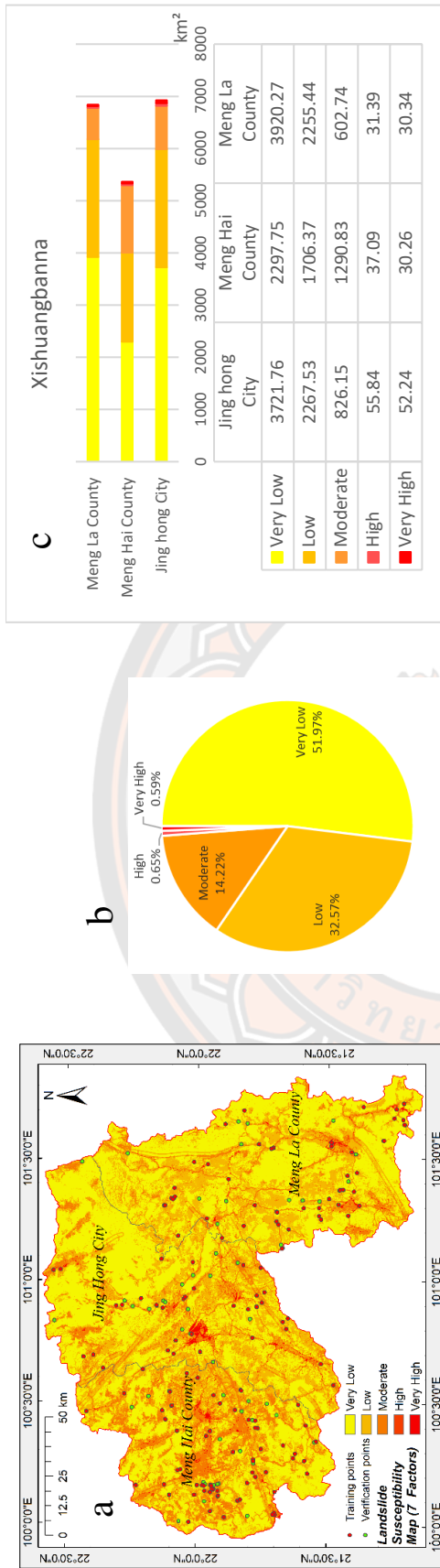


Figure 38 Final Landslide Susceptibility Mapping (LSM) Result (a), the Susceptibility Proportion for Each Level (b), and the Susceptibility Proportion for the County-Level Administrative Division

Table 14 Landslide Susceptibility Distribution in Township-Level of Final Landslide Susceptibility Mapping (LSM) Result

Region	Very Low		Low		Moderate		High		Very High	
	Area (km ²)	Area (%)	Area (km ²)	Area (%)	Area (km ²)	Area (%)	Area (km ²)	Area (%)	Area (km ²)	Area (%)
Jing Hong City	3721.76	19.46	2267.53	11.86	826.15	4.32	55.84	0.29	52.24	0.27
Meng Hai County	2297.75	12.01	1706.37	8.92	1290.83	6.75	37.09	0.19	30.26	0.16
Meng La County	3920.27	20.50	2255.44	11.79	602.74	3.15	31.39	0.16	30.34	0.16
Total	9939.78	51.97	6229.34	32.57	2719.72	14.22	124.32	0.65	112.84	0.59

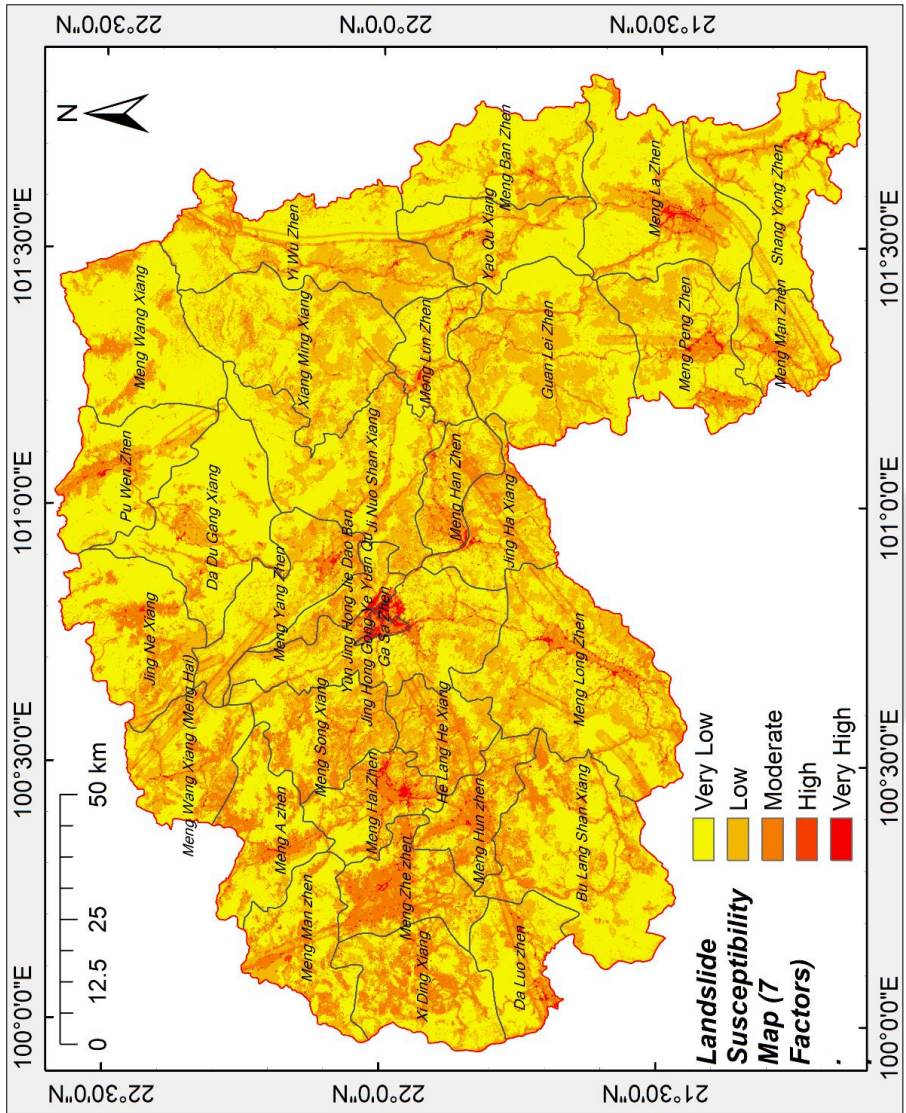


Figure 39 Final Landslide Susceptibility Mapping (LSM) Result for the Township-Level Administrative Division

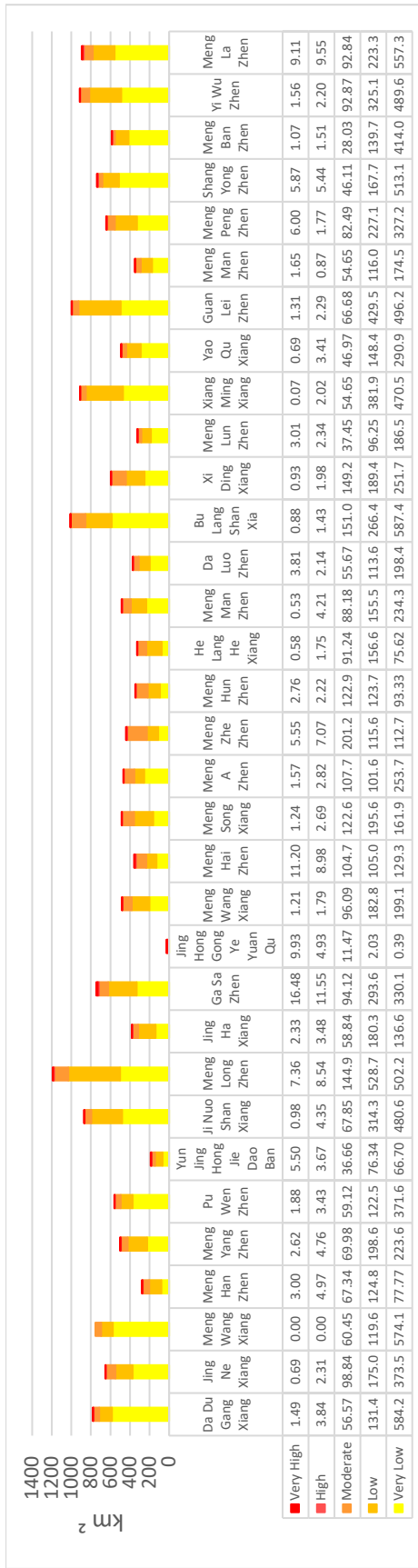


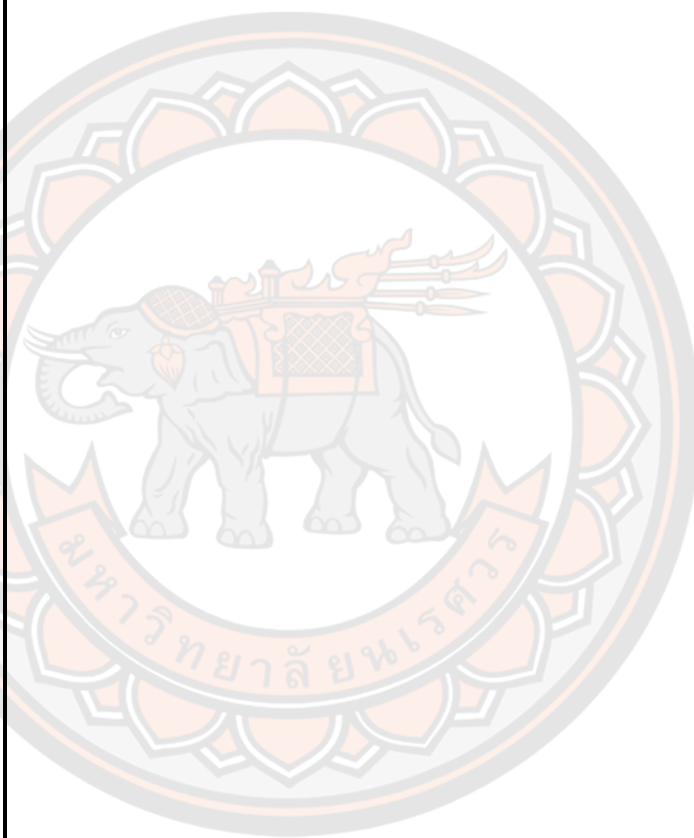
Figure 40 Landslide Susceptibility Proportion for Township-Level Administrative Divisions

Table 15 Landslide Susceptibility Distribution in Township-Level of Final Landslide Susceptibility Mapping (LSM) Result

Region	Township	Very Low		Low		Moderate		High		Very High	
		Area (km ²)	Area (%)	Area (km ²)	Area (%)	Area (km ²)	Area (%)	Area (km ²)	Area (%)	Area (km ²)	Area (%)
Jing Hong City	Da Du Gang Xiang	584.21	3.05	131.41	0.69	56.57	0.30	3.84	0.02	1.49	0.01
	Jing Ne Xiang	373.50	1.95	175.06	0.92	98.84	0.52	2.31	0.01	0.69	0.00
	Meng Wang Xiang	574.14	3.00	119.66	0.63	60.45	0.32	0.00	0.00	0.00	0.00
	Meng Han Zhen	77.77	0.41	124.85	0.65	67.34	0.35	4.97	0.03	3.00	0.02
	Meng Yang Zhen	223.66	1.17	198.61	1.04	69.98	0.37	4.76	0.02	2.62	0.01
	Pu Wen Zhen	371.67	1.94	122.52	0.64	59.12	0.31	3.43	0.02	1.88	0.01

Region	Township	Very Low		Low		Moderate		High		Very High	
		Area (km ²)	Area (%)	Area (km ²)	Area (%)	Area (km ²)	Area (%)	Area (km ²)	Area (%)	Area (km ²)	Area (%)
Meng Hai County	Yun Jing Hong Jie Dao Ban	66.70	0.35	76.34	0.40	36.66	0.19	3.67	0.02	5.50	0.03
	Ji Nuo Shan Xiang	480.66	2.51	314.32	1.64	67.85	0.35	4.35	0.02	0.98	0.01
	Meng Long Zhen	502.27	2.63	528.76	2.76	144.92	0.76	8.54	0.04	7.36	0.04
	Jing Ha Xiang	136.65	0.71	180.30	0.94	58.84	0.31	3.48	0.02	2.33	0.01
	Ga Sa Zhen	330.12	1.73	293.68	1.54	94.12	0.49	11.55	0.06	16.48	0.09
	Jing Hong Gong Ye Yuan Qu	0.39	0.00	2.03	0.01	11.47	0.06	4.93	0.03	9.93	0.05
	Meng Wang Xiang	199.12	1.04	182.81	0.96	96.09	0.50	1.79	0.01	1.21	0.01
	Meng Hai Zhen	129.32	0.68	105.06	0.55	104.76	0.55	8.98	0.05	11.20	0.06
	Meng Song Xiang	161.96	0.85	195.68	1.02	122.68	0.64	2.69	0.01	1.24	0.01
	Meng A Zhen	253.71	1.33	101.69	0.53	107.78	0.56	2.82	0.01	1.57	0.01
Meng La County	Meng Zhe Zhen	112.74	0.59	115.63	0.60	201.20	1.05	7.07	0.04	5.55	0.03
	Meng Hun Zhen	93.33	0.49	123.72	0.65	122.96	0.64	2.22	0.01	2.76	0.01
	He Lang He Xiang	75.62	0.40	156.65	0.82	91.24	0.48	1.75	0.01	0.58	0.00
	Meng Man Zhen	234.37	1.23	155.54	0.81	88.18	0.46	4.21	0.02	0.53	0.00
	Da Luo Zhen	198.41	1.04	113.68	0.59	55.67	0.29	2.14	0.01	3.81	0.02
	Bu Lang Shan Xia	587.44	3.07	266.49	1.39	151.08	0.79	1.43	0.01	0.88	0.00
	Xi Ding Xiang	251.75	1.32	189.43	0.99	149.20	0.78	1.98	0.01	0.93	0.00
	Meng Lun Zhen	186.57	0.98	96.25	0.50	37.45	0.20	2.34	0.01	3.01	0.02
	Xiang Ming Xiang	470.50	2.46	381.90	2.00	54.65	0.29	2.02	0.01	0.07	0.00
	Yao Qu Xiang	290.97	1.52	148.45	0.78	46.97	0.25	3.41	0.02	0.69	0.00
Meng Ban Zhen	Guan Lei Zhen	496.22	2.59	429.56	2.25	66.68	0.35	2.29	0.01	1.31	0.01
	Meng Man Zhen	174.53	0.91	116.07	0.61	54.65	0.29	0.87	0.00	1.65	0.01
	Meng Peng Zhen	327.25	1.71	227.16	1.19	82.49	0.43	1.77	0.01	6.00	0.03
	Shang Yong Zhen	513.19	2.68	167.77	0.88	46.11	0.24	5.44	0.03	5.87	0.03
Meng Ban Zhen	414.05	2.16	139.76	0.73	28.03	0.15	1.51	0.01	1.07	0.01	

Region	Township	Very Low		Low		Moderate		High		Very High	
		Area (km ²)	Area (%)	Area (km ²)	Area (%)	Area (km ²)	Area (%)	Area (km ²)	Area (%)	Area (km ²)	Area (%)
	Yi Wu Zhen	489.65	2.56	325.16	1.70	92.87	0.49	2.20	0.01	1.56	0.01
	Meng La Zhen	557.36	2.91	223.36	1.17	92.84	0.49	9.55	0.05	9.11	0.05
	Total	9939.78	51.97	6229.34	32.57	2719.72	14.22	124.32	0.65	112.84	0.59



4.1.4.4 Landslide Susceptibility Mapping (LSM) Result Verification

Validation is an indispensable step to verify the predictive capabilities of the landslide susceptibility mapping production, the prediction model has no scientific evidence without validation (Wu et al., 2016). Landslide susceptibility maps constructed with the final 7 LCFs were validated by calculating the success rate and prediction rate of which the AUC value is calculated with the landslide inventory training data and the verification data respectively. The result is shown in **Figure 41**.

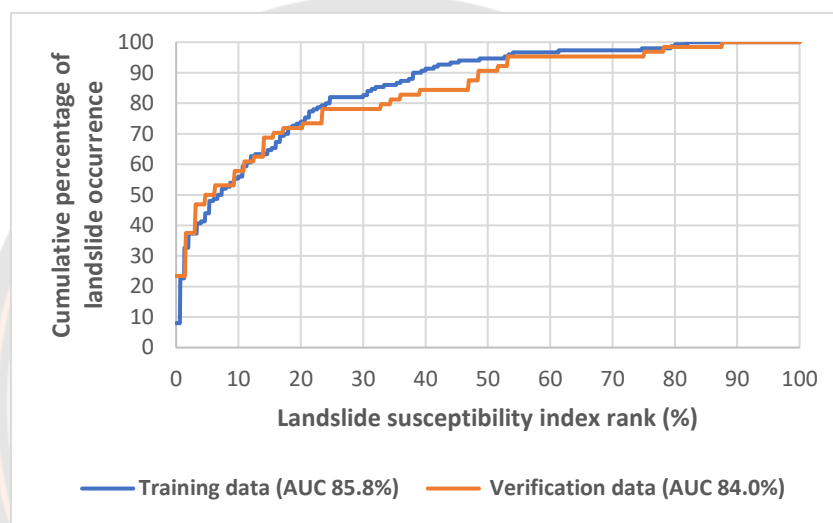


Figure 41 AUC Results of the Final Landslide Susceptibility Mapping Result with Inputting Both Landslide Inventory Training and Verification Data

4.1.5 Web-based Spatial Decision Support System Results

Figure 42 shows the Location Identification page of the “General” module which is also the default page of the system. On this page, the decision-makers/users are allowed to view the map for the study area, and decision-makers/users can select the map type between street and satellite map as they like by clicking the top right of the map. The raster data of the final landslide susceptibility map has been digitalized and the High and Very High-level susceptibility data have been extracted and imported to the map. As is shown in **Figure 43**, the red polygons in the map represent the Very High-level, and the orange color represents the High-

level landslide susceptibility areas. When decision-makers/users click on each of the polygons, the marker of the location that is clicked will be added to the map, and there will be an information window showing the coordinate of the clicked point, and the location is in High or Very High-level of landslide susceptibility area.



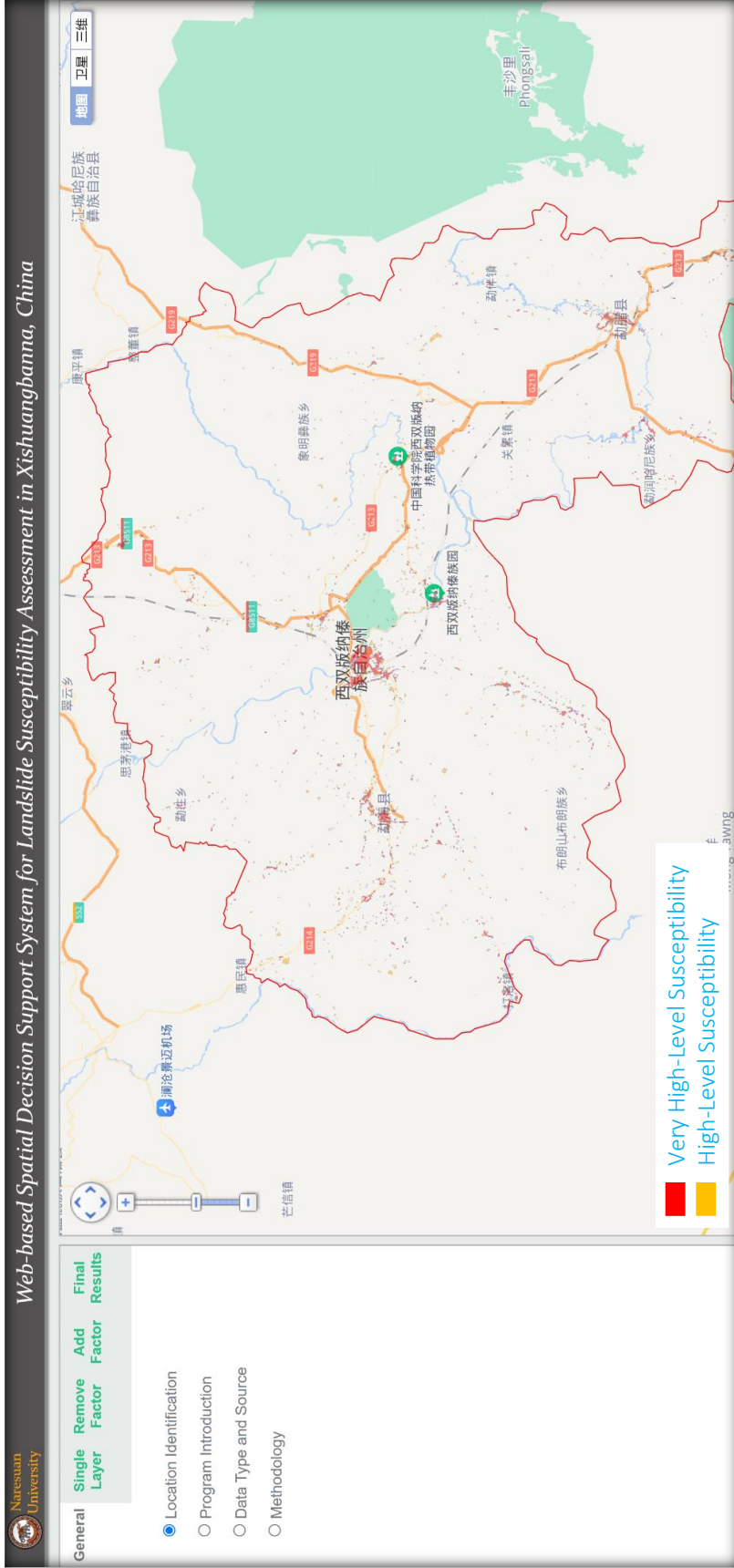


Figure 42 Location Identification Page of "General Module"

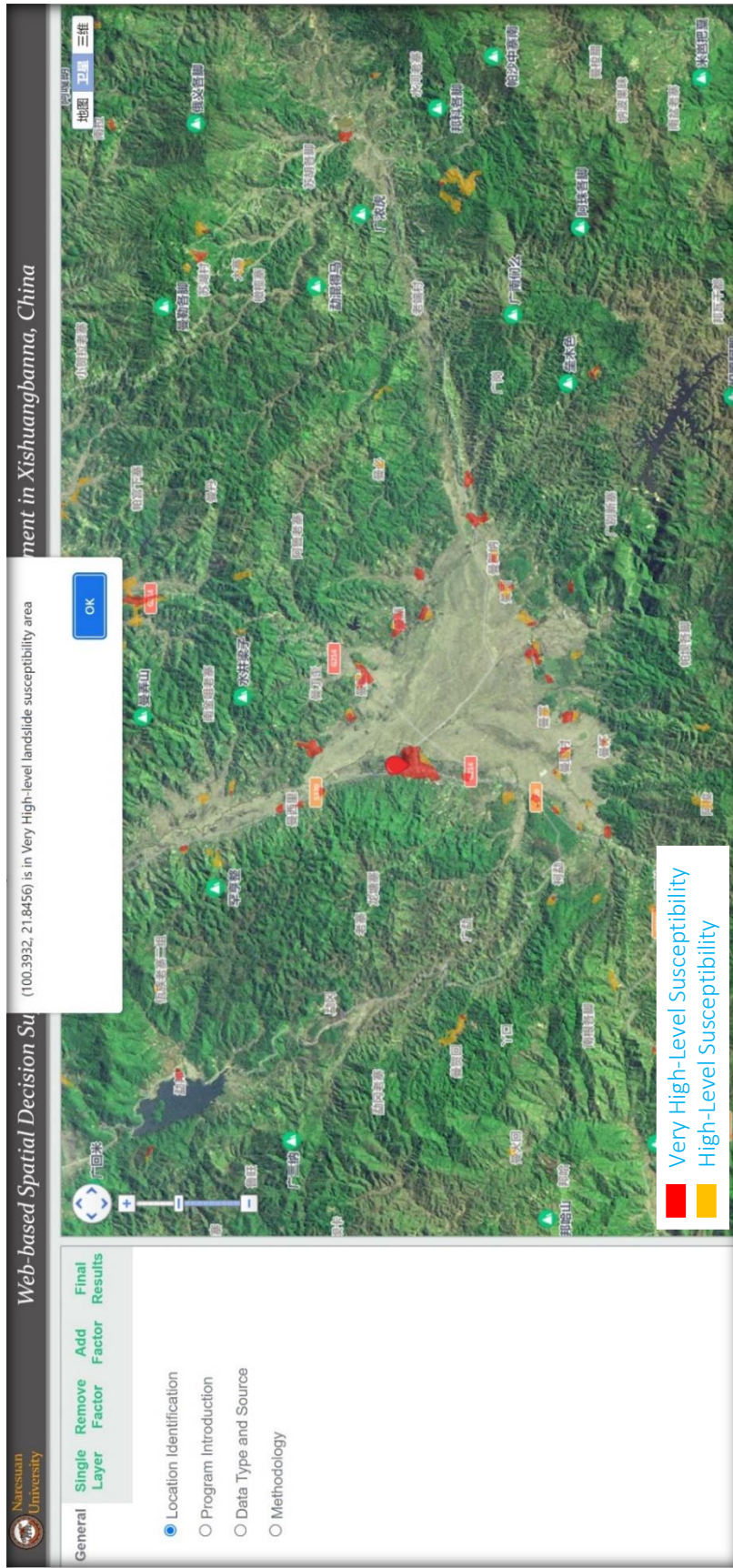


Figure 43 Example of Location Identification Function

Figure 44 shows the Program Introduction page of the “General” module. This page presents the background of the system, the process of the study, and the components of each module of the system.

Figure 45 is the Data Type and Source page of the “General” module. This page shows the data format, resolution, data source and the producing time of each single factor layer of the study.

Figure 46 is the Methodology page of the “General” module. This page shows the Landslide Conditioning Factor identification workflow, final Landslide Susceptibility Mapping workflow, and Design of Web-based Spatial Decision Support System for Landslide Susceptibility Assessment in Xishuangbanna, China. As well as the details of the equations used in the study.

Figure 47 is the About Us page of the “General” module. This page shows the technique background, the recommendations, and the copyright of the platform. Besides, the contact information of the admins is also shown in this page.

Figure 48 is the Slope Angle Layer overlaps with landslide inventory data sample page of “Single Layer” module. There are in total 14 different pages representing the different single factor layers of the study respectively.

Figure 49 is the Factor Weight & AUC Value page of the “Remove Factor” module. This page shows the factor weight and AUC value comparison of the inputting the 14 full factors case and removing each of the 14 factors from the whole cases.

Figure 50 is the Landslide Susceptibility Mapping result sample page of inputting all the 14 factors of the “Remove Factor” module. This page shows the landslide susceptibility map of inputting the 14 full factors, the AUC curve of the map, and the percentage of each landslide susceptibility level.

Figure 51 is the Factor Weight & AUC Value page of “Add Factor” module. This page shows the factor weight and AUC value comparison of the inputting the 3 minimum factors case and adding each of the other 11 factors to the 3 factors.

Figure 52 is the Landslide Susceptibility Mapping result sample page of inputting 3 minimum factors of “Add Factor” module. This page shows the

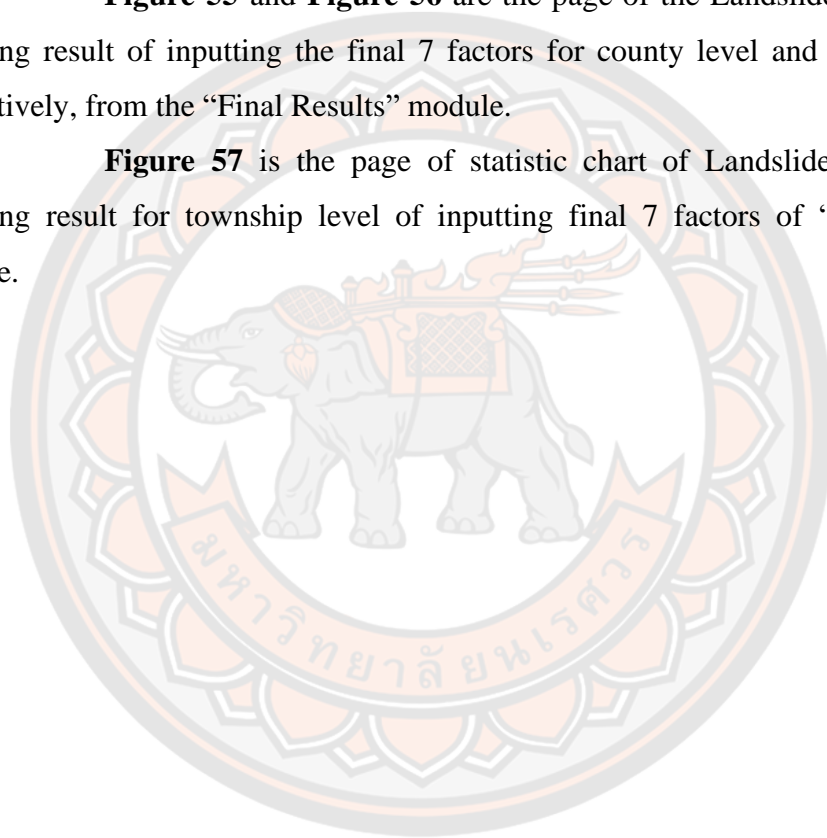
landslide susceptibility map of inputting the 3 minimum factors, the AUC curve of the map, and the percentage of each landslide susceptibility level.

Figure 53 is the page of AUC Value Compare of both cases of removing and adding factor except for the obligatory 3 minimum factors (Slope Angle, Lithology, and LULC) of the “Final Results” module.

Figure 54 is the page of Factor Weight Value for the final 7 factors of the “Final Results” module.

Figure 55 and **Figure 56** are the page of the Landslide Susceptibility Mapping result of inputting the final 7 factors for county level and township level respectively, from the “Final Results” module.

Figure 57 is the page of statistic chart of Landslide Susceptibility Mapping result for township level of inputting final 7 factors of “Final Results” module.



Web-based Spatial Decision Support System for Landslide Susceptibility Assessment in Xishuangbanna, China

General

- Single Layer
- Remove Factor
- Add Factor
- Final Results

Location Identification

Program Introduction

Data Type and Source

Methodology

This Web-based Spatial Decision Support System aims to present the Landslide Susceptibility Mapping results using Frequency Ratio Model. There are in total 14 landslide conditioning factors which are obtained from literature review at first. By analyzing the corresponding relationship between landslide inventory and each factor. Finally, there are 7 factors have been kept as the dominant landslide conditioning factors for Xishuangbanna, China.

The system reappears the process of our landslide susceptibility assessment for Xishuangbanna, which can be used as an effective decision-making support tool for decision makers, as well as providing a contemprable way of making use of the conventional landslide susceptibility assessment outcomes for researchers.

The Web-based Spatial Decision Support System including 5 modules including:

- 1) General - Consists of Location Identification, program introduction, data type and resource, and methodology pages;
- 2) Single Layer - Present landslide inventory distribution on each of the landslide conditioning factor classification map;
- 3) Remove Factor - Present factor weight & AUC value of the case of adopting all 14 factors, as well as the cases of removing one factor from the 14 factors in turn;
- 4) Add Factor - Present factor weight & AUC value of the case of adopting 3 minimum factors (Slope Angle, Lithology and Land Use & Land Cover (LULC)), as well as the cases of adding one factor into the 3 factor group in turn;
- 5) Final Results - Present AUC value compare of both cases of removing and adding factor except for the obligatory 3 minimum factors (Slope Angle, Lithology and LULC), factor weight value for the final 7 factors, the final Landslide Susceptibility Mapping result, the result for township level and the susceptibility statistic data of each township.

Figure 44 Program Introduction Page of “General” Module

- General
- Single Layer
- Remove Factor
- Add Factor
- Final Results

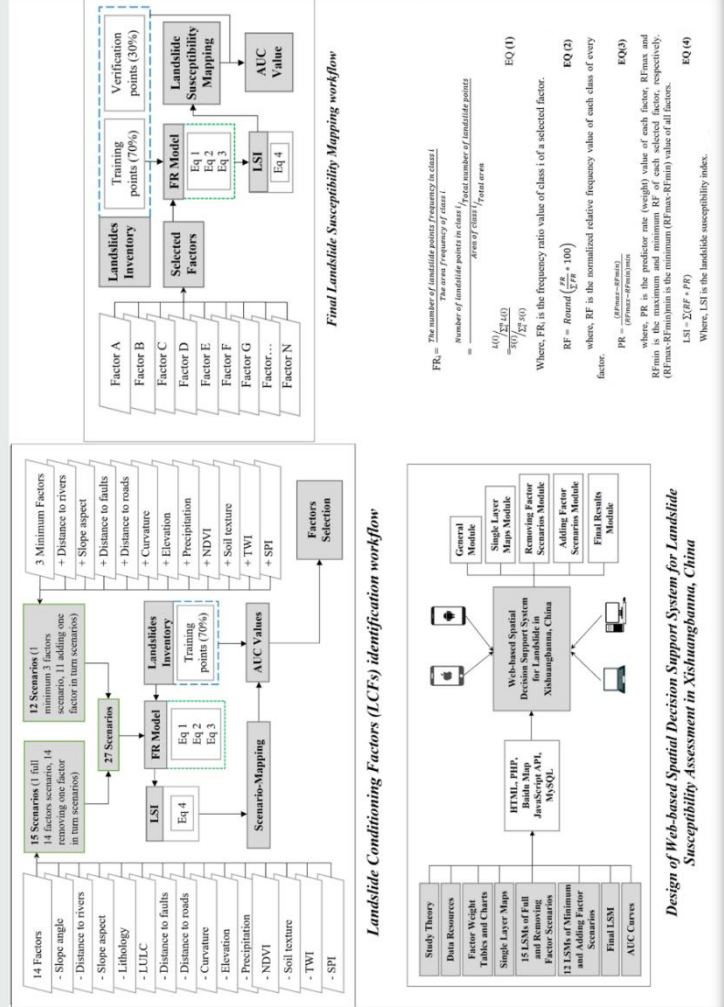
- Location Identification
- Program Introduction
- Data Type and Source
- Methodology

Data type and sources of each Landslide Conditioning Factor

Layer	Format	Resolution	Data source	Producing Time
Landslide Inventory	.shp	-	Resource and Environment Science and Data Center of China (RESDC) (http://www.resdc.cn)	
Elevation				
Slope angle				
Slope aspect	.tif	30m	The Advanced Spaceborne Thermal Emission and Reflection Radiometer (ASTER) Global Digital Elevation Model (GDEM) (https://earthexplorer.usgs.gov)	2000-2013
Curvature				
TWI				
SPI				
Distance to rivers	.shp	-	Water Bureau of Xishuangbanna Prefecture	2018
Distance to roads	.shp	-	OpenStreetMap (https://www.openstreetmap.org)	Up to date
Distance to faults	.jpg	-	Seismic Active Fault Survey Data Center of China (http://www.activefault-datacenter.cn)	2020
Precipitation	.nc	0.083°	National Tibetan Plateau Data Center (NTBDC) (https://data.tpdc.ac.cn/data)	1901-2017
NDVI	.tif	30 m	Landsat 8-9 OLI/TIRS C2 L2 Data Products (https://earthexplorer.usgs.gov)	2020
LULC	.tif	10 m	A ten-class global land use/land cover (LULC) map for the year 2020 at 10 meter resolution. (https://www.arcgis.com/)	2020
Lithology	.jpg	-	OSGeo China Center (https://www.osgeo.cn)	2004
Soil texture	.shp	-	Chinese Soil Database (http://vdb3.soil.esdb.cn)	1990

Figure 45 Data Type and Source Page of “General” Module

- Location Identification
- Program Introduction
- Data Type and Source
- Methodology



FR = $\frac{\text{The number of landslide points frequency in class } i}{\text{The area frequency of class } i}$

$$= \frac{\text{Number of landslide points in class } i / \text{Total number of landslide points}}{\text{Area of class } i / \text{Total area}}$$

EQ (1)

EQ (2)

EQ (3)

EQ (4)

Where, FR is the frequency ratio value of class i of a selected factor.

PR = $\frac{\text{RFmax}-\text{RFmin}}{\text{RFmax}+\text{RFmin}}$

LSI = $2(\text{FR} + \text{PR})$


Where, RF is the normalized relative frequency value of each class of every factor.

RFmax is the maximum and minimum RF of each selected factor, respectively. (RFmax, RFmin) is the maximum (RFmax, RFmin) value of all factors.

Where, LSI is the landslide susceptibility index.

Figure 46 Methodology Page of "General" Module

Web-based Spatial Decision Support System for Landslide Susceptibility Assessment in Xishuangbanna, China

 Naresuan University

- General
- Single Layer
- Remove Factor
- Add Factor
- Final Results

Location Identification

Program Introduction

Data Type and Source

Methodology

About Us

INTRODUCTION:

the platform is part of the outcome of Mr. Gen Long's Master's Thesis titled on "Web-based Spatial Decision Support System for Landslide Susceptibility Assessment in Xishuangbanna, China". The development of the platform is based on the programming languages and tools including HTML, PHP, Baidu JavaScript API, and MySQL. The platform starts a new way of thinking which has a broad potential for further development and provides a constructive way of making better use of the landslide susceptibility assessment outcomes, which can be used as an effective decision-making support tool. Furthermore, this process can be used not only for landslide-related studies but also for any type of GIS-based disaster hazard assessment studies.

CONTACT:

Mr. Gen Long, Civil Engineering Department, Faculty of Engineering, Naresuan University, THAILAND, email: genl63@nu.ac.th

Assoc. Prof. Dr. Sarintip Tantane, Center of Excellence on Energy Technology and Environment, Faculty of Engineering, Naresuan University, THAILAND, email: sarintipt@nu.ac.th

Asst. Prof. Dr. Korakod Nosit, Civil Engineering Department, Faculty of Engineering, Naresuan University, THAILAND, email: korakodn@nu.ac.th

COPYRIGHT @ Naresuan University

Figure 47 About Us Page of “General” Module

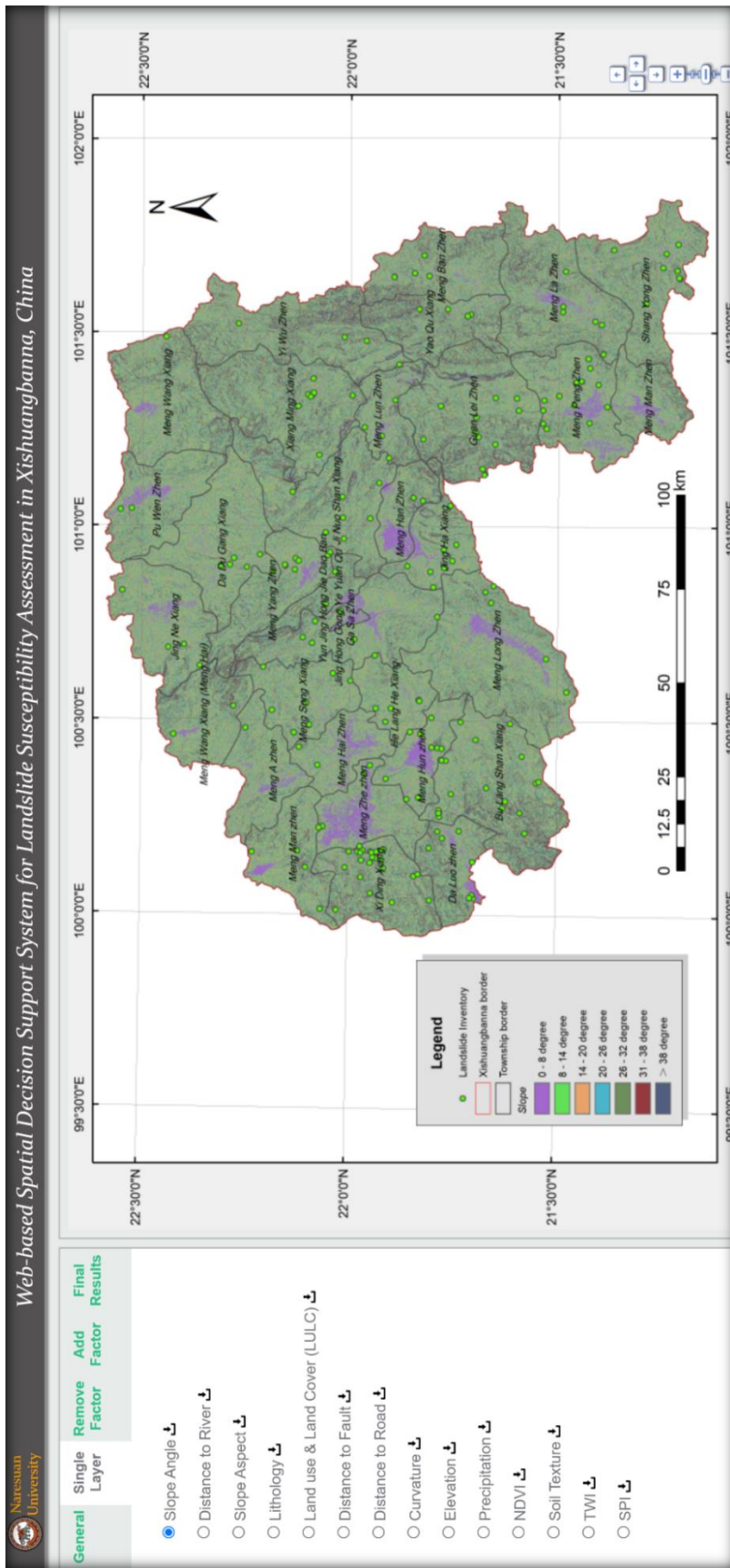
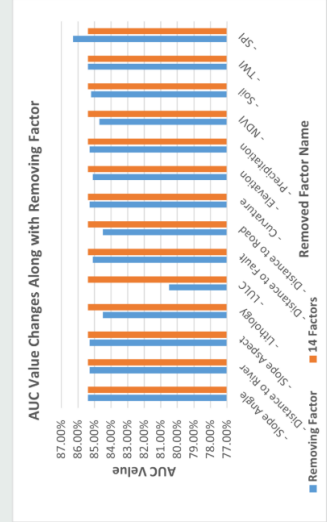
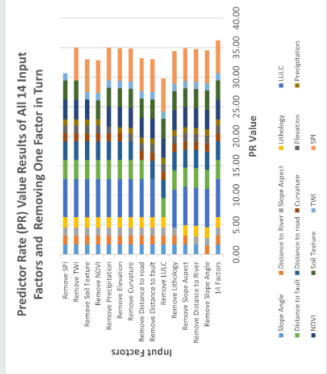


Figure 48 Slope Angle Sample Page of “Single Layer” Module

- Factor Weight & AUC Value
- 14 Factors (Maximum) ↓
- Remove Slope Angle ↓
- Remove Distance to River ↓
- Remove Slope Aspect ↓
- Remove Lithology ↓
- Remove Land Use & Land Cover ↓
- Remove Distance to Fault ↓
- Remove Distance to Road ↓
- Remove Curvature ↓
- Remove Elevation ↓
- Remove Precipitation ↓
- Remove NDVI ↓
- Remove Soil Texture ↓
- Remove TWI ↓
- Remove SPI ↓



Predictor Rate (PR) Value for each Landslide Conditioning Factor (LCF)

Factors Input	Slope Angle	Distance to River	Slope Aspect	Lithology	LULC	Distance to fault	Distance to road	Curvature	Elevation	Precipitation	NDVI	Soil Texture	TWI	SPI
14 Factors	1.70	1.48	1.35	1.80	6.49	3.24	3.06	1.41	1.34	1.00	3.37	3.22	1.23	5.56
Remove Slope Angle		1.48	1.35	1.80	6.49	3.24	3.06	1.41	1.34	1.00	3.37	3.22	1.23	5.56
Remove Distance to River	1.70		1.35	1.80	6.49	3.24	3.06	1.41	1.34	1.00	3.37	3.22	1.23	5.56
Remove Slope Aspect	1.70	1.48		1.80	6.49	3.24	3.06	1.41	1.34	1.00	3.37	3.22	1.23	5.56
Remove Lithology	1.70	1.48	1.35		6.49	3.24	3.06	1.41	1.34	1.00	3.37	3.22	1.23	5.56
Remove LULC	1.70	1.48	1.35	1.80		3.24	3.06	1.41	1.34	1.00	3.37	3.22	1.23	5.56
Remove Distance to fault	1.70	1.48	1.35	1.80	6.49		3.06	1.41	1.34	1.00	3.37	3.22	1.23	5.56
Remove Distance to road	1.70	1.48	1.35	1.80	6.49	3.24		1.41	1.34	1.00	3.37	3.22	1.23	5.56
Remove Curvature	1.70	1.48	1.35	1.80	6.49	3.24	3.06		1.34	1.00	3.37	3.22	1.23	5.56
Remove Elevation	1.70	1.48	1.35	1.80	6.49	3.24	3.06	1.41		1.00	3.37	3.22	1.23	5.56
Remove Precipitation	1.70	1.48	1.35	1.80	6.49	3.24	3.06	1.41	1.09		3.37	3.22	1.23	5.56
Remove NDVI	1.70	1.48	1.35	1.80	6.49	3.24	3.06	1.41	1.34	1.00		3.22	1.23	5.56
Remove Soil Texture	1.70	1.48	1.35	1.80	6.49	3.24	3.06	1.41	1.34	1.00	3.37		1.23	5.56
Remove TWI	1.70	1.48	1.35	1.80	6.49	3.24	3.06	1.41	1.34	1.00	3.37	3.22		5.56
Remove SPI	1.70	1.48	1.35	1.80	6.49	3.24	3.06	1.41	1.34	1.00	3.37	3.22	1.23	

Figure 49 Factor Weight & AUC Value Page of “Remove Factor” Module

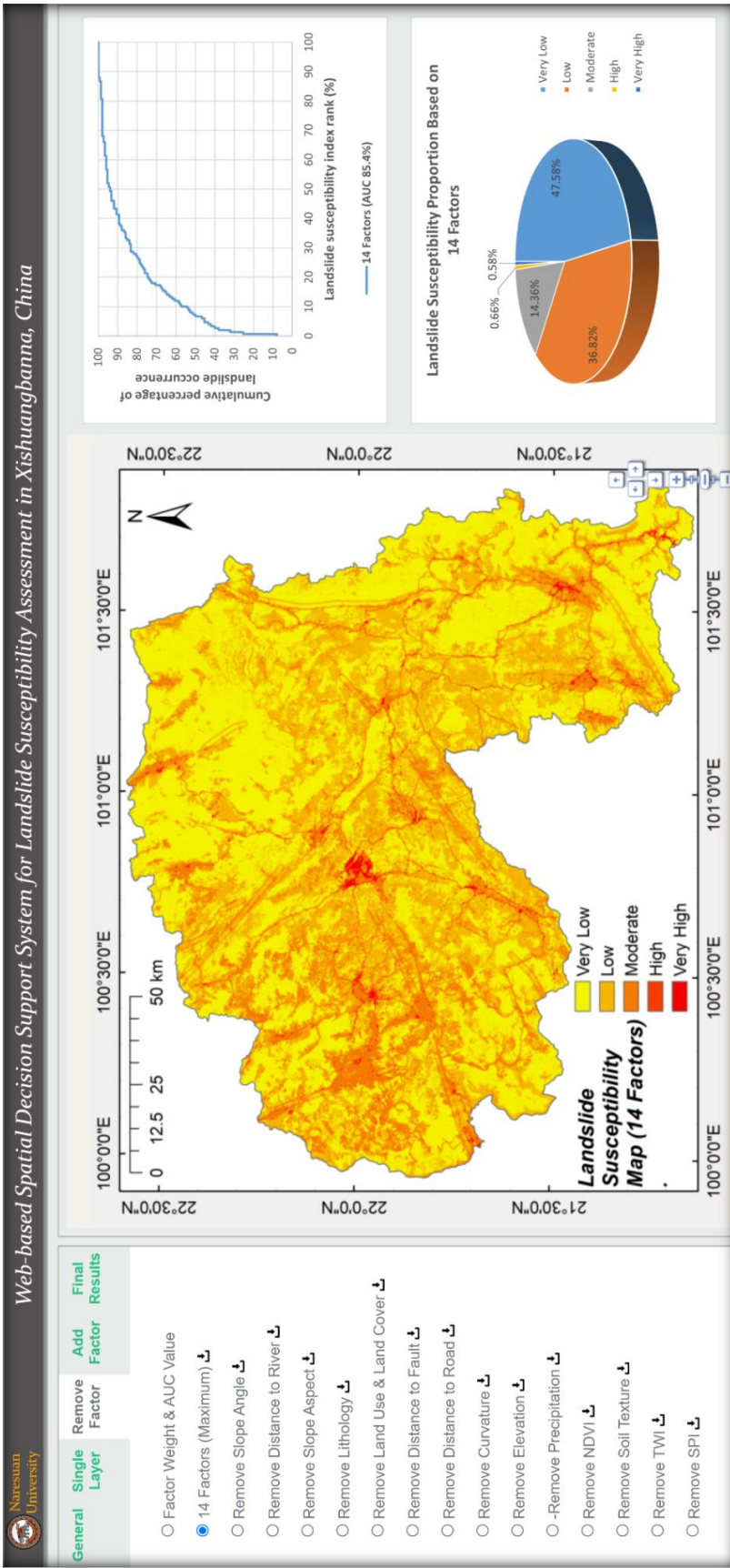
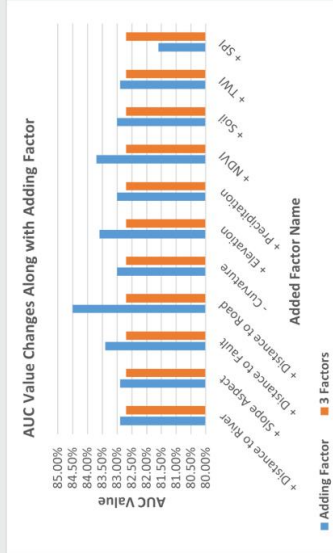
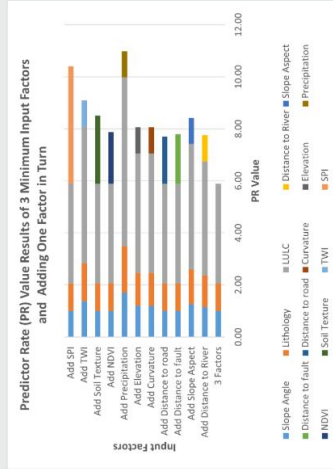


Figure 50 Landslide Susceptibility Mapping Result Sample Page of Inputting All the 14 Factors of “Remove Factor” Module

- Factor Weight & AUC Value
- 3 Factors (Minimum) ↓
- Add Distance to River ↓
- Add Aspect ↓
- Add Distance to Fault ↓
- Add Distance to Road ↓
- Add Curvature ↓
- Add Elevation ↓
- Add Precipitation ↓
- Add NDVI ↓
- Add Soil Texture ↓
- Add TWI ↓
- Add SPI ↓



Predictor Rate (PR) Value for each Landslide Conditioning Factor (LCF)

Factors Input	Slope Angle	Lithology	LULC	Distance to River	Slope Aspect	Distance to fault	Distance to road	Curvature	Elevation	Precipitation	NDVI	Soil Texture	TWI	SPI
3 Factors	1.00	1.06	3.83											
Add Distance to River	1.15	1.22	4.39	1.00										
Add Slope Aspect	1.26	1.34	4.82		1.00									
Add Distance to fault	1.00	1.06	3.83			1.91								
Add Distance to road	1.00	1.06	3.83				1.81							
Add Curvature	1.20	1.27	4.59					1.00						
Add Elevation	1.20	1.27	4.59						1.00					
Add Precipitation	1.70	1.80	6.49							1.00				
Add NDVI	1.00	1.06	3.83								1.99			
Add Soil Texture	1.00	1.06	3.83									2.62		
Add TWI	1.38	1.46	5.26										1.00	
Add SPI	1.00	1.06	3.83											4.51

Figure 51 Factor Weight & AUC Value Page of “Add Factor” Module

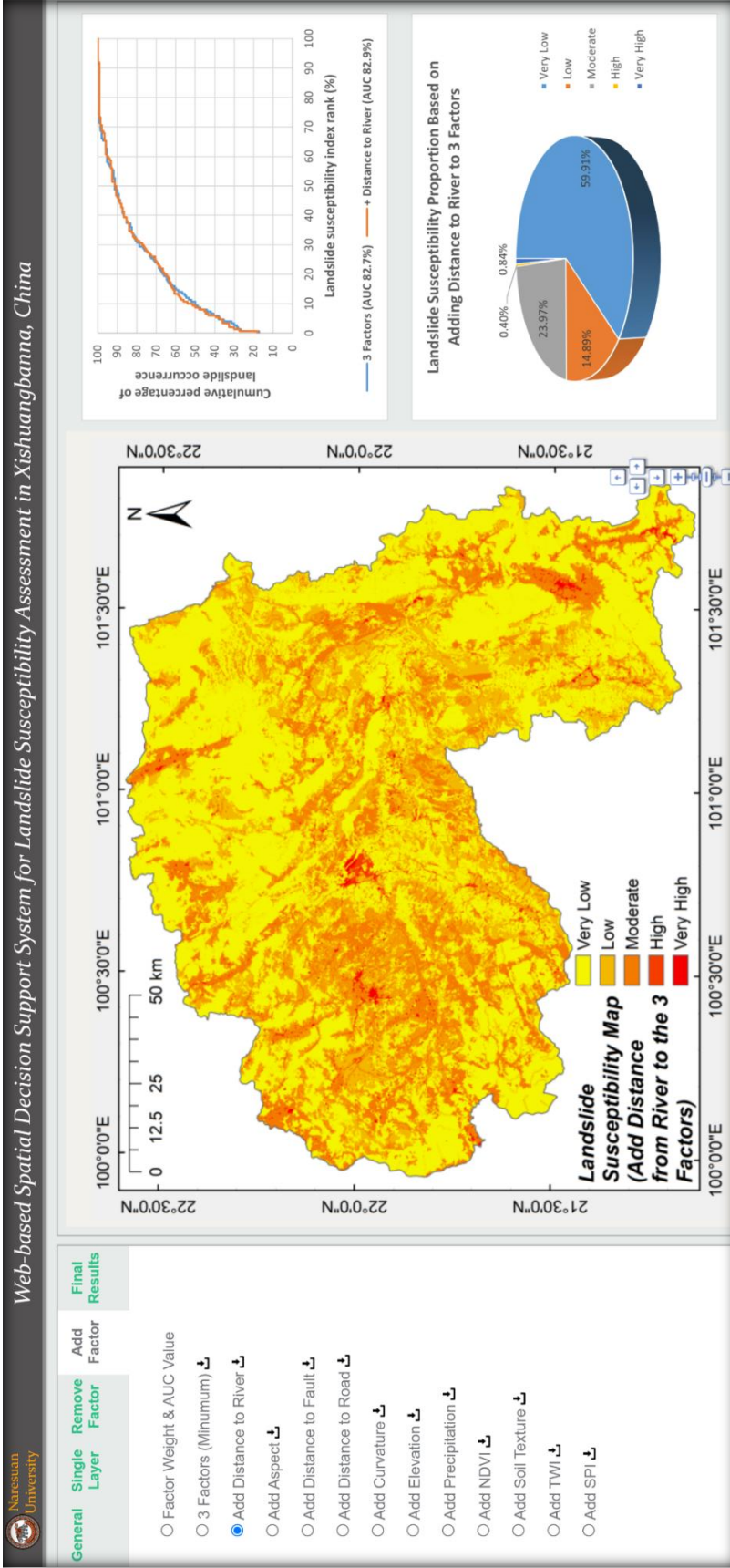


Figure 52 Landslide Susceptibility Mapping Result Sample Page of Inputting 4 Factors That Adding Distance to River to the 3 Minimum Factors of “Remove Factor” Module

General **Single Layer** **Remove Factor** **Add Factor** Final Results

- AUC Value Compare ↕
- Factor Weight Value ↕
- Landslide Susceptibility Map ↕
- LSM for Township ↕
- Statistic for Township ↕

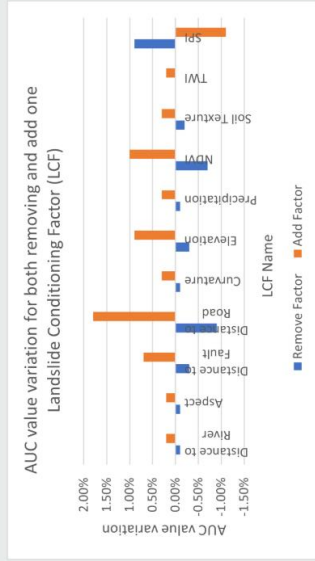


Figure 53 Page of AUC Value Compare of Both Cases of Removing and Adding Factor Except for the Obligatory 3 Minimum Factors (Slope Angle, Lithology, and LULC) of “Final Results” Module

General Single Layer Remove Factor Add Factor Final Results

- AUC Value Compare
- Factor Weight Value
- Landslide Susceptibility Map
- LSM for Township
- Statistic for Township

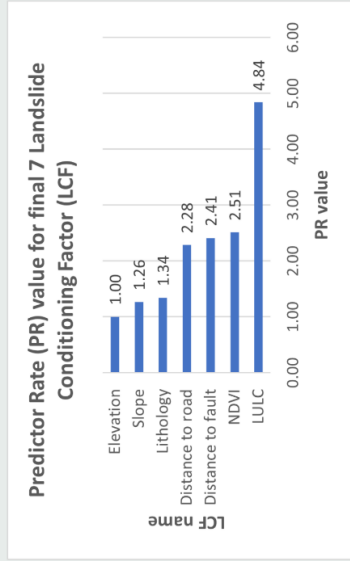


Figure 54 Page of Factor Weight Value for the Final 7 Factors of “Final Results” Module

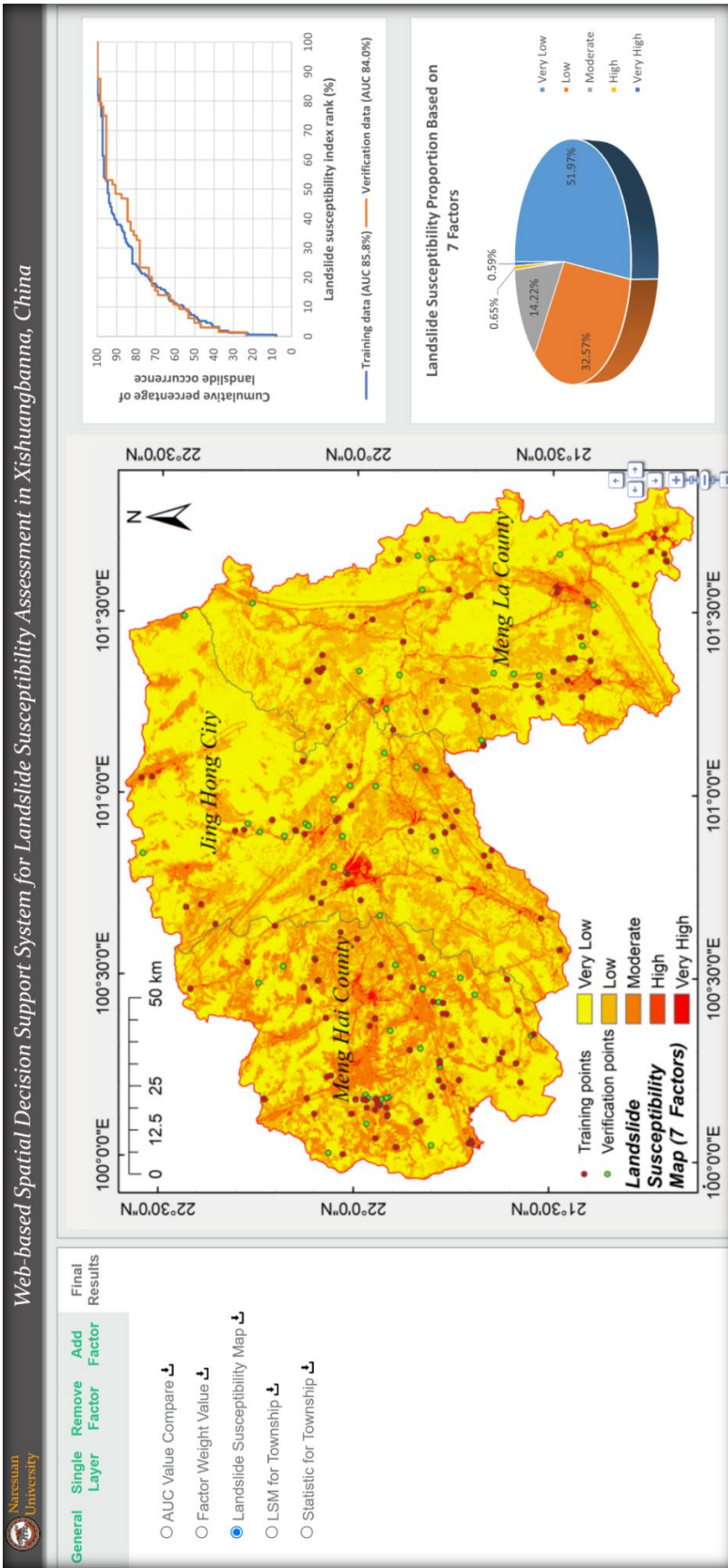


Figure 55 Page of Landslide Susceptibility Mapping Result of Inputting Final 7 Factors for County-Level of “Final Results” Module

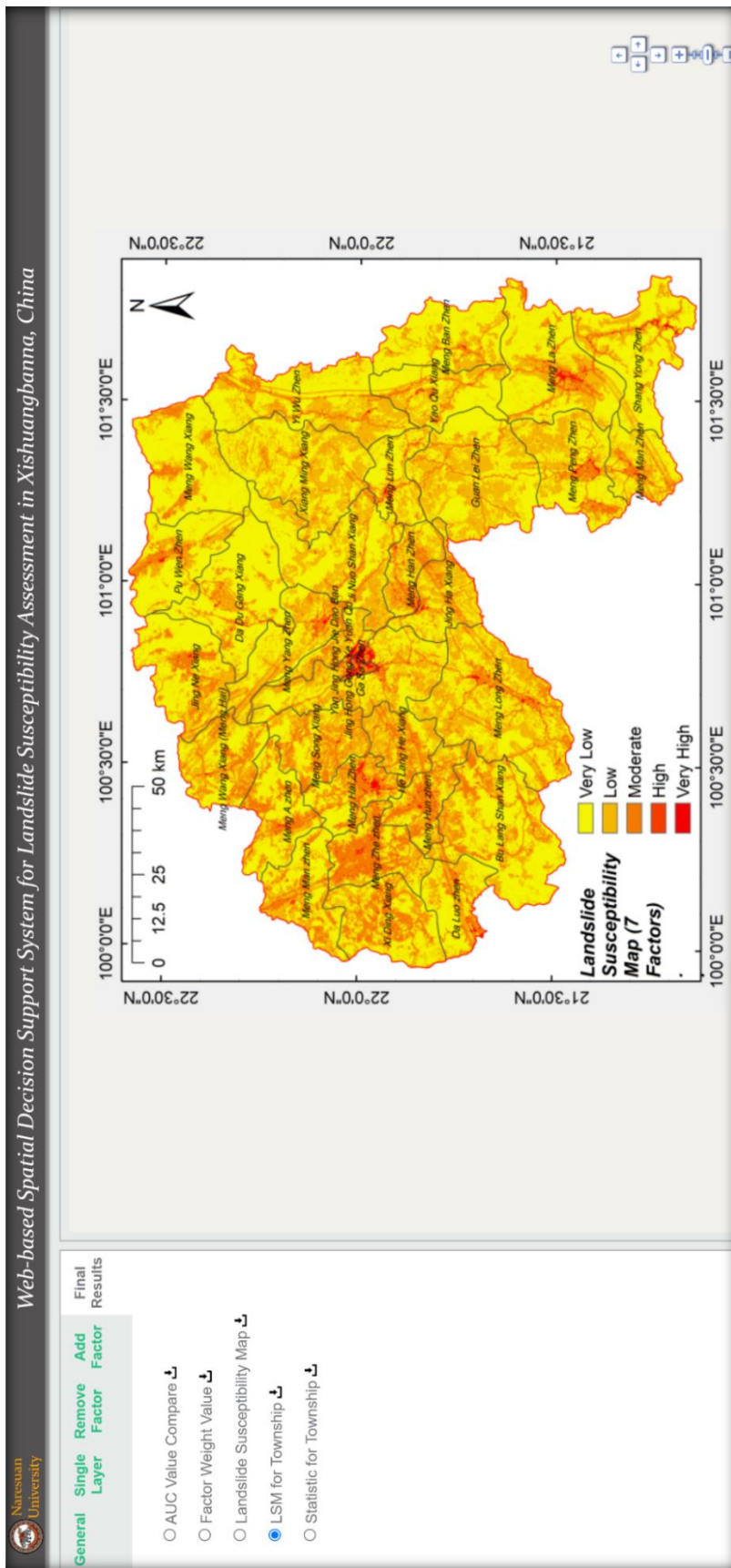


Figure 56 Page of Landslide Susceptibility Mapping Result of Inputting Final 7 Factors for Township-Level of “Final Results” Module

Final Results
General Thematic Maps Factor Add Factor

- AUC Value Compare
- Factor Weight Value
- Landslide Susceptibility Map
- LSM for Township
- Statistic for Township

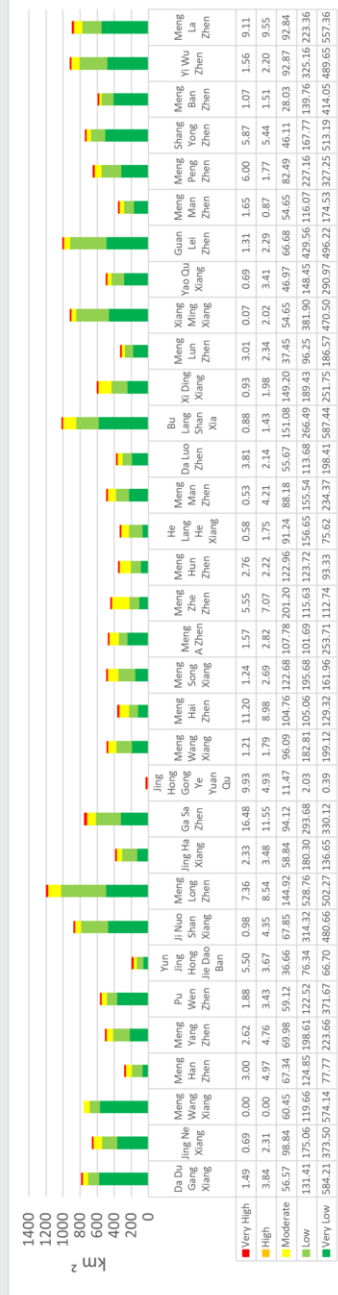


Figure 57 Page of Statistic Chart of Landslide Susceptibility Mapping Result for Township-Level of Inputting Final 7 Factors of "Final Results" Module

4.2 Discussion

As one of the most frequently used methods in LSA studies, the FR model was selected to assess the landslide susceptibility for Xishuangbanna Prefecture, Yunnan Province, China on a regional scale for the first time. Then a Web-based SDSS for LSA for the study area was developed. Generally, the study can be divided into 3 sections, the first section is the landslide conditioning factors identification for the study area. The second section is mapping the final landslide susceptibility for the study area by adopting the final 7 selected LCFs. The last step is developing the Web-based SDSS for the study area using the outcomes of the study.

4.2.1 Landslide Conditioning Factors Identification

In the landslide conditioning factors identification section, 14 most frequently used factors are extracted from a comprehensive literature review (52 studies) firstly, with setting the threshold utilization frequency of 21% out of the 52 studies. Then the parameters of each factor have been classified into different groups using the most frequently used-natural breaks classification method, except for the ones that have unique classifications themselves. Then the FR values were calculated by overlaying the landslide inventory training data with every single classified layer.

According to the FR values, for Slope Angle, classifications of 0 - 8°, 0 - 14°, and 14 - 20° show a higher correlation with landslide occurrence, while classifications of 20 - 26°, 26 - 32°, 32 - 38° shows a lower correlation. No historical landslides were found in the classification of > 38°, which is consistent with the conclusion that in almost vertical conditions, landslides are rare or absent. The lack of debris accumulation and soil development are the reasons for the areas under these topographic conditions (Abbaszadeh Shahri et al., 2019; Gómez & Kavzoglu, 2005).

For Distance to River, classifications of < 50m, 50 - 100m, 100 - 150m, and 150 - 200m show a higher correlation with landslide occurrence of which FR values are greater than 1, and classifications of 50 - 100m and 100 - 150m show higher correlation than other two with FR value greater than 2. Classification of > 200m shows a lower correlation which represents less landslide occurrence possibility for places that are too far away from rivers. This is generally consistent with the conclusion of - areas with a shorter distance to rivers has relatively more likelihood of

landslide formation than areas located far away (El Jazouli et al., 2019; Nohani et al., 2019; Sur et al., 2020; Wu et al., 2016; Youssef et al., 2014).

For Slope Aspect, according to the literature, although it has an important role in conditioning landslide occurrence, there is no consensus that have been reached regarding the relationship between them (Youssef et al., 2014). According to the FR values, classifications of Northeast (22.5-67.5), East (67.5-112.5), and South (157.5-202.5) show a higher correlation with landslide occurrence of which FR values are greater than 1, while there are no historical landslides were found in the flat areas of which classification is Flat (-1). Other classifications show a lower correlation that FR values less than 1.

For Lithology, the classification of Group L shows a relatively higher correlation with landslide occurrence with a FR value greater than 4. Classifications of Group A and Group D show the second higher correlation with a FR value greater than 2. Classifications of Group E, Group F, Group H, Group I, Group J, and Group P show the third higher correlation, while classifications of Group G, Group K, Group M, Group N, and Group O show the lower correlation with FR value less than 1. No landslides were found in the classification of Group B and Group C.

For LULC, the classification of Artificial Surfaces has a much higher FR value of 20.84 compared with other higher landslide correlation classifications such as Cultivated Land (1.47), Grass Land (1.82), and Shrubland (1.66). Forest shows a relatively lower correlation of 0.25. No historical landslides were found in Wetland and Water Body.

For Distance to Fault, classification of 500 - 1000m shows the highest FR value of 3.67 while classifications of < 500m and 1000m - 2000m also show a higher correlation with landslide occurrence but the FR values are less than 2. Classifications of 2000 - 3000m and 3000 - 4000m have FR value of 0.55 and 0.26 respectively, which mean a lower correlation with landslide occurrence. Classification of > 4000m has a FR value of 0.99 which is close to 1, which means this classification has a landslides density proportionally to the area of the classification. Generally, the FR values represent the conclusion that distance close to the geological faults often leads to high landslide susceptibility (Abedini & Tulabi, 2018; El Jazouli et al., 2019;

Le et al., 2021; Nohani et al., 2019; Shano et al., 2021; Wu et al., 2016; Youssef et al., 2014).

For Distance to Road, classification of 0 - 50m shows the highest correlation with landslide occurrence with the FR value of 7.01, while classifications of 50 - 100m and 100 - 150m show the second highest correlation with FR values of 3.58 and 3.55 respectively. Classification of 150 - 200m also shows a higher correlation but its FR value is less than 2. The classification of > 200m has a FR value of less than 1, which means a lower correlation with landslide occurrence. Generally, the FR results are consistent with the conclusion of the nearer the distance to the road system, the higher the risk of landslide hazards (Le et al., 2021; Nohani et al., 2019; Sur et al., 2020; Wu et al., 2016; Youssef et al., 2014).

For Curvature, classification of Flat has a FR value equals to 1.58 which means a higher correlation with the occurrence of landslides, while classifications of Convex and Concave have FR value of 1.00 and 0.96 respectively, which shows curvature has not an obvious influence on the occurrence of landslides in the study area.

For Elevation, the lowest and highest two classifications of elevation which are < 760m, between 760 - 940m, between 1470 - 1710m, and > 1710m have FR values greater than 1, which show these classifications have a higher correlation with landslide occurrence, while the classifications of elevation within 940m - 1470m have lower correlation with their FR values less than 1. For Precipitation, classifications of annual precipitation < 1450mm, between 1450 - 1580mm, and 1720 - 1840 mm show a higher correlation with landslide occurrence, but with only a bit greater FR value than 1. Classifications of annual precipitation between 1580 - 1720mm, 1840 - 1970mm, 1970 - 2140mm and > 2140mm show a lower correlation with landslide occurrence with FR values less than 1. However, according to the FR values, Precipitation does not show a strong effect on influencing landslide occurrence in the study area.

For NDVI, classifications of NDVI value < 0.18 and between 0.18 - 0.24 show a higher correlation with landslide occurrence with FR values of 3.85 and 2.82 respectively. Classifications of NDVI values between 0.29 - 0.34 and > 0.34

show a lower correlation with FR values of 0.41 and 0.34. Classification of NDVI value between 0.24 - 0.29 shows its landslides density proportionally to the area of the classification. This is consistent with the conclusion that NDVI values close to -1 reveal that the bare earth surface is lack of vegetation, while a value close to +1 means a healthier and higher coverage of vegetation (Abbaszadeh Shahri et al., 2019; Nohani et al., 2019; Sur et al., 2020; Wu et al., 2016; Youssef et al., 2014).

For Soil Texture, the classification of Clay Loam shows a higher correlation with the occurrence of landslides with a FR value of 1.75, while classifications of Clay, Sandy Clay Loam, and Sandy Loam show a lower correlation with FR values of 0.80, 0.82, and 0.93, respectively. No historical landslides were found in the classification of Sandy Silt Loam.

For TWI, according to the FR values, generally, the greater TWI value has the higher FR value. Classifications of the TWI value that is less than 7.35 show a lower correlation with landslide occurrence while classifications of the TWI value greater than 7.35 show a higher correlation.

For SPI, the classification of SPI value < 604 shows it has landslides density proportionally to the area of the classification with a FR value of 0.97 which is close to 1. Classification of SPI value $604 - 2,719$ shows a higher correlation with landslide occurrence with a FR value of 2.12. No historical landslides were found in the other 3 classifications that SPI values are greater than 2,719.

RPD has not been kept as the final LCF for no corresponding relationship was found with landslide occurrence.

To meet the “integer only” inputting requirement of the reclassification function of ArcGIS, all FR values have been normalized into RF values. 27 scenarios were designed including one inputting the 14 full factors and fourteen removing one factor from the whole in turn, and one inputting 3 minimum factors (Slope Angle, Lithology and LULC) and eleven adding other factors into the minimum group in turn, to generate the landslide susceptibility maps, then calculate and compare the AUC value of each scenario. The mandatory factors including Slope Angle, Lithology, and LULC are directly included in the final LCFs group. The bar chart in **Figure 36** shows the other 11 factors’ influence in increasing or decreasing the AUC value when the factor is participating or absent, the result shows 7 factors including

Distance to Road, NDVI, Elevation, and Distance to Fault have a distinctly positive effect on AUC value variation compared with other factors, while SPI has a negative effect.

4.2.2 Landslide Susceptibility Mapping with the 7 Final Landslide Conditioning Factors

Finally, 7 factors including Slope Angle, Lithology, LULC, Distance to Road, NDVI, Elevation, and Distance to Fault have been selected as the final landslide conditioning factors for the study area. In the landslide susceptibility mapping with the final LCFs section, according to the PR value for each factor (**Figure 37**), LULC has the most dominant effect with landslide occurrence with PR value greater than 4, NDVI, Distance to Fault, and Distance to Road show the second level of that with PR value greater than 2 and smaller than 3, while Lithology, Slope Angle, and Elevation show the least effect with PR value between 1 – 2. According to the mapping result in **Figure 38**, overall, about 51.97%, 32.57%, 14.22%, 0.65% and 0.59% of the total area have Very Low, Low, Moderate, High, and Very High levels of landslide susceptibility respectively. Of which, there are 52.24 km², 30.26 km², and 30.34 km² of the 0.59% (112.84 km²) Very High landslide susceptibility level areas are located in Jing Hong City, Meng Hai County, and Meng La County respectively. There are 55.84 km², 37.09 km², and 31.39 km² of the 0.65% (124.32 km²) High landslide susceptibility levels are in the aforesaid regions respectively. For the township level, both the High and Very High landslide susceptibility level areas are distributed in every township except for Meng Wang Xiang as is presented in **Table 15** and **Figure 40**. Of which, the area from high to low, the top 5 townships including Ga Sa Zhen, Meng Hai Zhen, Jing Hong Gong Ye Yuan Qu, Meng La Zhen, and Meng Long Zhen are located in Very High landslide susceptibility level region with the area of 16.48 km², 11.20 km², 9.93 km², 9.11 km², and 7.36 km² respectively. The area from high to low, the top 5 townships including Ga Sa Zhen, Meng La Zhen, Meng Hai Zhen, Meng Long Zhen, and Meng Zhe Zhen are located in High landslide susceptibility level region with the area of 11.55 km², 9.55 km², 8.98 km², 8.54 km², and 7.07 km² respectively. The AUC value obtained with inputting training and verification data is 85.8% and 84.0% respectively, it is shown that the model adopted obtained a very good result for LSM in the study area.

4.2.3 Development of the Web-based Spatial Decision Support System

As a decision support system, the location identification function of the General module is the core function of the Web-based SDSS, which can be used to support the decision-making processes which may strongly rely on the landslide susceptibility distribution status such as disaster prevention fund allocation plan, landslide monitoring system installation site selection, early warning system installation site selection, land use planning, infrastructure construction site selection, etc. As is shown in **Figure 42**, only High and Very High-level landslide susceptibility data have been extracted from the final landslide susceptibility map and digitalized and imported to the Web-based SDSS. This is because the Baidu Map JavaScript Application Programming Interface (API) has not been able to support importing “.kml”, “.shp”, or other vector formats of data yet. Currently, every compositive point of the polygons needs to be stored with text format, which enlarges the data size to a great extent, with only inputting the aforesaid two-level data, it already takes more than 15 seconds to load the Location Identification page, and cause response delay of the map. Though Google Map JavaScript API support importing vector files directly and can solve these problems, due to political issue, Google Map products are banned to use in China. Nevertheless, the proposed Web-based SDSS provides a new way of making better use of the landslide susceptibility assessment outcomes.

CHAPTER V

CONCLUSION AND RECOMMENDATION

5.1 Conclusion

The objective of the study is to assess the landslide susceptibility of Xishuangbanna, China, then develop a Web-based SDSS using the outcomes of the LSA. As one of the most popular landslide susceptibility assessment methods, the FR model is selected as the assessing tool in this study. There is not a consensus on the selection process of the landslide conditioning factors for a specific area, the decisive factors may completely be different from one area to another. The study, therefore, summarized 14 most frequently used factors which are Slope Angle, Distance to River, Slope Aspect, Lithology, LULC, Distance to Fault, Distance to Road, Curvature, Elevation, Precipitation, NDVI, Soil Texture, TWI and SPI from a comprehensive literature review first. Then 27 scenarios including one case of inputting all the 14 factors and 14 cases of removing one of the 14 factors from the whole in turn, one case of inputting 3 minimum factors (Slope Angle, Lithology and LULC) and 11 cases of adding one of the other factors to the 3 minimum, are designed to generate the landslide susceptibility maps of the 27 scenarios with inputting landslide inventory training data. Then the AUC value of each map is calculated using the extension of ESRI's ArcGIS namely Arc – SDM, to evaluate whether when a specific factor is participating and absent, how positive or negative effect it has in influencing the model quality. Finally, 7 factors including 3 obligatory factors (Slope Angle, Lithology and LULC), Distance to Road, NDVI, Elevation, and Distance to fault are identified to be the most positive factors in improving the model quality and are selected as the final landslide conditioning factors for the study area. Final Landslide Susceptibility Mapping is done based on the final factors, the AUC values of both with inputting the landslide inventory training data (success rate) and verification data (prediction rate) show the model of the study obtained a very good result. Finally, the outcomes of the landslide susceptibility assessment process including study theory, data sources, factor weight tables and charts, single layer

maps, 15 LSMs of full and removing factor scenarios, 12 LSMs of minimum and adding factor scenarios, the final LSM, and all the AUC values of all LSMs have been utilized to develop the Web-based SDSS for LSA in the study area.

The study's actual benefits in real-world can be summarized as follows:

a) It can make up the missing of the regional scale of LSA product for the study area;

b) 14 mostly used factors are extracted from a comprehensive literature review, which can be used as a useful reference by other researchers;

c) The scenarios design that adopting or excluding a specific possible landslide conditioning factor, then calculate their AUC values and analyze their positive or negative affect, can be used as a thinkable method when identifying the landslide conditioning factors for other study areas;

d) The Web-based SDSS starts a new way of thinking which has a broad potential for further development and provides a constructive way of making better use of the landslide susceptibility assessment outcomes, which not only can be used as an effective decision-making support tool but also can be used as a significative reference for other researchers;

e) The proposed Web-based SDSS not only applicable for landslide susceptibility assessment outcomes, but also for assessment outcomes of other types of disasters such as flood hazard assessment which is also based on GIS data.

5.2 Recommendations

The insufficiency and the future works of the study may include:

a) The FR model is based on landslide inventory rather than experts' opinion; thus, the quality of the landslide data is fatal. However, the landslide inventory obtained from the Resource and Environment Science and Data Center of China (RESDC) may need to be further verified (e.g., filed investigation and data refining). Moreover, the comparison with other models that are based on experts' opinions such as the AHP method also can be helpful and can be one of the future works;

b) The accuracy of the precipitation data the study used is less than 30m*30m resolution, which is the finest data we can obtain for the moment. Although

finally precipitation has not been included as one of the most decisive landslide conditioning factors for the study area, a reconsideration might be necessary when more accurate precipitation data is available in the future;

c) The proposed Web-based SDSS that uses landslide susceptibility assessment outcomes opened a new window for making better use of the existing data. However, as a decision support system, the development level of the decision support part in this study is still relatively low, extension of other decision support modules can be set as one of the goals in the future;

d) Baidu map JavaScript API is one of the most popular tools for developing Web-based map system, however, it has some limitations. For example, it has not been able to support importing vector files (".shp", ".kml") yet. The main displaying language is Chinese, which may cause inconvenience to the decision makers or experts who do not understand Chinese in understanding the labels in the map. Adopting Google Map JavaScript API can be an effective way of boosting the performance of the system, as well as improving the human-computer interaction experience. Which can be the prioritized consideration when the study area is not in China.



REFERENCES

REFERENCES

- Abbaszadeh Shahri, A., Spross, J., Johansson, F., & Larsson, S. (2019). Landslide susceptibility hazard map in southwest Sweden using artificial neural network. *Catena*, 183. <https://doi.org/10.1016/j.catena.2019.104225>
- Abedini, M., & Tulabi, S. (2018). Assessing LNRF, FR, and AHP models in landslide susceptibility mapping index: a comparative study of Nojian watershed in Lorestan province, Iran. *Environmental Earth Sciences*, 77(11). <https://doi.org/10.1007/s12665-018-7524-1>
- Acharya, T. D., & Lee, D. H. (2018). Landslide Susceptibility Mapping using Relative Frequency and Predictor Rate along Araniko Highway. *KSCE Journal of Civil Engineering*, 23(2), 763-776. <https://doi.org/10.1007/s12205-018-0156-x>
- Ahmed, B., & Dewan, A. (2017). Application of Bivariate and Multivariate Statistical Techniques in Landslide Susceptibility Modeling in Chittagong City Corporation, Bangladesh. *Remote Sensing*, 9(4). <https://doi.org/10.3390/rs9040304>
- Aleotti, P., & Chowdhury, R. (1999). Landslide hazard assessment: summary review and new perspectives. *Bulletin of Engineering Geology and the Environment*, 58(1), 21-44. <https://doi.org/10.1007/s100640050066>
- Anbalagan, R., Kumar, R., Lakshmanan, K., Parida, S., & Neethu, S. (2015). Landslide hazard zonation mapping using frequency ratio and fuzzy logic approach, a case study of Lachung Valley, Sikkim. *Geoenvironmental Disasters*, 2(1). <https://doi.org/10.1186/s40677-014-0009-y>
- Arabameri, A., Saha, S., Roy, J., Chen, W., Blaschke, T., & Tien Bui, D. (2020). Landslide Susceptibility Evaluation and Management Using Different Machine Learning Methods in The Gallicash River Watershed, Iran. *Remote Sensing*, 12(3). <https://doi.org/10.3390/rs12030475>
- Baidu. (2022). *JavaScript API Service Introduction*. Retrieved March 26 from <https://lbsyun.baidu.com/index.php?title=jspopular>

- Beven, K. J., & Kirkby, M. J. (1979). A physically based, variable contributing area model of basin hydrology / Un modèle à base physique de zone d'appel variable de l'hydrologie du bassin versant. *Hydrological Sciences Bulletin*, 24(1), 43-69. <https://doi.org/10.1080/02626667909491834>
- Brown, J. L., Bennett, J. R., & French, C. M. (2017). SDMtoolbox 2.0: the next generation Python-based GIS toolkit for landscape genetic, biogeographic and species distribution model analyses. *PeerJ*, 5, e4095. <https://doi.org/10.7717/peerj.4095>
- Cao, H., Liu, J., Fu, C., Zhang, W., Wang, G., Yang, G., & Luo, L. (2017). Urban Expansion and Its Impact on the Land Use Pattern in Xishuangbanna since the Reform and Opening up of China. *Remote Sensing*, 9(2). <https://doi.org/10.3390/rs9020137>
- Chung, C.-J. F., & Leclerc, Y. (2003). *Use of quantitative techniques for zoning landslide hazard*. Earthquake Hazard Mapping for Landuse and Emergency Planning , Summary of Conference Presentations, British Columbia, Canada. <https://citeseerx.ist.psu.edu/viewdoc/download?doi=10.1.1.624.3037&rep=rep1&type=pdf>
- Chung, C. F., & Leclerc, Y. (2003). *Use of quantitative techniques for zoning landslide hazard* Earthquake Hazard Mapping for Landuse and Emergency Planning, Summary of Conference Presentations,
- Dao, D. V., Jaafari, A., Bayat, M., Mafi-Gholami, D., Qi, C., Moayedi, H., Phong, T. V., Ly, H.-B., Le, T.-T., Trinh, P. T., Luu, C., Quoc, N. K., Thanh, B. N., & Pham, B. T. (2020). A spatially explicit deep learning neural network model for the prediction of landslide susceptibility. *Catena*, 188. <https://doi.org/10.1016/j.catena.2019.104451>
- de Lima, L. M. M., de Sa, L. R., Dos Santos Macambira, A. F. U., de Almeida Nogueira, J., de Toledo Vianna, R. P., & de Moraes, R. M. (2019). A new combination rule for Spatial Decision Support Systems for epidemiology. *Int J Health Geogr*, 18(1), 25. <https://doi.org/10.1186/s12942-019-0187-7>

- Devkota, K. C., Regmi, A. D., Pourghasemi, H. R., Yoshida, K., Pradhan, B., Ryu, I. C., Dhital, M. R., & Althuwaynee, O. F. (2012). Landslide susceptibility mapping using certainty factor, index of entropy and logistic regression models in GIS and their comparison at Mugling–Narayanghat road section in Nepal Himalaya. *Natural Hazards*, 65(1), 135-165.
<https://doi.org/10.1007/s11069-012-0347-6>
- El Jazouli, A., Barakat, A., & Khellouk, R. (2019). GIS-multicriteria evaluation using AHP for landslide susceptibility mapping in Oum Er Rbia high basin (Morocco). *Geoenvironmental Disasters*, 6(1). <https://doi.org/10.1186/s40677-019-0119-7>
- Esri. (2016). *RemapValue—Help | ArcGIS for Desktop*. Environmental Systems Research Institute, Inc.
<https://desktop.arcgis.com/en/arcmap/10.3/analyze/arcpy-spatial-analyst/remapvalue-class.htm>
- ESRI. (2022). *RemapValue—Help | ArcGIS for Desktop*. (n.d.). *An Overview of Spatial Analyst Classes*. Retrieved March 26 from <https://desktop.arcgis.com/en/arcmap/10.3/analyze/arcpy-spatial-analyst/remapvalue-class.htm>
- Fang, Z., Wang, Y., Peng, L., & Hong, H. (2020). Integration of convolutional neural network and conventional machine learning classifiers for landslide susceptibility mapping. *Computers & Geosciences*, 139.
<https://doi.org/10.1016/j.cageo.2020.104470>
- Fayez, L., Pazhman, D., Pham, B. T., Dholakia, M. B., Solanki, H. A., Khalid, M., & Prakash, I. (2018). Application of frequency ratio model for the development of landslide susceptibility mapping at part of Uttarakhand State, India. *Int. J. Appl. Eng. Res*, 13(9). <https://www.researchgate.net/publication/324835919>
- Fayez, L., Pham, B. T., H.A.Solanki, Pazhman, D., Dholakia, M. B., Khalid, M., & Prakash, I. (2018). Application of Frequency Ratio Model for the Development of Landslide Susceptibility Mapping at Part of Uttarakhand State, India. *International Journal of Applied Engineering Research*, 13.

- Ghavami, S. M. (2019). Multi-criteria spatial decision support system for identifying strategic roads in disaster situations. *International Journal of Critical Infrastructure Protection*, 24, 23-36.
<https://doi.org/10.1016/j.ijcip.2018.10.004>
- Gómez, H., & Kavzoglu, T. (2005). Assessment of shallow landslide susceptibility using artificial neural networks in Jabonosa River Basin, Venezuela. *Engineering Geology*, 78(1-2), 11-27.
<https://doi.org/10.1016/j.enggeo.2004.10.004>
- Goyal, Y. (2022). *Advantages of HTML*. Retrieved March 26 from <https://www.educba.com/advantages-of-html/>
- Groetz, P. A., Aenis, T., Tang, L., Nagel, U. J., & Hoffmann, V. (2010). *The Introduction of Rubber and its Consequences-an Assessment of New Risks and Changes for Upland Farmers in the Nabanhe National Nature Reserve in Xishuangbanna, Southwest-China*
<https://www.researchgate.net/publication/337682295>
- Hemati, Z., Selvalakshmi, S., Xia, S., & Yang, X. (2020). Identification of indicators: Monitoring the impacts of rubber plantations on soil quality in Xishuangbanna, Southwest China. *Ecological Indicators*, 116.
<https://doi.org/10.1016/j.ecolind.2020.106491>
- Herold, S., Sawada, M., & Wellar, B. (2005). *Integrating Geographic Information Systems, Spatial Databases and the Internet A Framework for Disaster Management* Proceedings of the 98th Annual Canadian Institute of Geomatics Conference,
- Hervás, J. (2013). Landslide Inventory. In P. T. Bobrowsky (Ed.), *Encyclopedia of Natural Hazards* (pp. 610-611). Springer Netherlands.
https://doi.org/10.1007/978-1-4020-4399-4_214
- Hervás, J., & Bobrowsky, P. (2009). Mapping: Inventories, Susceptibility, Hazard and Risk. In *Landslides – Disaster Risk Reduction* (pp. 321-349).
https://doi.org/10.1007/978-3-540-69970-5_19

- Hidayat, S., Pachri, H., & Alimuddin. (2019). *Analysis of Landslide Susceptibility Zone using Frequency Ratio and Logistic Regression Method in Hambalang, Citeureup District, Bogor Regency, West Java Province* Earth and Environmental Science,
- Huang, F., Yao, C., Liu, W., Li, Y., & Liu, X. (2018). Landslide susceptibility assessment in the Nantian area of China: a comparison of frequency ratio model and support vector machine. *Geomatics, Natural Hazards and Risk*, 9(1), 919-938. <https://doi.org/10.1080/19475705.2018.1482963>
- Hung, L. Q., Van, N. T. H., Duc, D. M., Ha, L. T. C., Van Son, P., Khanh, N. H., & Binh, L. T. (2015). Landslide susceptibility mapping by combining the analytical hierarchy process and weighted linear combination methods: a case study in the upper Lo River catchment (Vietnam). *Landslides*, 13(5), 1285-1301. <https://doi.org/10.1007/s10346-015-0657-3>
- Intarawichian, N., & Dasananda, S. (2010). Analytical hierarchy process for landslide susceptibility mapping in lower mae chaem watershed, northern Thailand. . *Suranaree J. Sci. Technol*, 17(3), 16. <https://www.thaiscience.info/Journals/Article/SJST/10890515.pdf>
- Intarawichian, N., & Dasananda, S. (2011). Frequency ratio model based landslide susceptibility mapping in lower Mae Chaem watershed, Northern Thailand. *Environmental Earth Sciences*, 64(8), 2271-2285. <https://doi.org/10.1007/s12665-011-1055-3>
- Javier, D. N., & Kumar, L. (2019). Frequency Ratio Landslide Susceptibility Estimation in a Tropical Mountain Region. *The International Archives of the Photogrammetry, Remote Sensing and Spatial Information Sciences*, XLII-3/W8, 173-179. <https://doi.org/10.5194/isprs-archives-XLII-3-W8-173-2019>
- Jelokhani-Niaraki, M. (2018). Knowledge sharing in Web-based collaborative multicriteria spatial decision analysis: An ontology-based multi-agent approach. *Computers, Environment and Urban Systems*, 72, 104-123. <https://doi.org/10.1016/j.compenvurbsys.2018.05.012>
- Jelokhani-Niaraki, M., & Malczewski, J. (2015). A group multicriteria spatial decision support system for parking site selection problem: A case study. *Land Use Policy*, 42, 492-508. <https://doi.org/10.1016/j.landusepol.2014.09.003>

- Jeong, J. S., & García-Moruno, L. (2016). The study of building integration into the surrounding rural landscape: Focus on implementation of a Web-based MC-SDSS and its validation by two-way participation. *Land Use Policy*, *57*, 719-729. <https://doi.org/10.1016/j.landusepol.2016.07.005>
- JianhouZhang, & MinCao. (1995). Tropical forest vegetation of Xishuangbanna, SW China and its secondary changes, with special reference to some problems in local nature conservation. *Biological Conservation*, *73*(3). [https://doi.org/10.1016/0006-3207\(94\)00118-A](https://doi.org/10.1016/0006-3207(94)00118-A)
- Khan, H., Shafique, M., Khan, M. A., Bacha, M. A., Shah, S. U., & Calligaris, C. (2019). Landslide susceptibility assessment using Frequency Ratio, a case study of northern Pakistan. *The Egyptian Journal of Remote Sensing and Space Science*, *22*(1), 11-24. <https://doi.org/10.1016/j.ejrs.2018.03.004>
- Kumar, R., & Anbalagan, R. (2016). Landslide susceptibility mapping using analytical hierarchy process (AHP) in Tehri reservoir rim region, Uttarakhand. *Journal of the Geological Society of India*, *87*(3), 271-286. <https://doi.org/10.1007/s12594-016-0395-8>
- Le, T. T. T., Tran, T. V., Hoang, V. H., Bui, V. T., Bui, T. K. T., & Nguyen, H. P. (2021). Developing a Landslide Susceptibility Map Using the Analytic Hierarchical Process in Ta Van and Hau Thao Communes, Sapa, Vietnam. *Journal of Disaster Research*, *16*(4), 529-538. <https://doi.org/10.20965/jdr.2021.p0529>
- Lee, S., & Pradhan, B. (2006). Landslide hazard mapping at Selangor, Malaysia using frequency ratio and logistic regression models. *Landslides*, *4*(1), 33-41. <https://doi.org/10.1007/s10346-006-0047-y>
- Lee, S., & Sambath, T. (2006). Landslide susceptibility mapping in the Damrei Romel area, Cambodia using frequency ratio and logistic regression models. *Environmental Geology*, *50*(6), 847-855. <https://doi.org/10.1007/s00254-006-0256-7>
- Lee, S., & Talib, J. A. (2005). Probabilistic landslide susceptibility and factor effect analysis. *Environmental Geology*, *47*(7), 982-990. <https://doi.org/10.1007/s00254-005-1228-z>

- Li, H., Ma, Y., Aide, T. M., & Liu, W. (2008). Past, present and future land-use in Xishuangbanna, China and the implications for carbon dynamics. *Forest Ecology and Management*, 255(1), 16-24.
<https://doi.org/10.1016/j.foreco.2007.06.051>
- Lin, Q., & Wang, Y. (2018). Spatial and temporal analysis of a fatal landslide inventory in China from 1950 to 2016. *Landslides*, 15(12), 2357-2372.
<https://doi.org/10.1007/s10346-018-1037-6>
- Mahalingam, R., Olsen, M. J., & O'Banion, M. S. (2016). Evaluation of landslide susceptibility mapping techniques using lidar-derived conditioning factors (Oregon case study). *Geomatics, Natural Hazards and Risk*, 7(6), 1884-1907.
<https://doi.org/10.1080/19475705.2016.1172520>
- Mansourian, A., Taleai, M., & Fasihi, A. (2011). A web-based spatial decision support system to enhance public participation in urban planning processes. *Journal of Spatial Science*, 56(2), 269-282.
<https://doi.org/10.1080/14498596.2011.623347>
- Marjanović, M., Kovačević, M., Bajat, B., & Voženilek, V. (2011). Landslide susceptibility assessment using SVM machine learning algorithm. *Engineering Geology*, 123(3), 225-234. <https://doi.org/10.1016/j.enggeo.2011.09.006>
- Marsala, V., Galli, A., Paglia, G., & Miccadei, E. (2019). Landslide Susceptibility Assessment of Mauritius Island (Indian Ocean). *Geosciences*, 9(12).
<https://doi.org/10.3390/geosciences9120493>
- Meena, S., Ghorbanzadeh, O., & Blaschke, T. (2019). A Comparative Study of Statistics-Based Landslide Susceptibility Models: A Case Study of the Region Affected by the Gorkha Earthquake in Nepal. *ISPRS International Journal of Geo-Information*, 8(2). <https://doi.org/10.3390/ijgi8020094>
- Milevski, I., Dragičević, S., & Zorn, M. (2019). Statistical and expert-based landslide susceptibility modeling on a national scale applied to North Macedonia. *Open Geosciences*, 11(1), 750-764. <https://doi.org/10.1515/geo-2019-0059>
- Min, S., Huang, J., Waibel, H., Yang, X., & Cadisch, G. (2019). Rubber Boom, Land Use Change and the Implications for Carbon Balances in Xishuangbanna, Southwest China. *Ecological Economics*, 156, 57-67.
<https://doi.org/10.1016/j.ecolecon.2018.09.009>

- Mind'je, R., Li, L., Nsengiyumva, J. B., Mupenzi, C., Nyesheja, E. M., Kayumba, P. M., Gasirabo, A., & Hakorimana, E. (2019). Landslide susceptibility and influencing factors analysis in Rwanda. *Environment, Development and Sustainability*, 22(8), 7985-8012. <https://doi.org/10.1007/s10668-019-00557-4>
- Mohd, M. M., Amin, M. S. M., Kamal, M. R., Wayayok, A., & Yazid, S. A. A. a. M. (2014). *Application of Web Geospatial Decision Support System for Tanjung Karang Rice Precision Irrigation Water Management* Food and Environmental Engineering, Malaysia.
- Mondal, S., & Maiti, R. (2014). Integrating the Analytical Hierarchy Process (AHP) and the frequency ratio (FR) model in landslide susceptibility mapping of Shiv-khola watershed, Darjeeling Himalaya. *International Journal of Disaster Risk Science*, 4(4), 200-212. <https://doi.org/10.1007/s13753-013-0021-y>
- Moore, I., Grayson, R., & Ladson, A. (1991). Digital terrain modelling: A review of hydrological, geomorphological, and biological applications. *Hydrological Processes*, 5, 3-30.
- Muavhi, N., Thamaga, K. H., & Mutoti, M. I. (2021). Mapping groundwater potential zones using relative frequency ratio, analytic hierarchy process and their hybrid models: case of Nzhelele-Makhado area in South Africa. *Geocarto International*, 1-20. <https://doi.org/10.1080/10106049.2021.1936212>
- Nohani, Moharrami, Sharafi, Khosravi, Pradhan, Pham, Lee, & Melesse. (2019). Landslide Susceptibility Mapping Using Different GIS-Based Bivariate Models. *Water*, 11(7). <https://doi.org/10.3390/w11071402>
- Nyimbili, P. H., & Erden, T. (2017). Spatial decision support systems (SDSS) and software applications for earthquake disaster management with special reference to Turkey. *Natural Hazards*, 90(3), 1485-1507. <https://doi.org/10.1007/s11069-017-3089-7>
- Oliveira, T. H. M. d., Painho, M., & Henriques, R. (2012). A Spatial Decision Support System for the Portuguese Public Transportation Sector. *ACM SIGSPATIAL IWGS*.

- Persichillo, M. G., Bordoni, M., Meisina, C., Bartelletti, C., Barsanti, M., Giannecchini, R., D'Amato Avanzi, G., Galanti, Y., Cevasco, A., Brandolini, P., & Galve, J. P. (2016). Shallow landslides susceptibility assessment in different environments. *Geomatics, Natural Hazards and Risk*, 8(2), 748-771. <https://doi.org/10.1080/19475705.2016.1265011>
- Phrakonkham, S., Kazama, S., & Daisuke, K. (2020). Integrated evaluation of water-related disasters using the analytical hierarchy process under land use change and climate change issues in Laos. In (pp. 32): *Natural Hazards and Earth System Science*.
- Pirasteh, S., & Li, J. (2017). Probabilistic frequency ratio (PFR) model for quality improvement of landslide susceptibility mapping from LiDAR-derived DEMs. *Geoenvironmental Disasters*, 4(1). <https://doi.org/10.1186/s40677-017-0083-z>
- Poudyal, C. P., Chang, C., Oh, H.-J., & Lee, S. (2010). Landslide susceptibility maps comparing frequency ratio and artificial neural networks: a case study from the Nepal Himalaya. *Environmental Earth Sciences*, 61(5), 1049-1064. <https://doi.org/10.1007/s12665-009-0426-5>
- Pourghasemi, H. R., Moradi, H. R., & Fatemi Aghda, S. M. (2013). Landslide susceptibility mapping by binary logistic regression, analytical hierarchy process, and statistical index models and assessment of their performances. *Natural Hazards*, 69(1), 749-779. <https://doi.org/10.1007/s11069-013-0728-5>
- Pourghasemi, H. R., Pradhan, B., & Gokceoglu, C. (2012). Application of fuzzy logic and analytical hierarchy process (AHP) to landslide susceptibility mapping at Haraz watershed, Iran. *Natural Hazards*, 63(2), 965-996. <https://doi.org/10.1007/s11069-012-0217-2>
- Pradhan, B. (2010). Landslide Susceptibility mapping of a catchment area using frequency ratio, fuzzy logic and multivariate logistic regression approaches. *J. Indian Soc. Remote Sens*, 38.
- Rabby, Y. W., & Li, Y. (2020). Landslide Susceptibility Mapping Using Integrated Methods: A Case Study in the Chittagong Hilly Areas, Bangladesh. *Geosciences*, 10(12). <https://doi.org/10.3390/geosciences10120483>

- Rasyid, A. R., Bhandary, N. P., & Yatabe, R. (2016). Performance of frequency ratio and logistic regression model in creating GIS based landslides susceptibility map at Lompobattang Mountain, Indonesia. *Geoenvironmental Disasters*, 3(1). <https://doi.org/10.1186/s40677-016-0053-x>
- Roznovsky, A. (2022). *WHY USE PHP? MAIN ADVANTAGES AND DISADVANTAGES*. Retrieved March 26 from <https://light-it.net/blog/why-use-php-main-advantages-and-disadvantages/>
- Sangeeta, & Maheshwari, B. K. (2018). Earthquake-Induced Landslide Hazard Assessment of Chamoli District, Uttarakhand Using Relative Frequency Ratio Method. *Indian Geotechnical Journal*, 49(1), 108-123. <https://doi.org/10.1007/s40098-018-0334-2>
- Sarathchandra, C., Alemu Abebe, Y., Worthy, F. R., Lakmali Wijerathne, I., Ma, H., Yingfeng, B., Jiayu, G., Chen, H., Yan, Q., Geng, Y., Weragoda, D. S., Li, L.-L., Fengchun, Y., Wickramasinghe, S., & Xu, J. (2021). Impact of land use and land cover changes on carbon storage in rubber dominated tropical Xishuangbanna, South West China. *Ecosystem Health and Sustainability*, 7(1). <https://doi.org/10.1080/20964129.2021.1915183>
- Shahabi, H., Khezri, S., Ahmad, B. B., & Hashim, M. (2014). Landslide susceptibility mapping at central Zab basin, Iran: A comparison between analytical hierarchy process, frequency ratio and logistic regression models. *Catena*, 115, 55-70. <https://doi.org/10.1016/j.catena.2013.11.014>
- Shano, L., Raghuvanshi, T. K., & Meten, M. (2021). Landslide susceptibility mapping using frequency ratio model: the case of Gamo highland, South Ethiopia. *Arabian Journal of Geosciences*, 14(7). <https://doi.org/10.1007/s12517-021-06995-7>
- Solaimani, K., Mousavi, S. Z., & Kavian, A. (2012). Landslide susceptibility mapping based on frequency ratio and logistic regression models. *Arabian Journal of Geosciences*, 6(7), 2557-2569. <https://doi.org/10.1007/s12517-012-0526-5>
- Sreekanth, P. D., Soam, S. K., & Rao, K. V. K. a. N. H. (2021). Spatial decision support system for managing agricultural experimental farms. *Current Science*.

- Srivastava, V., Srivastava, H. B., & Lakhera, R. C. (2010). Fuzzy gamma based geomatic modelling for landslide hazard susceptibility in a part of Tons river valley, northwest Himalaya, India. *Geomatics, Natural Hazards and Risk*, 1(3), 225-242. <https://doi.org/10.1080/19475705.2010.490103>
- Statistics, X. M. B. o. (2020). *Population: Yunnan: Xishuangbanna*. <https://www.ceicdata.com/en/china/population-prefecture-level-region/population-yunnan-xishuangbanna>
- Sugumaran, V., & Sugumaran, R. (2007). Web-based Spatial Decision Support Systems (WebSDSS): Evolution, Architecture, Examples and Challenges. *Communications of the Association for Information Systems*, 19. <https://doi.org/10.17705/1cais.01940>
- Sur, U., Singh, P., & Meena, S. R. (2020). Landslide susceptibility assessment in a lesser Himalayan road corridor (India) applying fuzzy AHP technique and earth-observation data. *Geomatics, Natural Hazards and Risk*, 11(1), 2176-2209. <https://doi.org/10.1080/19475705.2020.1836038>
- Tan, M. L., Ullah, K., & Zhang, J. (2020). GIS-based flood hazard mapping using relative frequency ratio method: A case study of Panjkora River Basin, eastern Hindu Kush, Pakistan. *Plos One*, 15(3). <https://doi.org/10.1371/journal.pone.0229153>
- Trifonova, O. P., Lokhov, P. G., & Archakov, A. I. (2014). [Metabolic profiling of human blood]. *Biomed Khim*, 60(3), 281-294. <https://doi.org/10.18097/pbmc20146003281>
- UNISDR. (2016). *Exposure and Vulnerability* UNISDR Science and Technology Conference on the implementation of the Sendai Framework for Disaster Risk Reduction 2015-2030,
- University, C. (2022). *Soil Texture Triangle Particle size class estimator*. Retrieved August 26 from <http://www.landis.org.uk/services/tools.cfm>
- Vakhshoori, V., & Zare, M. (2016). Landslide susceptibility mapping by comparing weight of evidence, fuzzy logic, and frequency ratio methods. *Geomatics, Natural Hazards and Risk*, 7(5), 1731-1752. <https://doi.org/10.1080/19475705.2016.1144655>

- Valencia Ortiz, J. A., & Martínez-Graña, A. M. (2018). A neural network model applied to landslide susceptibility analysis (Capitanejo, Colombia). *Geomatics, Natural Hazards and Risk*, 9(1), 1106-1128.
<https://doi.org/10.1080/19475705.2018.1513083>
- Van Westen, C. J., Rengers, N., & Soeters, R. (2003). Use of Geomorphological Information in Indirect Landslide Susceptibility Assessment. *Natural Hazards*, 30(3), 399-419. <https://doi.org/10.1023/B:NHAZ.0000007097.42735.9e>
- Wangdi, K., Banwell, C., Gatton, M. L., Kelly, G. C., Namgay, R., & Clements, A. C. (2016). Development and evaluation of a spatial decision support system for malaria elimination in Bhutan. *Malar J*, 15, 180.
<https://doi.org/10.1186/s12936-016-1235-4>
- Wicaksono, Y. S., Sihombing, F. M. H., & Indra, T. L. (2020). *Landslide susceptibility map of Bogor Area using analytical hierarchy process* Life and Environmental Sciences Academics Forum,
- Wu, Y., Li, W., Wang, Q., Liu, Q., Yang, D., Xing, M., Pei, Y., & Yan, S. (2016). Landslide susceptibility assessment using frequency ratio, statistical index and certainty factor models for the Gangu County, China. *Arabian Journal of Geosciences*, 9(2). <https://doi.org/10.1007/s12517-015-2112-0>
- Xiao, C., Li, P., & Feng, Z. (2019). Monitoring annual dynamics of mature rubber plantations in Xishuangbanna during 1987-2018 using Landsat time series data: A multiple normalization approach. *International Journal of Applied Earth Observation and Geoinformation*, 77, 30-41.
<https://doi.org/10.1016/j.jag.2018.12.006>
- Xu, J., Grumbine, R. E., & Beckschäfer, P. (2014). Landscape transformation through the use of ecological and socioeconomic indicators in Xishuangbanna, Southwest China, Mekong Region. *Ecological Indicators*, 36, 749-756.
<https://doi.org/10.1016/j.ecolind.2012.08.023>
- Yalcin, A., Reis, S., Aydinoglu, A. C., & Yomralioglu, T. (2011). A GIS-based comparative study of frequency ratio, analytical hierarchy process, bivariate statistics and logistics regression methods for landslide susceptibility mapping in Trabzon, NE Turkey. *Catena*, 85(3), 274-287.
<https://doi.org/10.1016/j.catena.2011.01.014>

- Yanhui Zhu, T. H., Wang, J., Luo, Y., & Yang, K. (2018). *Landslide and Debris Flow Hazard Risk Analysis and Assessment in Yunnan Province 2018 Eighth International Conference on Instrumentation & Measurement, Computer, Communication and Control (IMCCC)*,
<https://ieeexplore.ieee.org/document/9045070>
- Yatsalo, B., & Sullivan, T. (2012). Environmental risk management with the use of multi-criteria spatial decision support system. *Risk Assessment and Management*.
- Youssef, A. M., Al-Kathery, M., & Pradhan, B. (2014). Landslide susceptibility mapping at Al-Hasher area, Jizan (Saudi Arabia) using GIS-based frequency ratio and index of entropy models. *Geosciences Journal*, 19(1), 113-134.
<https://doi.org/10.1007/s12303-014-0032-8>
- Zhang, G., Cai, Y., Zheng, Z., Zhen, J., Liu, Y., & Huang, K. (2016). Integration of the Statistical Index Method and the Analytic Hierarchy Process technique for the assessment of landslide susceptibility in Huizhou, China. *Catena*, 142, 233-244. <https://doi.org/10.1016/j.catena.2016.03.028>
- Zhang, J.-Q., Corlett, R. T., & Zhai, D. (2019). After the rubber boom: good news and bad news for biodiversity in Xishuangbanna, Yunnan, China. *Regional Environmental Change*, 19(6), 1713-1724. <https://doi.org/10.1007/s10113-019-01509-4>
- Zhang, Y.-x., Lan, H.-x., Li, L.-p., Wu, Y.-m., Chen, J.-h., & Tian, N.-m. (2020). Optimizing the frequency ratio method for landslide susceptibility assessment: A case study of the Caiyuan Basin in the southeast mountainous area of China. *Journal of Mountain Science*, 17(2), 340-357. <https://doi.org/10.1007/s11629-019-5702-6>
- Zhu, Y., Xu, J., Li, Q., & Mortimer, P. E. (2014). Investigation of rubber seed yield in Xishuangbanna and estimation of rubber seed oil based biodiesel potential in Southeast Asia. *Energy*, 69, 837-842.
<https://doi.org/10.1016/j.energy.2014.03.079>